

# The Jordan Journal of Earth and Environmental Sciences (JJES)

JJES is An International Peer-Reviewed Research Journal Issued by Higher Scientific Research Committee Ministry of Higher Education and Scientific Research and Deanship of Academic Research and Graduate Studies The Hashemite University.

## EDITORIAL BOARD

---

### Editor-in-Chief

**Professor Abdul Rahim A. Hamdan**  
The Hashemite University

### Editorial board

- **Professor Abdulkader M. Abed**  
University of Jordan
- **Professor Hani N. Khoury**  
University of Jordan
- **Professor Zuhair El-Isa**  
University of Jordan
- **Professor Ibrahim Al-Dwari**  
Yarmouk University
- **Professor Ahmad Abu Hilal**  
Yarmouk University
- **Professor Issa Makhoulouf**  
Hashemite University

## THE INTERNATIONAL ADVISORY BOARD

---

- **Prof. Sayed Abdul Rahman,**  
Cairo University, Egypt.
- **Prof. Abdullah Al-Amri,**  
King Saud University, Saudi Arabia.
- **Prof. Waleed Al-Zubair,**  
Arabian Gulf University, Bahrain.
- **Prof. Ute Austermann-Haun,**  
Fachhochschule und Lipp, Germany.
- **Prof. Ibrahim Banat,**  
University of Ulster, UK.
- **Prof. Matthias Barjenbruch,**  
Technisch Universitat Berlin, Germany.
- **Prof. Mohamed Boukhary,**  
Ain Shams University, Egypt.
- **Prof. Mohammad El-Sharkawy,**  
Cairo University, Egypt
- **Prof. Venugopalan Ittekkot.**  
Center for Tropical Marine Ecology, Bremen,  
Germany.
- **Prof. Christopher Kendall,**  
University of North Carolina, U.S.A.
- **Prof. Elias Salameh,**  
University of Jordan, Jordan.
- **Prof. V. Subramanian,**  
Jawaharlal Nehru University, India.
- **Prof. Omar Rimawy,**  
University of Jordan, Jordan.
- **Prof. Hakam Mustafa,**  
Yarmouk University, Jordan.
- **Dr. Michael Crosby,**  
The National Science Board, National Science  
Foundation, Virginia, U.S.A.
- **Dr. Brian Turner,**  
Durham University, U.K..
- **Dr. Friedhelm Krupp,**  
Senckenberg Research Institute and Natural History  
Museum, Germany.
- **Dr. Richard Lim,**  
University of Technology, Australia.

## EDITORIAL BOARD SUPPORT TEAM

---

### Language Editor

Dr. Wael Zuraiq

### Publishing Layout

MCPD. Osama Alshareet

## SUBMISSION ADDRESS:

---

Professor **Abdul Rahim A. Hamdan**  
Deanship of Academic Research and Higher Studies  
Hashemite University, P.O. Box 330127, Postal Code 13133, Zarqa, Jordan.

Phone: +962-5-3903333 ext. 4151

E-Mail: [jjes@hu.edu.jo](mailto:jjes@hu.edu.jo) , [hamdan@hu.edu.jo](mailto:hamdan@hu.edu.jo)



Hashemite Kingdom of Jordan



Hashemite University

Jordan Journal of  
Earth and Environmental Sciences

JJEEES

*An International Peer-Reviewed Scientific*

<http://jjees.hu.edu.jo/>

ISSN 1995-6681

# The Jordan Journal of Earth and Environmental Sciences (JJEES)

JJEES is An International Peer-Reviewed Research Journal Issued by Higher Scientific Research Committee Ministry of Higher Education and Scientific Research and Deanship of Academic Research and Graduate Studies The Hashemite University

## Instructions to authors:

---

The Jordan Journal of Earth and Environmental Sciences (JJEES) is the national journal of Jordan in earth and environmental sciences. It is an internationally refereed journal dedicated to the advancement of knowledge. It publishes research papers that address both theoretical and applied valuable subjects and matters in both Arabic and English languages in the various fields of geoscience and environmental disciplines. JJEES is published quarterly by the Hashemite University. Submitted articles are blindly and rigorously reviewed by distinguished specialists in their respected fields. The articles submitted may be authentic research papers, scientific reviews, technical/scientific notes.

## FORMATE GUIDE:

1. The research papers should be printed on one side of the paper, be double-line spaced, have a margin of 30 mm all around, and no more than 30 pages (7,500 words, font size 13). Authors should submit three copies of the paper and a floppy diskette 3.5 or a CD under (Winword IBM) or by e-mail. The title page must list the full title and the names and affiliations of all authors (first name, middle name and last name). Also, their addresses, including e-mail, and their ranks/positions must be included. Give the full address, including e-mail, telephone and fax, of the author who is to check the proof.
2. The research must contain the title and abstract, keywords, introduction, methodology, results, discussion, and recommendations if necessary. The system of international units must also be used. Scientific abbreviations may be used provided that they are mentioned when first used in the text. Include the name(s) of any sponsor(s) of the research contained in the paper, along with grant number(s).
3. Authors should submit with their paper two abstracts, one in the language of the paper and it should be typed at the beginning of the paper followed by the keywords before the introduction. As for the other abstract, it should be typed at the end of the paper on a separate sheet. Each abstract should not contain more than 200 words.
4. Captions and tables should be numbered consecutively according to their occurrence in the research with headings. When mentioned in the text, the same consecutive numbers should be used. Captions and tables must be typed on separate sheets of paper and placed at the end of the paper.
5. The author(s) should submit a written consent that he or she will not publish the paper in any other journal at the same time of its publication in JJEES. After the paper is approved for publication by the editorial board, the author does not have the right to translate, quote, cite, summarize or use the publication in the other mass media unless the editor-in-chief submits a written consent according to the policy of JJEES. Submitted material will not be returned to the author unless specifically requested.
6. **DOCUMENTATION:**

### References:

- a. To cite sources in the text, use the author-date method; list the last name(s) of the author(s), then the year. Examples: (Holmes, 1991); (Smith and Hutton 1997).
- b. In the event that an author or reference is quoted or mentioned at the beginning of a paragraph or sentence or an author who has an innovative idea, the author's name is written followed by the year between two brackets. Example: Hallam(1990).
- c. If the author's name is repeated more than once in the same volume, alphabets can be used. Example: (Wilson, 1994 a; Wilson, 1994 b).
- d. Footnotes may be used to solve any ambiguity or explain something as in the case of a term that requires illustration. In this case, the term is given a number and the explanation is written in a footnote at the bottom of the page.
- e. If the number of authors exceeds two, the last name of the first author followed by et al. is written in the text. Example: (Moore et al.). Full names are written in the references regardless of their number.
- f. Prepare a reference section at the end of the paper listing all references in alphabetical order according to the first author's last name. This list should include only works that been cited.

### Books:

Hunt, J. 1996. Petroleum Geochemistry and Geology. 2<sup>nd</sup> Ed., H. W. Freeman and Company, New York.

### Chapter in a book:

Shinn E. A., 1983. Tidal Flat Environment, **In:** Carbonate Depositional Environments, edited by Scholle, P. A., Bebout, D. G., and Moore, C. H., The American Association of Petroleum Geologists, Tulsa, Oklahoma, U.S.A. pp. 171-210.

### Periodicals:

Sexton, P. F., Wilson, P. A., and Pearson, P. N., 2006. Paleoecology of Late Middle Eocene Planktonic Foraminifera and Evolutionary Implication, *Marine Micropaleontology*, 60(1): 1-16.

### Conferences and Meetings:

Huber, B. T. 1991. Paleogene and Early Neogene Planktonic Foraminifer Biostratigraphy of Sites 738 and 744, Kerguelen Plateau (southern Indian Ocean). In: Barron, J., Larsen, B., et al. (Eds.), Proceedings of the Ocean Drilling Program. Scientific Results, vol. 119. Ocean Drilling Program, College station, TX, pp. 427-449.

**Dissertations:**

Thawabteh, S. M. 2006. Sedimentology, Geochemistry, and Petrographic Study of Travertine Deposits along the Eastern Side of the Jordan Valley and Dead Sea, M. Sc. Thesis, The Hashemite University.

**Unpublished:**

Makhlouf, I. M. and El-Haddad, A. 2006. Depositional Environments and Facies of the Late Triassic Abu Ruweis Formation, Jordan, J. Asian Earth Sciences, England, in Press.

**Illustrations:**

- a. Supply each illustration on a separate sheet, with the lead author's name, the figure number and the top of the figure indicated on the reverse side.
  - b. Supply original photographs; photocopies and previously printed material are not acceptable.
  - c. Line artwork must be high-quality laser output (not photocopies).
  - d. Tints are not acceptable; lettering must be of reasonable size that would still be clearly legible upon reduction, and consistent within each figure and set of figure.
  - e. Electronic versions of the artwork should be supplied at the intended size of printing; the maximum column width is 143mm.
  - f. The cost of printing color illustrations in the Journal may be charged to the author(s).
7. Arranging articles in JJEES is based on the editorial policy.
  8. The author should submit the original and two copies of the manuscript, together with a covering letter from the corresponding author to the Editor-in-Chief.
  9. The editorial board's decisions regarding suitability for publication are final. The board reserves the right not to justify these decisions.
  10. In case the paper was initially accepted, it will be reviewed by two specialized reviewers.
  11. The accepted papers for publication shall be published according to the final date of acceptance.
  12. If the author chooses to withdraw the article after it has been assessed, he/she shall reimburse JJEES the cost of reviewing the paper.
  13. The author(s) will be provided with one copy of the issue in which the work appears in addition to 20 off prints for all authors. The author(s) must pay for any additional off prints of the published work.
  14. statement transferring copyright from the authors to the Hashemite University to enable the publisher to disseminate the author's work to the fullest extent is required before the manuscript can be accepted for publication. A copy of the Copyright Transfer Agreement to be used (which may be photocopied) can be found in the first issue of each volume of JJEES.
  15. Articles, communications or editorials published by JJEES represent the sole opinion of the authors. The publisher bears no responsibility or liability whatsoever for the use or misuse of the information published by JJEES.

**Manuscript Submission:**

Submit three copies of the manuscript (including copies of tables and illustrations) to the Editor-in-Chief

Professor **Abdul Rahim A. Hamdan**

Deanship of Academic Research and Higher Studies

Hashemite University, P.O. Box 330127, Postal Code 13133, Zarqa, Jordan.

Phone: +962-5-3903333 ext. 4151

E-Mail: [jjees@hu.edu.jo](mailto:jjees@hu.edu.jo) , [hamdan@hu.edu.jo](mailto:hamdan@hu.edu.jo)

Submitted manuscript should not have been previously published or submitted for publications elsewhere while they are under consideration by JJEES. Research articles, communications, and technical notes are subject to critical review by competent referees. Manuscript submitted in Arabic should be accompanied by abstract and keywords in English.

**Organization of the Manuscript:**

The research papers should be printed on one side of the paper, be double-line spaced, have a margin of 30 mm all around, and no more than 30 pages (7,500 words, font size 13). Authors should submit three copies of the paper and a floppy diskette 3.5 or a CD under (Winword IBM) or by e-mail. The title page must list the full title and the names and affiliations of all authors (first name, middle name and last name). Also, their addresses, including e-mail, and their ranks/positions must be included. Give the full address, including e-mail, telephone and fax, of the author who is to check the proof.

The research must contain the title and abstract, keywords, introduction, methodology, results, discussion, and recommendations if necessary. The system of international units must also be used. Scientific abbreviations may be used provided that they are mentioned when first used in the text. Include the name(s) of any sponsor(s) of the research contained in the paper, along with grant number(s).

**Copyright:**

A statement transferring copyright from the authors to the Hashemite University to enable the publisher to disseminate the author's work to the fullest extent is required before the manuscript can be accepted for publication. A copy of the Copyright Transfer Agreement to be used (which may be photocopied) can be found in the first issue of each volume of JJEES.

**Disclaimer:**

Articles, communications or editorials published by JJEES represent the sole opinion of the authors. The publisher bears no responsibility or liability whatsoever for the use or misuse of the information published by JJEES.



## **PAGES**

## **PAPERS**

53 – 62

Geochemistry, Mineralogy and Petrogenesis of El-Lajjoun Pleistocene Alkali Basalt of Central Jordan.

*Tayel El-Hasan and Ahmad Al-Malabeh*

63 – 72

Time Series Analysis of Air Pollution in Al-Hashimeya Town Zarqa, Jordan

*G. Saffarini and S. Odat*

73 – 80

Analyzing Correlation Coefficients of the Concentrations of Trace Elements in Urinary Stones

*Iyad Ahmed Abboud*

81 – 88

Structural Control on Groundwater Distribution and Flow in Irbid Area, North Jordan

*Al-Taj, M.*

89 – 94

Characterization of A Hard Opaline Clayey Bed Overlying Phosphates from Esh-Shidiya Area, SE of Jordan.

*Zayed Al-Hawari*

---



# Geochemistry, Mineralogy and Petrogenesis of El-Lajjoun Pleistocene Alkali Basalt of Central Jordan.

Tayel El-Hasan <sup>\*a</sup> and Ahmad Al-Malabeh <sup>b</sup>

<sup>a</sup> Faculty of science, Mu'tah University, Al-Karak, Jordan,

<sup>b</sup> Department of Earth and Environmental Science, the Hashemite, University, Zarka, Jordan.

## Abstract

The El-Lajjoun basalt (hereafter, LB) is a Wadi-fill flow that covers an area of about 10 km<sup>2</sup> in Central Jordan. The tectonic evaluation carried out through lineament and fracture analyses indicates that the regional development is tectonically related to the opening of the Red Sea, and the development of the Dead Sea transform fault and other distinct regional tectonic features. The age of the LB (middle Pleistocene) can be correlated with the second stage of the opening of the Red Sea over the last 5 Ma. Petrographic data shows that rocks are plagioclase, olivine, pyroxene, and magnetite-phyric basalts. They correspond to alkali olivine basalts and basanites. The LB rocks are very similar in composition, and have comparable ranges of major and trace element concentrations. They are of undersaturated silica type and belong to sodic to mildly alkaline magma series. The distinctive geochemical characteristics of LB indicated that LB was derived from a slightly fractionated magma as reflected by its high MgO (7-8 wt%) concentration, the Mg-number (0.60-0.63), the low silica content (<43-46 wt%), and the relatively high Ni and Cr concentrations (193-271 ppm and 243-374 ppm, respectively). This basalt is resulted from a low degree of partial melting (10%) of a homogeneous garnet peridotite mantle source in the asthenosphere at a depth > 100 km.

© 2008 Jordan Journal of Earth and Environmental Sciences. All rights reserved

**Keywords:** Pleistocene, Alkali-olivine basalt, Within-plate basalt, Partial melting

## 1. Introduction

The tectonic evolution of the Arabian plate is determined by the main regional structures of the region including the African Arabian rift system, the collision of the Arabian and Eurasian plates, and the Arabian dome (Barberi et al. 1970; Almond, 1986; Garfunkel, 1988; Burke, 1996; and Al-Malabeh et al. 2004) (Figure 1). This evolution led to different fractures and rifting systems, i.e. the East-African rift, the opening of the Red Sea, and the Dead Sea rift system. These tectonics were controlling the volcanic activity in the Arabian plate which are sporadically found over an area that covers a distance of 7,000 Km from Yemen in the south through Saudi Arabia, Jordan, Syria, and up to Turkey in the north (Coleman and McGuire 1988; Camp and Roobol 1992; and Pick et al. 1999).

The basaltic rocks in Jordan are mainly of Tertiary - Quaternary in age. They occupy 18 % of Jordan's area; and are distributed in three main regions based on their mode of occurrences according to (Bender, 1974; and Al-Malabeh, 1993): 1) within Jordan rift (e.g. Zara basalt), 2) central Jordan (e.g. El-Lajjun basalt) and 3) NE-Jordanian Harrat (with an area 11,400 km<sup>2</sup>) which is a part of the largest Harrat Al-Shaam (Al-Malabeh, 2003) as shown in (Figure 2a).

Based on K-Ar, Barbari et al. 1979; Moffat, 1988; Duffield et al. 1988; and Ilani et al. 2001 have divided the volcanic activity of Jordan into three major episodes: Oligocene to early Miocene (26.23-22.17 Ma), middle to late Miocene (13.97-8.94 Ma), and late Miocene to Pleistocene (6.95 Ma to < 0.15 Ma). Previous petrochemical studies of basaltic rocks indicated that NE basaltic plateau is composed of alkali basalts and basanites with minor nephelinites (e.g. Barberi et al. 1979; Moffat, 1988; Saffarini et al. 1985; Al-Malabeh, 1994; Al-Malabeh et al. 2002; Shaw et. al. 2003; Ibrahim and Al-Malabeh 2006).

The basalt in central Jordan, which is of our concern here, is found mainly in six places, namely El-Lajjoun, Jabal Shihan, Tafila, Wadi Dana, Jurf Al-Darawish and Ghor Al-Katar. They occur either as plateau basalts, or as local flows, (e.g., Wadi fills) or as individual volcanic bodies (cones, plugs, sills, and dikes). In spite of the fact that substantial horizontal sinistral displacement of N-S striking the Dead Sea Transform Fault (DST) is accompanied by sinistral fan-like rotation of the Arabian plate., this might have led to the opening of fissures for the ascent of magmas. The available geochronological data for these basalts suggests a different story. The several doleritic dikes along the NW-SE Al-Karak - Wadi Al-Fayha fault zone (graben) with the an age of 28.8- 18.9 Ma belong to the oldest phase of activity, whereas the ages of activities in the other sites are more recent; such as in Wadi Dana 9.3 – 5.1 Ma (Steinitz and Batrov, 1992); in Shihan plateau 6.0 Ma (Barberi et al. 1979) and in Tafila

\* Corresponding author.; tayel@mutah.edu.jo

3.7 -1.7 Ma (Steinitz and Batrov, 1992). Therefore, the association of these basalts only with the DST is questionable since some of them are dated older than the rift. Therefore it is better to relate them to the development of the Arabian plate, coeval on a large scale with the regional uplifting, and with rifting phases (Garfunkel, 1989).

This work aims at investigating the geochemical, mineralogical, and petrographical features of the Neogene-Quaternary intra-continental basaltic flows at El-Lajjoun area - central Jordan. And to determine their origin and type of parental magma, and to investigate their relationship to the tectonic evolution of the whole region.

## 2. Study Area Settings

The LB is located about 15 km east of Al-Karak city at 31°13'40"N and 35°51'52"E (Figure 2a). The flow covers an area of about 10 km<sup>2</sup>; and it forms an NE-SW striking, arc-like strip with a width of about 0.5 km with an average thickness of 1-3 m. The exposure starts along the sides of Wadi Adir, and then passes through the El-Lajjoun grazing station, and then along the sides of Wadi Al-Dakain (Figure 2b). This basalt belongs to the middle Pleistocene (Bender, 1968; Heimbach & Huseibeh, 1975; and Steinitz and Batrov, 1992). This is in consistence with the second stage of the opening of the Red Sea over the last 5 Ma.

The basalt is seen in the field to cover Al-Hisa Phosphorite Unit of Mastrichtian age (Al-Shawabkeh, 1991; Latafeh, et al. 2002; and Al-Malabeh et al. 2002); and is covered by fluvial and lacustrine gravels and soil (Figs. 2b). The lithostratigraphy of El-Lajjoun area is presented in (Figure 2c).

The results of joint and fault measurements are presented as rose diagrams in (Figure 2d). The LB displays two dominant joint directions, namely N-S and E-W and two minor directions, i.e., NW-SE and NE-SW. These directions are coincided with the main regional and local structural directions. The N-S trending fractures are parallel to (DST). The E-W fractures lie parallel to Salwan Fault and perpendicular to DST, Suwaqa normal fault (Hatcher et al. 1981), Zarka Main fault and El-Lajjoun graben. Moreover, the NE-SW trending joints are consistent with the late Pan-African stress pattern as reported by (Bentor, 1985; and Stern, 1985). They suggested that these trends are formed by extensional stresses normal to their direction. Also, this direction is consistent with the Jurf Al-Darawish fault, which has a vertical displacement of at least 100 m, downthrown to the east (Barjous & Mikbel, 1990). The NW-SE trending directions are shown by a number of prominent regional faults such as the Al-Karak - Al-Fayha fault system (graben) and the Wadi Sirhan fault zone, which extends about 325 km in the same direction starting from Saudi Arabia in the south and continuing to the north of Jordan (Bender, 1974) (Figure 2a).

## 3. Sampling and Analytical Techniques

Twelve representative rock samples from the LB were crushed and powdered using geochemical techniques. Major oxides and trace elements were analysed on fused

glass disks at the Geological Institute, University of Wuerzburg, Germany, by multi-channel XRF spectrometry. Powdered samples were dried for two hours at 110 °C and ignited in an electric furnace at 100 °C for one hour. Ignited samples were then mixed with sodium tetra-borate and fused in crucibles over gas burners for 1-1.5 hours. Melts were poured into a mold creating 32 mm diameter glass disks. Major and trace elements analytical results are given in Table 1. The Loss On Ignition (LOI) was determined by weight lost after melting at 1000 °C.

## 4. Results

### 4.1. Petrography and Mineralogy

The LB, in hand specimen, is melanocratic, holocrystalline, medium-grained, and porphyritic. Vesicles have an elongated and oval shape and show pahoehoe structure and fragmented ropy chilled surfaces. The flows exhibit uniform petrographical characteristics. Moreover, the main mineral constituents are plagioclase, olivine, pyroxene, and opaque minerals (mainly magnetite). The secondary minerals include iddingsite, calcite, sericite, and serpentine. Common textures occurring in the LB are intergranular, seriate, subpliotaxitic, glomeroporphyritic, ophitic, sub-ophitic, vesicular and amygdaloidal textures. The calculated CIPW-norm is listed in Table (2).

#### 4.1.1. Plagioclase

Plagioclase occurs in two generations as larger phenocrysts and as small tabular to elongated microlites in the groundmass. The phenocrysts are subhedral laths, from < 0.5 mm up to 6 mm in length and forming about 35-45 vol.% of the rock. The crystals are quite fresh and well developed; and show lamellar twinning. The extinction angles on several plagioclase phenocrysts range from 28° to 32°, indicating a labradorite composition (An50-An70) by using the method described by Michel-Levy's (Kerr, 1977). The crystals show intergranular, radiated and subpliotaxitic textures. Glomeroporphyritic texture is occasionally present with clusters of up to four crystals. Seritization is observed along borders and along cleavage planes of the crystals as yellow to turbid rims. Albitization of plagioclase is also recorded where Ca-plagioclase is converted to Na-plagioclase, a process caused by the instability of the Ca-plagioclase during weathering.

#### 4.1.2. Olivine

Olivine occurs as phenocrysts and in groundmass. It forms 10-16 vol. % of the rock. The phenocrysts are euhedral to subhedral. They are colourless to pale grey, and range between 0.08 mm and 5 mm in size, displaying seriate texture. Moreover, the crystals occur both as individuals and as glomeroporphyritic aggregates of more than six crystals. Olivine in the groundmass has subhedral to rounded shape. The larger crystals are fractured slightly-to-moderately. Iddingitization is common, particularly along fractures and along edges of the crystals. Some crystals are partially to completely pseudomorphed to dull brown iddingsite. Groundmass olivine is also iddingsitized.

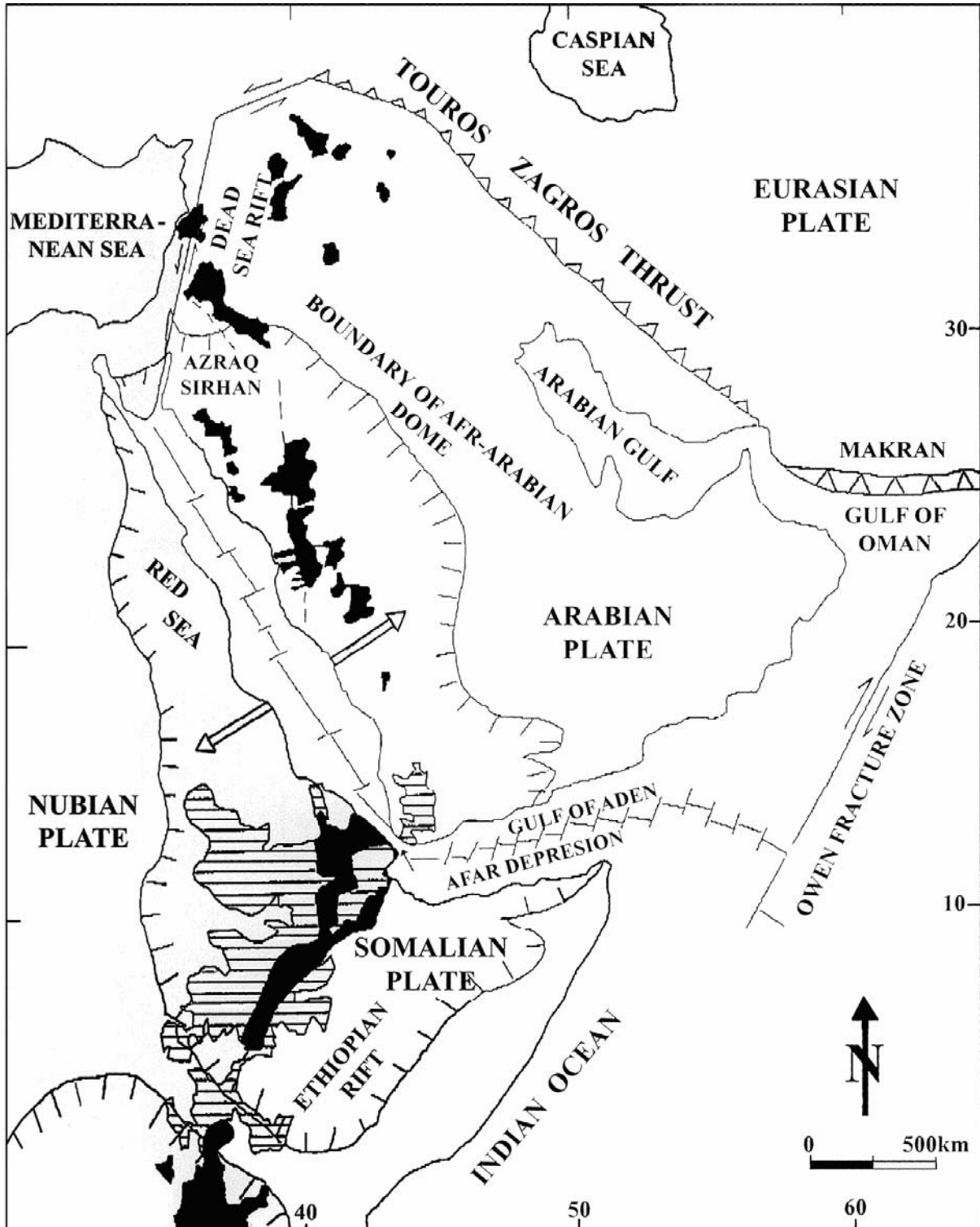


Figure 1: Regional tectonic map of the eastern Mediterranean region and the associated volcanic feature (After Al-Malabeh, 1993).

These alteration products are considered to be resulted because of relatively low-temperature deuteric alteration process, or the result of primary olivine oxidation. Due to embayment, Corroded outlines are noticed. Such embayments of olivine crystals were described by (Cox et al. 1979) as a result of interaction between melt and olivine crystals during the crystallization processes. The

LB has a normative olivine value that ranges from 14.13 to 19.04 wt %, and averages 15 wt%, which matches the value of modal olivine of 10-16 %. The normative nepheline content ranges between 3.17 and 12.87 wt% (Table 2), which allows classifying the rocks according to criteria of (Le Bas et al. 1986) as alkali olivine basalt and basanite(olv.>10%).

Table 1. Geochemical analytical results of El-Lajjoun basalt (LB), major oxides are in (wt%), trace elements are in (ppm).

Sample#	L1	L2	L3	L4	L5	L6	L7	L8	L9	L10	L11	L12
SiO <sub>2</sub>	45.16	43.63	45.01	43.11	45.12	46.52	46.61	45.22	46.34	45.17	45.26	43.85
TiO <sub>2</sub>	1.61	1.60	1.63	1.64	1.67	1.66	1.71	1.64	1.76	1.72	1.66	1.68
Al <sub>2</sub> O <sub>3</sub>	13.45	13.98	14.48	14.92	14.69	14.56	13.42	14.63	13.71	15.07	14.31	14.57
FeOt	12.81	12.68	12.99	12.01	12.12	12.17	11.92	12.11	12.52	12.29	12.46	12.56
MnO	0.16	0.16	0.16	0.16	0.16	0.16	0.17	0.16	0.18	0.16	0.16	0.16
MgO	8.87	8.16	8.78	8.46	8.66	8.84	7.87	8.54	8.30	7.66	8.52	8.41
CaO	11.40	12.94	11.23	12.01	11.98	12.14	11.27	11.78	10.46	11.02	10.68	11.62
Na <sub>2</sub> O	2.83	3.35	3.46	3.54	3.45	3.81	3.43	3.33	3.54	3.68	2.92	3.68
K <sub>2</sub> O	0.52	0.57	0.60	0.69	0.73	0.67	0.71	0.69	0.68	0.69	0.57	0.69
P <sub>2</sub> O <sub>5</sub>	0.27	0.26	0.28	0.30	0.29	0.27	0.23	0.31	0.33	0.29	0.41	0.38
LOI	2.68	2.85	2.87	2.14	2.56	1.89	2.01	1.84	1.97	2.13	2.78	2.03
Sum	99.56	99.29	100.20	99.73	99.85	99.62	99.55	100.2	99.74	99.88	99.73	99.63
Mg #	0.62	0.60	0.62	0.63	0.63	0.62	0.62	0.62	0.61	0.63	0.63	0.63
<b>Trace Elements ppm</b>												
Cr	303	319	316	317	320	323	318	234	343	306	291	374
Ni	231	215	230	225	233	227	239	271	265	211	193	214
Sc	21	17	21	23	20	28	22	27	19	21	23	28
Co	59	50	57	54	58	61	52	57	62	51	71	53
V	190	203	196	201	195	213	210	180	195	211	193	214
Sn	14	12	14	13	15	12	14	13	12	16	15	14
Pb	6	6	5	6	5	6	5	6	5	5	6	6
Mo	4	4	4	5	4	6	4	4	5	4	5	5
Sr	727	505	517	546	523	524	520	714	673	571	518	534
Rb	8	10	10	7	9	9	10	9	8	9	7	10
Ba	269	230	199	226	245	255	239	242	262	256	231	259
Zr	103	102	106	104	105	104	107	104	108	107	106	107
Nb	13	13	16	14	13	15	14	13	15	14	15	13
Y	16	17	18	21	20	16	16	20	18	17	17	19
Cr/Ni	1,31	1,48	1,37	1,41	1,37	1,42	1,33	0,86	1,29	1,45	1,5	1,75
Rb/Sr	0,011	0,019	0,019	0,012	0,017	0,017	0,019	0,012	0,012	0,0158	0,013	0,012
Zr/Nb	7,92	7,85	6,62	7,43	8,08	6,93	7,64	8	7,2	7,64	7,067	8,2331
Zr/Y	6,44	6	5,88	4,95	5,25	6,5	6,68	5,2	6	6,29	6,24	5,6347
Y/Nb	1,23	1,31	1,125	1,5	1,54	1,07	1,14	1,54	1,2	1,21	1,133	1,4662

Table 2. CIPW-Norms for El-Lajjoun Basalt (LB).

Sample#	L1	L2	L3	L4	L5	L6	L7	L8	L9	L10	L11	L12
Il	3.06	3.04	3.1	3.12	3.17	3.15	3.25	3.12	3.34	3.27	3.15	3.19
Ap	0.64	0.62	0.66	0.71	0.69	0.64	0.54	0.73	0.78	0.69	0.97	0.9
Or	3.07	3.37	3.55	4.08	4.31	3.96	4.2	4.08	4.02	4.08	3.37	4.08
Ab	14.99	5.85	12.79	6.19	10.48	11.82	18.39	12.21	19.58	14.71	18.86	8.96
An	25.44	21.43	22.21	22.78	22.44	20.65	19.12	22.93	19.51	22.56	24.26	21.2
Di	24.26	33.86	26.11	28.64	28.83	31.05	29.05	27.59	24.96	24.97	21.49	27.99
Mt	4.51	4.49	4.54	4.55	4.6	4.58	4.65	4.55	4.73	4.67	4.58	4.61
Ol	19.04	14.15	18.42	15.59	15.84	15.62	14.13	16.29	17.09	15.69	18.83	16.39
Ne	4.85	12.19	8.93	12.87	10.14	11.06	5.76	8.65	5.62	8.9	3.17	12.01

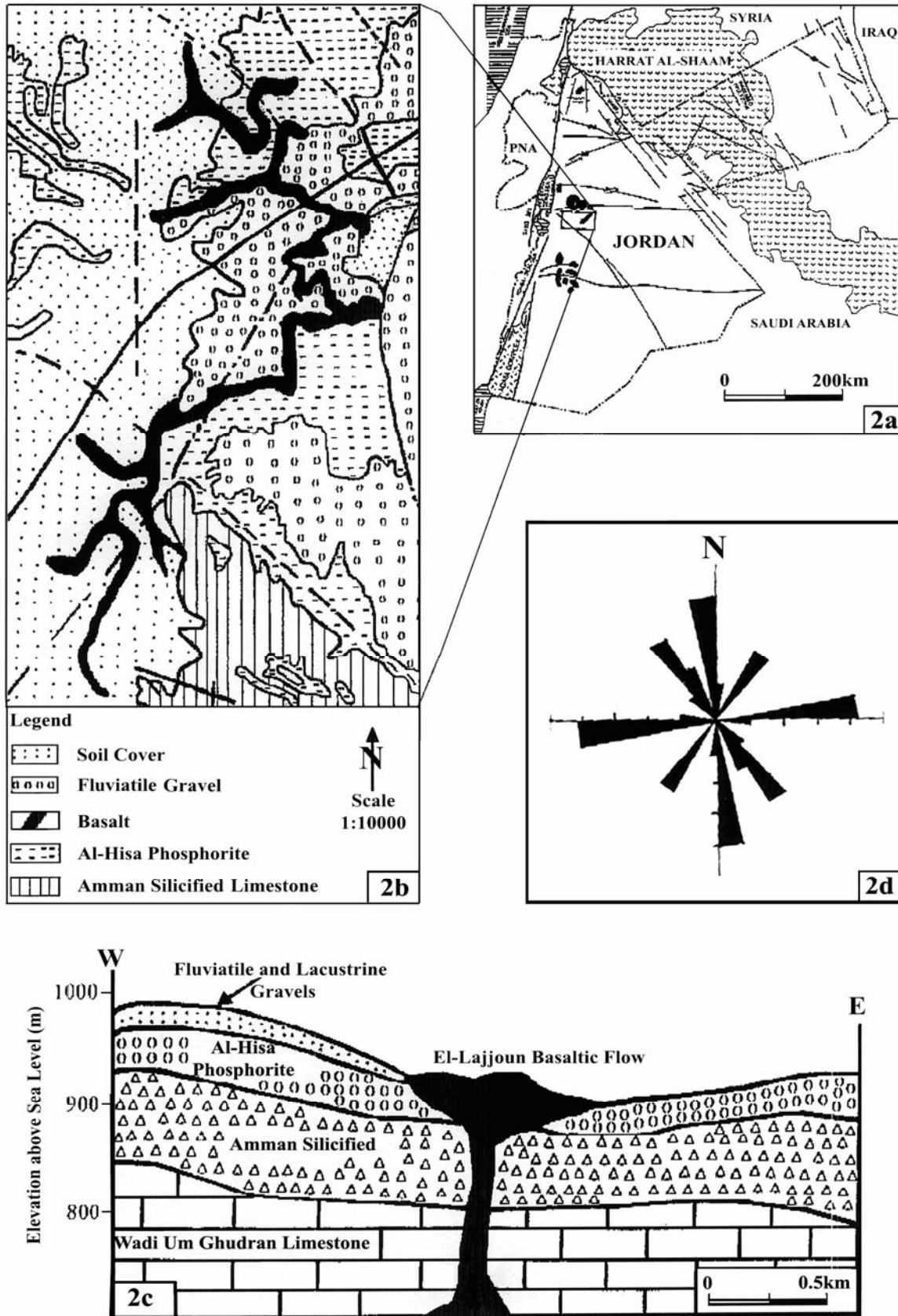


Figure 2: Generalized figure showing: a) Tectonic and volcanic map of Jordan showing the location of the El-Lajjoun basalt (modified after Barjous & Mikbel, 1990; Al-Malabeh, 1993; and Ibrahim, 1996), b) Geologic map of El-Lajjoun basalt and the surrounding area (modified after Al-Shawabkeh, 1991), c) Cross section shows the lithostratigraphy of El-Lajjoun area. d) Rose diagram depicting the orientation pattern of brittle deformation in El-Lajjoun area.

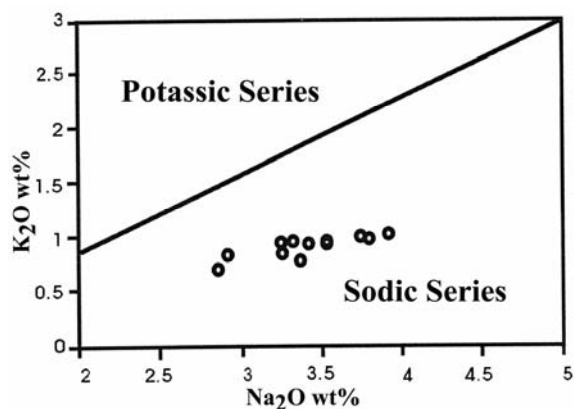


Figure 3: K<sub>2</sub>O vs. Na<sub>2</sub>O diagram showing the sodic affinity of the LB samples, (after Middlemost, 1975).

#### 4.1.3. Pyroxene

Pyroxene occurs as brownish anhedral crystals, forming about 10-15 vol. % of the rock. They show perfect cleavage parallel to [110], and cleavage intersects at ca. 90° in cross sections. The crystals have sizes between 0.3 to 2 mm. These grains exhibit moderately curved fractures. The pyroxene crystals have an inclined extinction of between 49° and 53°, indicating clinopyroxene of augite composition. Pyroxene crystals are affected by chloritization. Green chlorite is present along fractures and along crystal rims. Pyroxene interacts with plagioclase crystals yielding a sub-ophitic texture.

#### 4.1.4. Opaque Minerals

Opaque minerals are common in LB. Opaque minerals range in size from 0.03 mm to 4 mm, forming about 4-6 vol. % of the rock Table (2). They are mostly magnetite phenocrysts scattered throughout the rock and throughout inclusions within olivine and pyroxene crystals. Generally, magnetite is black; and shows homogeneous optical properties. Most of it is anhedral to subhedral, but crystals with square outline are also presented.

#### 4.1.5. Groundmass

The LB groundmass consists mainly of plagioclase (labradorite), olivine, pyroxene (augite), and opaque minerals (mainly magnetite). Iddingsite, gypsum and calcite are secondary minerals. However, no modal nepheline is recorded.

#### 4.1.6. Vesicles

LB shows spherical to ovoid and elongated vesicles. The long axis ranges from 0.1 to 5 mm. Most of the vesicles are empty, but some are filled with calcite and other secondary minerals (probably gypsum and zeolites). They form about 3-5 vol. % of the rock.

### 4.2. Rock Geochemistry

#### 4.2.1. Major oxides

The contents of major oxides are in weight percentage, and trace elements are in ppm, listed in Table (1). All samples are very similar in composition. This is evident from the very narrow ranges of major and trace element concentrations. This is mainly illustrated by the narrow range in silica content between 43.63 and 46.61 wt% with an average of 45.08 wt%. This content falls within the

averages reported for alkali olivine basalt and basanite by many authors (e.g. Barberi et al. 1979; Cebria and Lopez-Ruiz, 1995; Ibrahim and Al-Malabeh, 2006) and is demonstrated by the nomatiline nepheline.

The MgO content of LB ranges from 7.66 to 8.87 wt% with an average 8.42 wt%. The Mg-number (Mg#), which is defined by Jenner et al. 1987; and Downes et al. 1995, as the molecular proportion of Mg<sup>2+</sup>/(Mg<sup>2+</sup>+Fe<sup>2+</sup>) is usually used as a petrogenetic indicator for magma fractionation and its primitive nature. LB has a high Mg-number ranging between 0.60 and 0.63 with an average 0.62. For the purpose of Mg# calculations, the Fe<sub>2</sub>O<sub>3</sub> is considered to equal to TiO<sub>2</sub> + 1.5 (Irvine and Barager, 1971). Wedephol (1975) and Wilson (1989) reported that a value of (Mg#) > 0.7 as a threshold that characterizes primitive magmas while Clague and Ferry (1982) suggested a value of 0.65 as distinction value. Moreover, the total Fe-content of LB, calculated as FeO, ranges between 11.92 and 12.99 wt% with average 12.38 wt%. It reflects that the rock is enriched in iron. Shaw et al. (2003) suggested that SiO<sub>2</sub> under saturated magma with a high MgO > 7 wt% and high FeO > 11 wt%. All these are evidences for a smaller degree of partial melting at high pressures (i.e. a deep-seated mantle source).

LB has Na<sub>2</sub>O and K<sub>2</sub>O averages of 3.42 and 0.65 wt%, respectively. The total Na<sub>2</sub>O+K<sub>2</sub>O values are very similar throughout the samples amounting to 4.72 wt% on average. The average value of Na<sub>2</sub>O/K<sub>2</sub>O ratio is 5.82, reflecting the sodic affinity of the rock (Figure 3). Furthermore, the Al<sub>2</sub>O<sub>3</sub>/TiO<sub>2</sub> ratio average is 8.60 wt%, which indicates basic affinity of the rock.

#### 4.2.2. Trace Elements

The LB has relatively high Ni and Cr contents. Ni varies between 193 ppm and 271 ppm and averages 230 ppm. This may reflect that the LB has a limited olivine fractionation. Cr content ranges from 234 ppm to 374 ppm, and averages 313 ppm, with a Cr/Ni ratio about 0.074. The high content of Ni and Cr may also indicate that parental magma have been derived through partial melting of a peridotite mantle source (Wilson, 1989).

Rb content in LB is relatively low, ranging from 7 to 10 ppm and averages 8.8 ppm. This value is lower than the value of 22 ppm reported for alkali basalt by (Coleman and McGuire, 1988) and provides an argument against plagioclase fractionation. This was further supported by the high K/Rb ratio, which averages at 625. Sr content ranges from 505 to 727 with an average of 552.5 ppm. The LB has Zr content ranging from 102 to 108 ppm. Nb content ranges between 13 and 16 ppm. The average of Zr/Nb ratio is 7.5. The Y content is low and shows a very limited variation that ranges from 16 to 21 ppm, with an average Y/Nb ratio that equals 1.3. This ratio is consistent with the ratio of >1 reported by Pearce and Cann (1973) for the intra-continental alkali basalt.

## 5. Discussion and Conclusions

Several discriminatory diagrams were applied to help in the classification, nomenclature and interpretation of the tectonic setting of the LB. On the Middlemost et al. (1975) diagram, samples were plotted in the mildly alkali field (Figure 4). The Zr versus Y/Zr diagram of Pearce and

Norry (1979) illustrated the behavior of Zr and Y relative to the index of fractionation of three non-cumulate basalts settings. Here, LB samples fall within the intraplate basalt field with higher Zr/Y ratios than the MORB and Island Arc basalts (Figure 5).

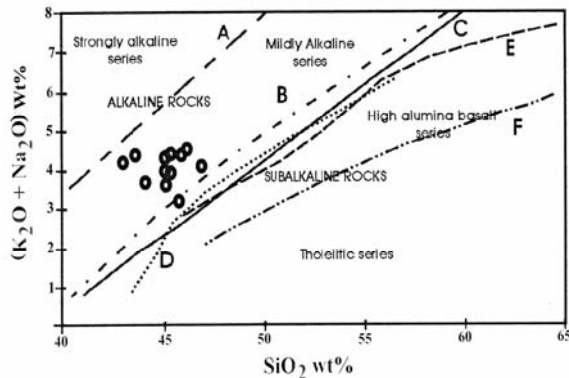


Figure 4: Total Alkali-silica diagram from LB. Dividers are A: Saggerson and Williams (1964), B: Irvine and Baragar (1971), C: Macdonald & Katsura (1964), D, E, F: Shwarzer & Roger (1974).

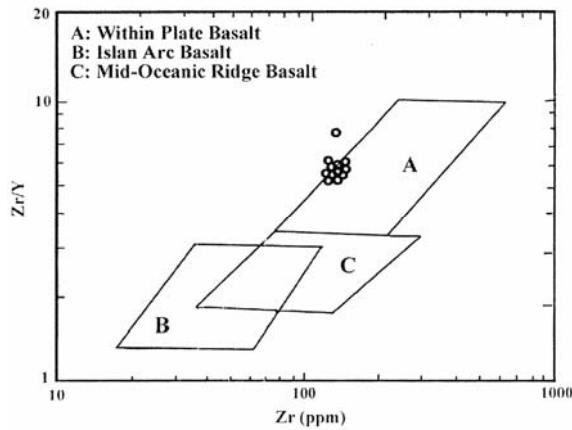


Figure 5: Zr-Zr/y diagram (Pearce & Norry, 1979) for the LB.

This is further supported by the ternary diagram of Pearce and Can (1973), which uses the Ti, Zr and Y to distinguish between island-arc tholeiites, MORB, calc-alkaline and intraplate basalts. On this diagram, all samples were plotted in the intraplate basalt field (Figure 6). Floyd and Winchester (1975) diagram is based on TiO<sub>2</sub> versus Y/Nb in order to distinguish between oceanic alkali basalt (OAB), continental alkali basalt (CAB), oceanic tholeiites (OTB) and continental tholeiites (CTB). LB samples fall on the CAB field (Figure 7) indicated also a continental intraplate tectonic setting. Moreover, the TAKTIP-diagram (K<sub>2</sub>O/total alkali versus TiO<sub>2</sub>/P<sub>2</sub>O<sub>5</sub> diagram) of (Chandrasekharam and Parthasarthy, 1978) is another helpful plot to discriminate intraplate basalt from rift volcanic. Here, LB samples fall in the field of rift volcanic (Figure 8).

One of the primary purposes of the present research is to study the kind of primitive nature of magma that gave rise to LB alkali olivine basalt. As mentioned previously, the low SiO<sub>2</sub> content (43.63 to 46.61 wt%), the high MgO content (mostly > 7 wt%) and the total FeO content (> 11 wt%) are distinctive criteria for the slightly fractionation nature of the LB. Moreover, they exhibit relatively high concentration of Cr (between 234 and 374 ppm) as

compared to values reported for relatively primary magmas (e.g. Hughes, (1982), a value of 142 ppm, Al-Malabeh, (1994), a value of 185). This is also a good geochemical indicator for slightly clino-pyroxene fractionation of LB magmas.

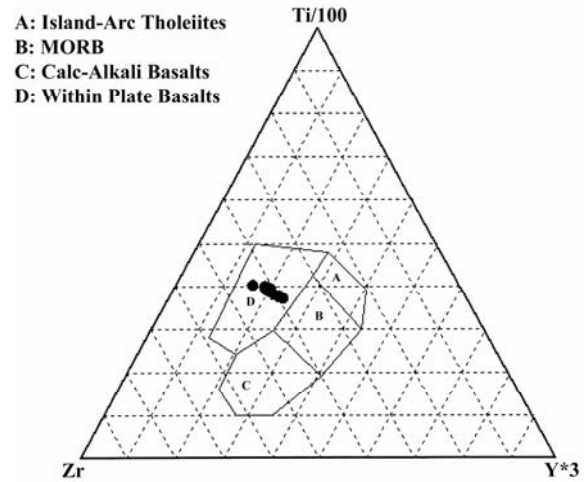


Figure 6: Ti-Zr-Y diagram (Pearce & Can, 1973) for the LB.

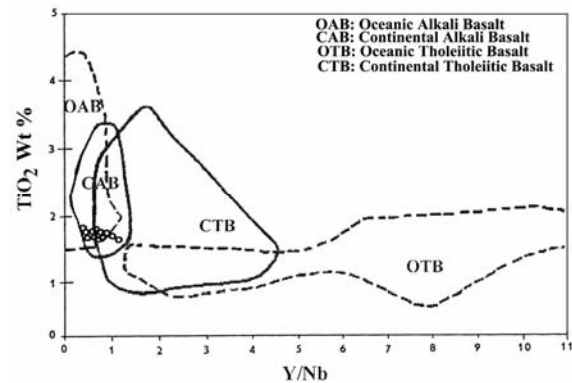


Figure 7: TiO<sub>2</sub>-Y/Nb diagram (Floyd and Winchester, 1975) for the LB.

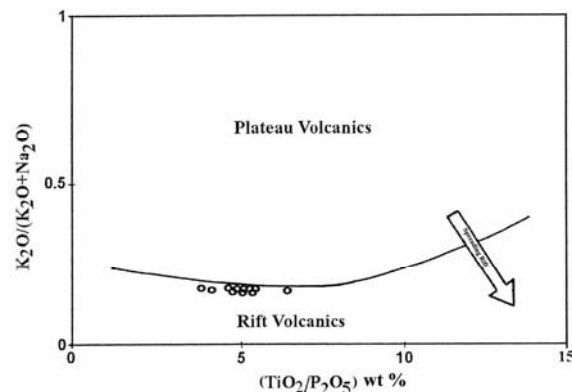


Figure 8: TAKTIP diagram-weight % K<sub>2</sub>O/total alkalis versus TiO<sub>2</sub>/P<sub>2</sub>O<sub>5</sub> (Chandasekharamand & Parthasarthy, 1978), with arrow due to Solyom et al. (1985) for the LB.

Trace element ratios such as Ba/Rb, Rb/Sr, K/Ba and K/Rb and the low Rb content exclude magma mixing and crustal contamination, and provide an evidence for a primitive homogeneous source (Clague and Ferry, 1982); and Cebria and Lobez-Ruiz, 1995). This result is further supported by the Sr-Zr plot after (Camp and Roobol, 1992), where all samples fall into a partial melting trend rather than suggesting plagioclase

fractionation (Figure 9). However, the limited variation may reflect slight plagioclase fractionation.

The degree of partial melting is quantified by the non-modal batch melting equation of (Shaw, 1970) as follows:

$$C_1 = C_0/D_0 + F(1 - P_1) \quad (1)$$

Where  $F$  is the melting degree,  $C_0$  and  $C_1$  are the concentrations of elements in the source and in the liquid, respectively.  $D_0$  and  $P_1$  are the bulk distribution coefficients of elements in the initial assemblage and for the minerals entering into the liquid, respectively. Using the mineral melt distribution coefficient model for Rb and Zr (Clague and Frey, 1982), these incompatible elements have very low  $D_0$  and  $P_1$  values, which are much smaller than the numerical values for partial melting (Camp and Roobol, 1989). In that case  $C_1/C_0 \approx 1/F$  and  $F = C_0/C_1$ , the  $F$  values are calculated using concentrations in a primordial mantle source ( $C_0$ ) of 11.2 and 0.64ppm for Zr and Rb, respectively. Using these parameters, the studied samples give partial melting degrees averaging around 10% (Rollinson, 1993). These values compare well with the previous published studies for the Jordanian and Arabian intraplate basalt (e.g. Camp and Roobol, 1989; Shaw et al. 2003; Al-Malabeh et al. 2002).

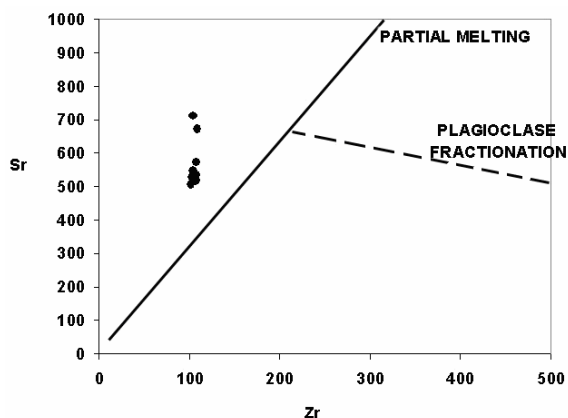


Figure 9: Plot of LB samples on Sr-Zr diagram (Camp & Roobol, 1989) showing the limited plagioclase fractionation.

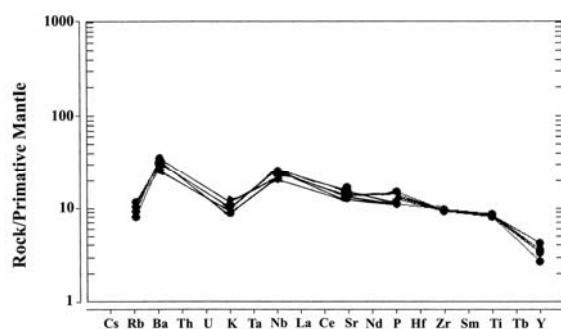


Figure 10: Spider diagram of incompatible elements from LB normalized to primitive mantle source. Elements are arranged in order of increasing incompatibility with mantle rocks.

Fundamental information regarding the nature of the inferred source origin can be obtained based on the heterogeneity of the major oxides and trace elements patterns that suggest that LB is most likely to be a result of partial melting of a relatively homogeneous mantle source. This is further supported by trace elements ratios such as

K/Ba, Ba/Rb and Zr/Nb (Peltz and Bratosin, 1986). As well the low and consistent Y content, the high Zr/Y and the  $TiO_2/Y$  ratios (Frey and Roy, 1978; and Downes et al. 1995) indicate that the sources are garnet rather than spinel bearing rocks. The normalized trace elements spider diagram of the rock/primitive mantle shows a positive Nb peak, which is a good indicator that LB is a product of the asthenospheric part of the mantle rather than the lithospheric part (Thompson, 1986; and Wilson, 1989) (Figure 10).

#### Acknowledgment

The authors would like to express their deep thanks to the staff of Geological Institute, University of Wuerzburg/Germany, for their help in analytical procedures. Also thanks are due to Prof. Dr. S. Kembe, University of Darmstadt / Germany for his valuable reviewing of the manuscript.

#### References

- [1] Al-Malabeh, A., 2003. Geochemistry and Volcanology of Jabal Al-Rufiyat, Strombolian Monogenic Volcano, Jordan, *Dirasat*, 30: 125-140.
- [2] Al-Malabeh, A., Al-Fugha, H., and El-Hasan, T., 2004. Petrology and Geochemistry of Late Precambrian magmatic rocks from southern Jordan, *N. JB. Palaent. Abh.*, 233 (3): 333-350.
- [3] Al-Malabeh, A., 1993. The volcanology, mineralogy and geochemistry of selected pyroclastic cones from NE-Jordan and their evaluation for possible industrial applications, Ph.D. thesis, Erlangen University, Germany.
- [4] Al-Malabeh, A., 1994. Geochemistry of two volcanic cones from the intra-continental plateau basalt of Harra El-Jabban, NE-Jordan, *Geochemical Journal*, 28:517-540.
- [5] Al-Malabeh, A., El-Hasan, T., Lataifeh, M., and O'Shea, M., 2002. Geochemical- and Mineralogical-Related Magnetic Characteristics of the Tertiary-Quaternary (Umm A-Qutein) Basaltic Flows from the Basaltic Field of Harra El-Jabban, Northeast Jordan, *Physica B-Physics of Condensed Matter*, Netherlands. 321 (1-4): 396-403.
- [6] Almond, D.C., 1986. The relation of Mesozoic magmatic volcanicity to tectonics in the Afro-Arabian Dome, *J. Volcanol. Geotherm Res.*, 28: 225-246.
- [7] Al-Shawabkeh, K., 1991. The geology of the Adir area. Unpublished report, NRA, Jordan.
- [8] Barberi, F., Borsi, S., Ferra, G., Marinelli, G., & Vareet, J., 1970. Relations between tectonics and magmatology in the northern Dankil depression (Ethiopia). *Philos. Trans. R. Soc. London*, 267: 293-311.
- [9] Barberi, F., Capaldi, G., Gasperini, P., Marinelli, G., Santacroce, R., Scandone, R., Treuil, M., Varet, J., 1979. Recent basaltic volcanism of Jordan and its implications on the geodynamic evolution of the Afro-Arabian rift system, *Accademia Nazionale Dei Lincei, Att Del Convegno Lincei*, 47, Rome, 667-83.
- [10] Barjous, M., and Mikbel, S., 1990. Tectonic evolution of the Gulf of Aqaba-Dea Sea transform fault. In: R. Kovach and Z. Ben Avraham (Eds.) *Geologic and tectonic processes of the Dead Sea Rift zone*, *Tectonophysics*, 180: 49-59.
- [11] Bender, F. (1974): *Geology of the Arabian peninsula*, Jordan. *US Geol. Surv. Prof. Paper*, 560-1, 36 p.
- [12] Bendor, Y., 1985. The crustal evolution of the Arabo-Nubian massif with special reference to the Sinai Peninsula, *Precamb. Res.*, 28: 1-74.

- [13] Burke, K., 1996. The African plate, *South African Journal of Geology*, 99: 341-409.
- [14] Camp, V., & Roobol, M., 1992. Upwelling asthenosphere beneath western Arabia and its regional implications, *Journal of Geophysical Research*, 97: 15255-15271.
- [15] Camp, V., Roobol, M., 1989. The Arabian continental alkali province: Part I Evolution of Harrat Rahat, Kingdom of Saudi Arabia, *Geological Society of America Bulletin*, 101: 71-95.
- [16] Cebria, J.; and Lopez-Ruiz, J., 1995. Alkali basalt and leucites in an extensional Intra plate setting: The Late Cenozoic Calatrava volcanic province (Central Spain), *Lothos*, 35: 27-46.
- [17] Chandrasekhar, D., and Parthasarthy, A., 1978. Geochemical and tectonic studies on the coastal and inland Deccan Trap volcanics and a model for the evolution of Deccan Trap volcanism, *N. JB. Mineral. Abh.*, 132:128-145.
- [18] Clague, D., Frey, F., 1982. Petrology and trace elements geochemistry of Honolulu volcanism: Implications for the ocean mantle below Hawaii, *Journal of Petrology*, 23: 447-504.
- [19] Coleman, R., and McGuire, A., 1988. Magma systems related to the Red Sea opening, *Tectonophysics*, 150:77-100.
- [20] Cox, K., Bell, J., and Pankhurst, R., 1979. The interpretation of igneous rocks, 4<sup>th</sup> in press., London.
- [21] Downes, H., and Seghedi, I., Szakacs, A., Dobosi, G., James, D., Vaselli, O., Rigby, I., Ingram, G., Rex, D. and Peckskay, Z., 1995. Petrology and geochemistry of Late Tertiary/Quaternary mafic alkali volcanism in Romania, *Lithos*, 35: 65-81.
- [22] Duffield, W. Mc Kee, E., El Salem, F., Feimeh, M., 1988. K-Ar ages, chemical composition and geothermal significance of Cenozoic basalt near the Jordan Rift, *Geothermics*, 17: 635-644.
- [23] Floyd, P., and Winchester, J., 1975. Magma type and tectonic setting discrimination using immobile elements. *Earth and Planetary discrimination using immobile elements*, *Earth and Planetary science letters*, 27: 211-218.
- [24] Frey, F., Green, D. and Roy, S., 1978. Integrated models of Basalt Petrogenesis: A study of Quartz tholeiites to olivine melilites from South Eastern Australia utilizing geochemical and experimental petrological data, *J. Petrol.*, 19: 463-513.
- [25] Garfunkel, Z., 1988. Relation between continental rifting and uplift: evidence from Suez rift and northern Red Sea, *Tectonophysics*, 150: 33-49.
- [26] Garfunkel, Z., 1989. Tectonic setting of Phanerozoic magmatism in Israel, *Isr. J. Earth Sci.*, 38: 51-74.
- [27] Hatcher, R. Zietz, I., Regan, R. and Abu-Ajammieh, M., 1981. Sinistral strike-slip motion on the Dead Sea rift: confirmation from new magnetic data, *Geology*, 9: 458-462
- [28] Heimbach, W., and Huseibeh, M., 1975. The geological and hydrogeological surveys in the area between the Hejaz Railway Qatrana-El Hasa and the eastern border of Jordan, Unpublished report and maps, NRA, Jordan.
- [29] Hughes, C., 1982. *Igneous petrology. Development in petrology.* Elsevier, New York.
- [30] Ibrahim, K. (1996): The regional geology of Al-Azraq area. NRA. Geol. Dir. Map Div. Bull. 36, P 67.
- [31] Ibrahim, K., and Al-Malabeh, A., 2006. Geochemistry and Volcanic Features of Harrat El Fahda, A young Volcanic Field in Northwest Arabia, Jordan. *Journal of Asian Sciences*. 127(2):127-154.
- [32] Ilani, S., Harlavan, Y., Tarawneh, K., Rabba, I., Weinberger, R., Ibrahim, K.M., Peltz, S., and Steinitz, G., 2001. New K-Ar ages of basalts from the Harrat Ash Shaam volcanic field in Jordan: implications for the span and duration of the upper mantle upwelling beneath the western Arabian plate, *Geology*, 29: 171-174.
- [33] Irvine, T., and Barager, W., 1971. A guide to the chemical classification of the common rocks, *Canadian Journal of Earth Science*, 8: 523-548.
- [34] Jenner, G., Gawood, P., Rautenschlein, M. and White, W., 1987. Composition of back-arc basin volcanics, Valufa ridge, Lau basin: evidence for a slab-derived component in their mantle source, *J. Volcanol. Geotherm. Res.*, 32: 209-222.
- [35] Kerr, P. (1977): *Optical Mineralogy.* John Wiley and Sons, New York.
- [36] Lataifeh, M., Al-Malabeh, A. and El-Hasan, T., 2002. Geochemical and Magnetic Investigations of El-Lajjoun Cenozoic Basaltic Rocks, Central Jordan, *Abhath Al-Yarmouk*, 11: 337-347.
- [37] Le Bas, M.J., Le Maitre, R.W., Streckeisen, A., Zanettin, B., 1986. A chemical classification of volcanic rocks based on the total alkalis-silica diagram, *Journal of Petrology*, 27: 745-750.
- [38] Macdonald, G., and Katsura, T., 1964. Chemical composition of Hawaiian lavas, *J. Petrol.*, 5: 82-133.
- [39] Middlemost, E., 1975. The basalt Clan., *Earth Sci. Rev.*, 11: 337-564.
- [40] Moffat, D., 1988. A volcanotectonic analysis of the Cenozoic continental basalts of northern Jordan: implications for hydrocarbon prospectively in the block B area, Unpubl. Report. University college of Swansen, Uk.
- [41] Pearce, J., and Cann, J. R., 1973. Tectonic setting of basic volcanic rocks determined using trace element analysis, *Earth Planet Sci. Lett.*, 19: 290-300.
- [42] Pearce, J., and Norry, M., 1979. Petrogenetic implications of Ti, Zr, Y, and Nb variations in volcanic rocks, *Contributions to Mineralogy and Petrology*, 69(1): 33-47.
- [43] Peltz, S., and Bratosin, W., 1986. New data on the geochemistry of the Quaternary basalts in Pensani mountains, D.S, *Inst. Geol. Geofiz.*, 71: 389-403.
- [44] Pick, R., Deniel, C., Coulon, C. Yirgu, G. and Marty, B., 1999. Isotopic and trace element signatures of Ethiopian flood basalts: evidence for plume-lithosphere interactions, *Geochimica et Cosmo-chimica Acta*, 63: 2263-2279.
- [45] Saffarini, G, Nassir, S., and Abed, A., 1985. A contribution to the petrology and geochemistry of the Quaternary-Neogene basalts of central Jordan, *Dirasat*, 12: 133-144.
- [46] Schwarzer R., and Rogers, J., 1974. A worldwide comparison of alkali olivine basalts and their differentiation trends, *Earth Plant. Sci. Lett.*, 23: 286-296.
- [47] Shaw, D.M., 1970. Development of the early continental crust, Part I. Use of trace elements distribution coefficient model for the proto-Archean crust, *Can. J. Earth. Sci.*, 9: 1577-1595.
- [48] Shaw, J., Baker, J., Menzies, M., Thirlwall, B., and Ibrahim, K., 2003. Petrogenesis of the largest intraplate volcanic field on the Arabian plate (Jordan): a mixed lithosphere-asthenosphere source activated by lithosphere extension, *J. Petrol.*, 44(9): 1657-1679.
- [49] Solyom, Z., Andreasson, P. Johansson, I., 1985. Petrochemistry of Late Proerozoic rift volcanism in Scandinavia, mafic dike swarms in constructive and abortive arms, *Intr. Conf. on Mafic Dyke Swarms*, Uni. Toronto Reindale Campus, Ont., Abstract book, Vol., p. 164-171.
- [50] Steinitz, G., and Bartov, Y., 1992. The Miocene-Pleistocene history of the Dead Sea segment of the Rift in light of K-Ar ages of basalts, *Isr. J. Earth Sci.*, 40: 199-208.
- [51] Stern, R., 1985. The Najed fault system, Saudi Arabia and Egypt. A late Precambrian rift system, *Tectonics.* 4: 497-511.
- [52] Thompson, R., 1986. Sources of basic magmas. *Nature*, 319: 448-449.
- [53] Rollinson, H., 1993. *Using Geochemical Data: Evaluation, Presentation, Interpretation.* Longman Scientific & Technical, Essex, pp352.

[54] Wilson, M., 1989. *Igneous petrogenesis, a global tectonic approach*. Unwin Hyman, London.

# Time Series Analysis of Air Pollution in Al-Hashimeya Town Zarqa, Jordan

G. Saffarini<sup>a</sup> and S. Odat<sup>b\*</sup>

<sup>a</sup> Faculty of geology and Environment, the University of Jordan, Jordan.

<sup>b</sup> Faculty of Education and Environment, Hail University, Saudi Arabia.

## Abstract

Different time series analysis of yearly air pollution at Al-Hashimeya Town, central of Jordan, has been performed in this study. Descriptive analysis showed different long-term variation of yearly air pollution. High persistence in yearly air pollution time series were identified using autocorrelation function. Autoregressive, integrated, and moving average (ARIMA) models were also calculated to predict future values of time series variable. It was found that time series analysis of Al -Hashimeya yearly air pollution data for the period 1992–2004 showed an overall decreasing trend in ambient air pollutants NO<sub>2</sub>, CO, H<sub>2</sub>S, NO and TSP. This is likely due to regulatory measures implemented by the government in the preceding 13 years. There was an increasing trend in PM<sub>10</sub>, NO<sub>x</sub> and Pb, whereas SO<sub>2</sub> did not change much.

© 2008 Jordan Journal of Earth and Environmental Sciences. All rights reserved

*Key words:* Air pollution, time series, ARIMA Autoregression, Autocorrelation

## 1. Introduction

Development and use of statistical and other quantitative methods in the environmental sciences have been a major communication between environmental scientists and statisticians (Hertzberg and Frew, 2003). In recent years, many statistical analyses have been used to study air pollution as a common problem in urban areas (Lee, 2002). The common descriptive statistical approach used for air quality measurement and modeling is rather limited as a method to understand behavior and variability of air quality (Voigt, 2004). Many investigators have used probability models to explain temporal distribution of air pollutants (Bencala and Seinfeld, 1979, Yee and Chen, 1997). Time series analysis is a useful tool for better understanding of cause and effect relationship in environmental pollution (Schwartz and Marcus, 1990, Salcedo *et al.*, 1999, Kyriakidis and Journal, 2001). The main aim of time series analysis is to describe movement history of a particular variable in time. Many authors have tried to detect changing behavior of air pollution through time using different techniques (Salcedo *et al.*, 1999, Hies *et al.*, 2000, Kocak *et al.*, 2000, among others). Many others have tried to relate air pollution to human health through time series analysis (Gouveia and Fletcher, 2000, Roberts, 2003, Touloumi *et al.*, 2004). Therefore, this study aims at extending time series analysis to give both qualitative and quantitative information about air pollution at Al -Hashimeya town, the most polluted city in Jordan, and to predict future concentrations of air pollutant.

## 2. Methodology

### 2.1. Study Site:

Al-Hashimeya area is located north of Zarqa city, 35 km northeast of Amman. It is bounded by Longitude 36° 04' to 39° 09' east and Latitude 32° 04' to 32 10 north (Figure 1). This town is the most polluted city in Jordan. The air pollution has resulted from many factories and companies in the vicinity. Potential air pollution sources include Jordan Oil Refinery, Khirbit Al-Samra Waste water treatment plant, and Al-Husseini Thermal Power station. These sources are called "Triange of Pollution". And each source has a different impact on air quality. Asemi-arid Mediterranean type climate is dominant in Al-Hashimeya town, which characterized by hot and dry weather conditions in summer and lack of rain in winter. The average annual rate of rainfall is 142 mm. Low precipitation rate worsens air quality in Al-Hashimeya, because rain is a natural process that help washing out soluble substances from the air (Shehadeh, Noaman, 1991).

### 2.2. Data Collection:

There have been several studies conducted by both Royal Scientific Society (RSS) and Ministry of Environment to monitor basic pollutants in the area, from 1992 to 2004 (Table1 and Figure1). Instruments installed in the monitoring sites samples ambient air continuously and analyze it automatically, (Table 2 illustrate the instruments).

\* Corresponding author.; [sa@hu.edu.jo](mailto:sa@hu.edu.jo).

Table1: Monitoring sites and their positions from pollution sources in Al-Hashimeya.

Monitoring sites	Distance and direction of station from pollution sources
IBN EL ANBARY SCHOOL	6 km south west from SWTP 0.5 km north from HTPS 1.5km east from JOR
UM SOLEH	3 km from Al Hashymia town
THERMAL PLANT	5.5km southwest from SWTP 0.5 km south /southeast from HTPS 2km southeast from JOR
ELEMENTARY SCHOOL	4 km west from SWTP
SECONDARY SCHOOL	1 km northeast from JOR
ELECTRICAL TRAINING CENTER	0.5 km south from HTPS
HASHIMYEH MUNICIPALITY	Main highway of Irbid- Al Hashymia-Azarqa
POLICE STATION/ZARQA	Main highway zarqa Amman
PROJECT SITE	2km south east from SWTP 2 km north from HTPS 2km northeast from JOR
E. SCHOOL/ KHERBEH	2 km from south east from SWTP 6.8 km from northeast HTPS 7 km northeast from JOR
UM SHURYK	2 km south /southwest from SWTP 2.5 km north from HTPS 3km from northeast JOR

Table 2 : Instruments and their uses.

Instruments	USES
Sulfure Dioxide Analyser UV-Flourescence	Analyses Sulfure Dioxide continously
Hydrogen Sulfide Analyser UV-Flourescence	Analyses Hydrogen Sulfide continously
Carbon Monoxide Analyser Non- Dispersive Infrared	Carbon Monoxide continously
High Volume Sampler with Selective PM10 Inlet, Gravimetric.	Collects PM10
Portable Calibrator Permeation Oven.	Calibrates instruments of pollutants measurement.
Wind Recorder Mechanical.	Measures wind direction and wind speed.

### 2.3. Preparing for the Data Analysis

We used the yearly mean concentration of seven criteria pollutants PM<sub>10</sub>, TSP, CO, NO<sub>x</sub>, SO<sub>2</sub>, H<sub>2</sub>S and Pb. The data were obtained from unpublished sources (RSS). Missing values were substituted. For example, if for a particular year the value was missing, then it was substituted by considering the average of the preceding and succeeding years. This was done to preserve seasonal patterning (as opposed to the effect of the procedure of substituting by the annual average.).

### 2.4. Time Series Analysis

In statistics, a time series is a sequence of data points measured typically at successive times, and spaced at (often uniform) time intervals. Three broad classes of partical importance for time series models can take many forms - these are Autoregressive (AR) models, integrated (I)models ,and moving average (MA) MODELS. It is generally referred to as an ARIMA (p,d,q) model where the p,d and q are integers greater than or equal to zero; and refer to the order of the Autoregressive, integrated, and moving average parts of the model respectively (Yee and Chen,1997).An ARMA (p,q) model is given by:

$$\left(1 - \sum_{i=1}^p \phi_i L^i\right) X_t = \left(1 + \sum_{i=1}^q \theta_i L^i\right) \varepsilon_t$$

Where L is the lag operator, the  $\phi_i$  are the parameters of the autoregressive part of the model ,the  $\theta_i$  are the parameters of the moving average part and the  $\varepsilon_t$  are error terms. The error terms  $\varepsilon_t$  are generally assumed to be variables sampeld from a normal distribution with zero mean:  $\varepsilon_t \sim N(0, \sigma^2)$  where  $\sigma^2$  is the variance (www.wikipedia.org).

### 2.5. Autocorrelation Correlogram

Seasonal patterns of time series can be examined via correlograms. The correlogram (autocorrelogram) displays the autocorrelation function (ACF) graphically and numerically - that is, serial correlation coefficients (and their standard errors) for consecutive lags in a specified range of lags (e.g., 1 through 30). Ranges of two standard errors for each lag are usually marked in correlograms, but typically the size of autocorrelation is of more interest than its reliability because we are usually interested only in very strong and thus highly significant autocorrelations.

### 2.6. Partial Autocorrelations:

Another useful method to examine serial dependencies is to examine partial autocorrelation function (PACF) - an extension of autocorrelation, where the dependence on the intermediate elements (those *within* the lag) is removed. In other words, partial autocorrelation is similar to autocorrelation, except that when calculating it, (auto) correlations with all the elements within the lag are partially out (Hay, 1980). If a lag of 1 is specified (i.e., there are no intermediate elements within the lag), then partial autocorrelation is equivalent to autocorrelation. In a sense, partial autocorrelation provides a "cleaner" picture of serial dependencies for individual lags (not confounded by other serial dependencies). (Sall and Lee 2001).

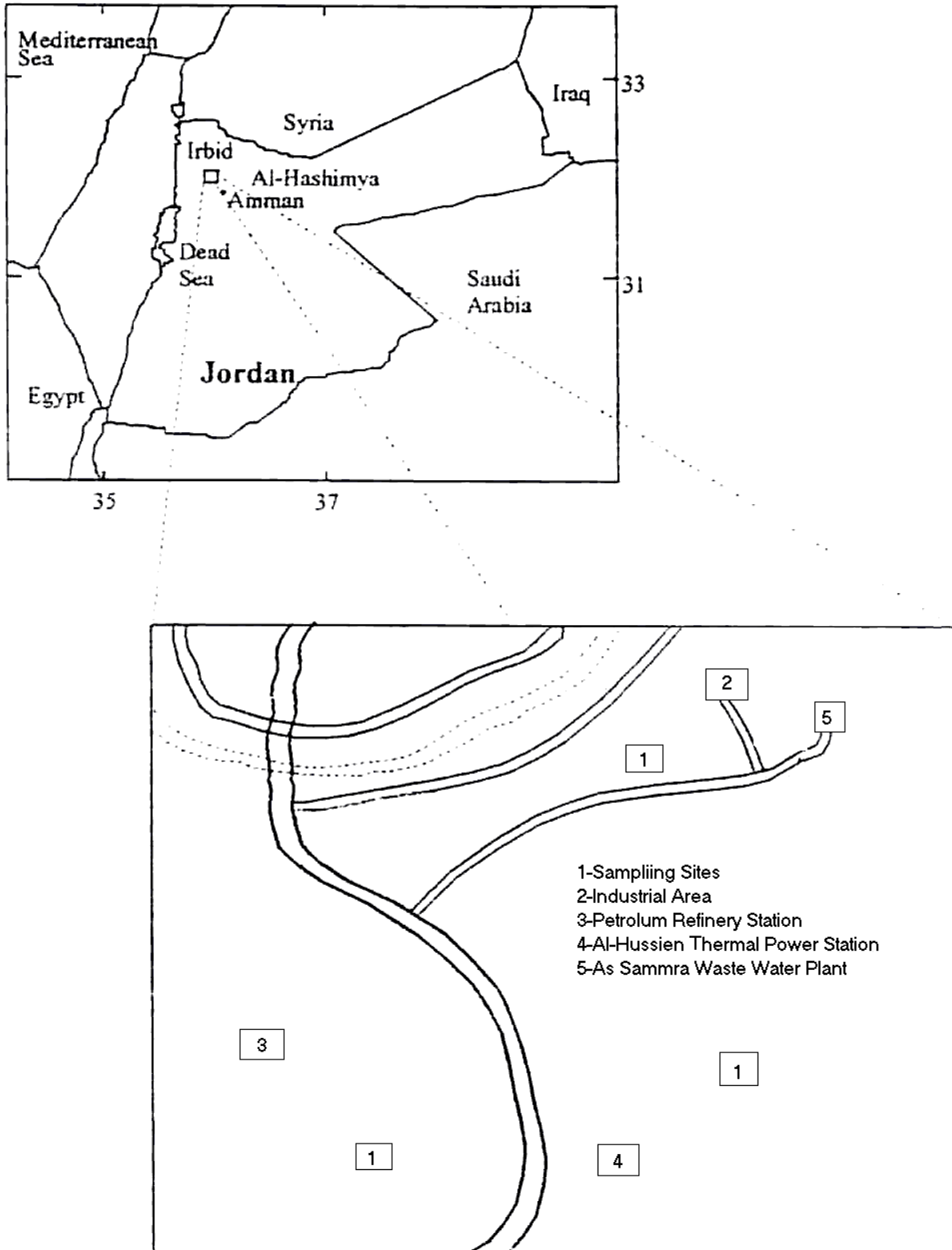


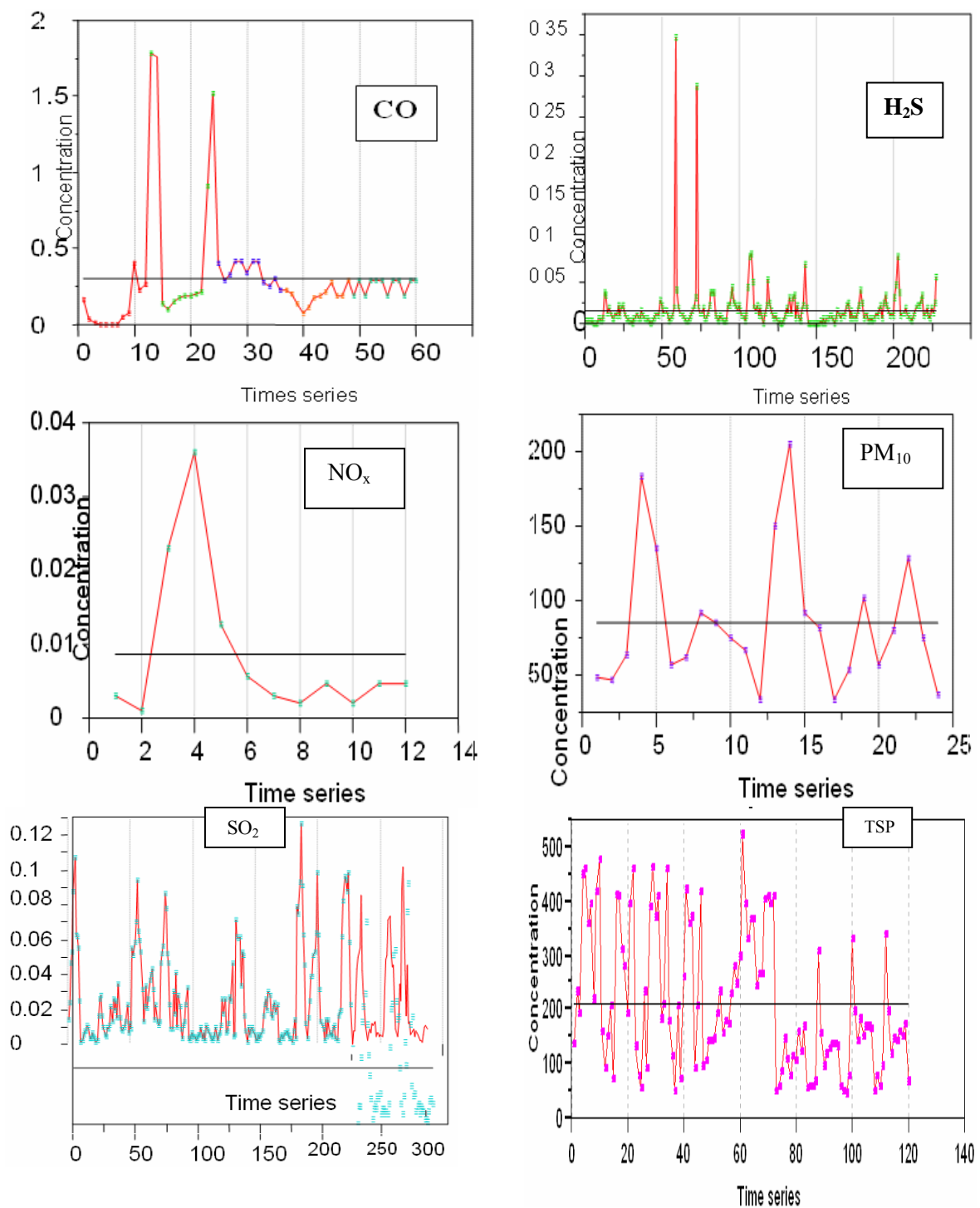
Figure 1: The locations of sampling sites

### 3. Results

#### 3.1. Time Series

The first step in time series analysis is to draw time series plot. Time series plot provide a preliminary understating of time behavior of the series. Figure2. shows time series plot of selected time series air pollution concentration. This Figure shows different time behavior of air pollutants. For example, the concentration of SO<sub>2</sub> and TSP seems to have a similar trend from the beginning to the end of the year, but maximum and minimum concentrations occur in different times.

It is also obvious that H<sub>2</sub>S and CO have not a significant trend through time. The fluctuations of Pb are more irregular at the end of the year, but the fluctuation of NO<sub>x</sub> and PM<sub>10</sub> are more obvious at the beginning of the year. The autocorrelation functions of the selected time series also show different time stationary of the series. The autocorrelation functions of them are presented in Figure 3. The significant models of ARMA lags for all selected pollutants are also presented in Table 3. all pollutants show non stationary (long serial correlation). The amplitude of autocorrelation functions does not become less pronounced for most of the series.



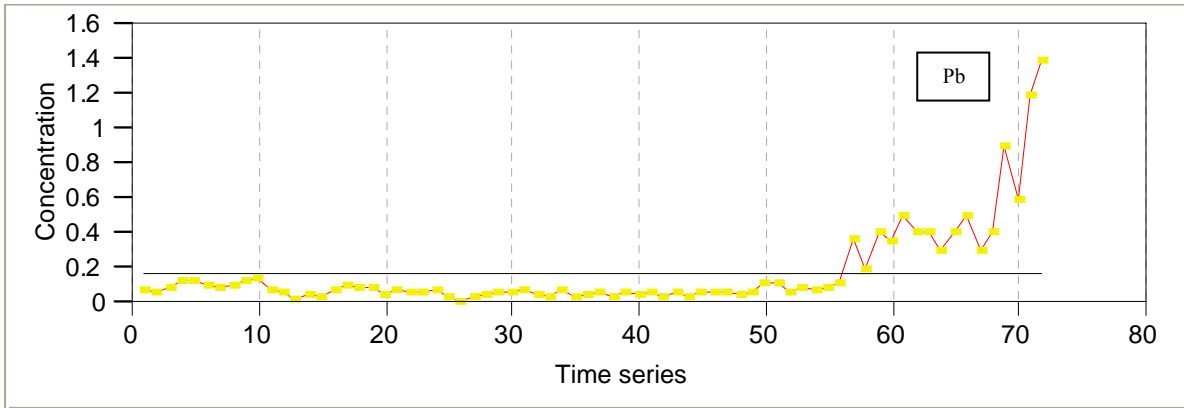


Figure 2: Time series plots of selected air pollutions.

Table 3: Models of ARMA (p, q) of pollutants concentrations.

Variables	-2LogLH	R <sup>2</sup>	SBC	AIC.	Variance.	DF	Model
PM10	161.73	0.55	201.10	186.96	888.96	12	ARMA (1, 10)
TSP	1055.75	0.57	1181.1741	1108.69	6673.02	94	ARMA (12, 13)
CO	-178.09	0.55	-74.05	-122.23	0.061	37	ARMA(11, 11)
NOx	-118.64	0.49	-99.11	-102.01	0.0000748	6	ARMA (1, 4)
SO <sub>2</sub>	-2456.72	0.70	-2376.71	-2424.33	0.0002018	275	ARMA(6, 6)
H <sub>2</sub> S	-1655.30	0.29	-1488.40	-1587.80	0.00073	199	ARMA (14, 14)
Pb	-349.08	0.89	-282.92	-319.34	0.0075984	56	ARMA(2, 13)

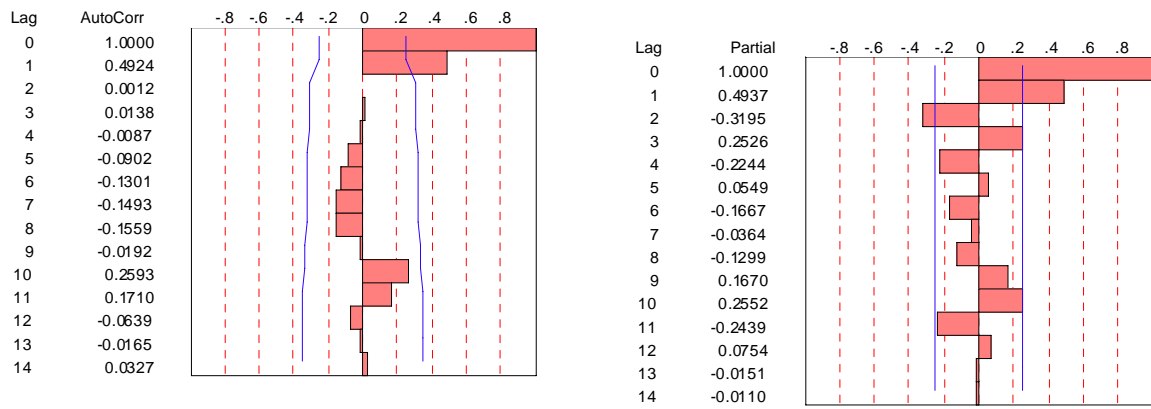


Figure 3a: Autocorrelation and partial auto correlation correlogram of CO.

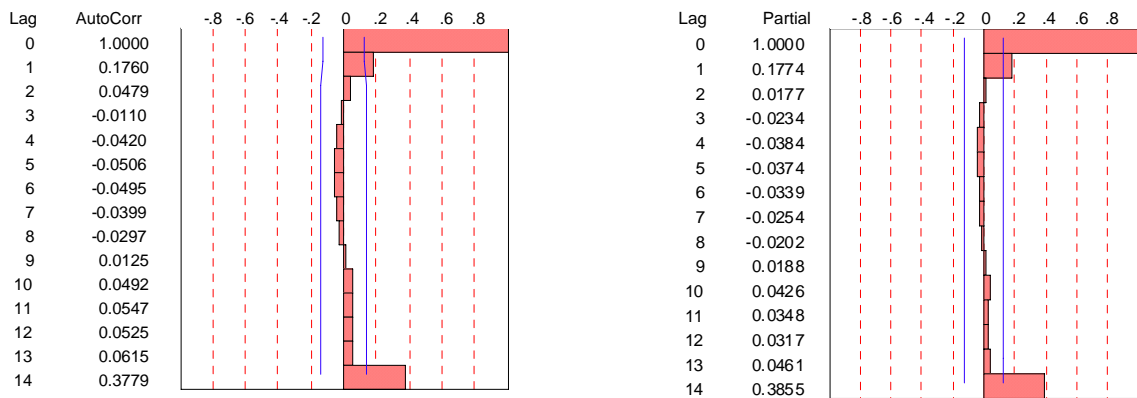


Figure 3b : Auto correlation and partial Auto correlation correlogram of H<sub>2</sub>S.

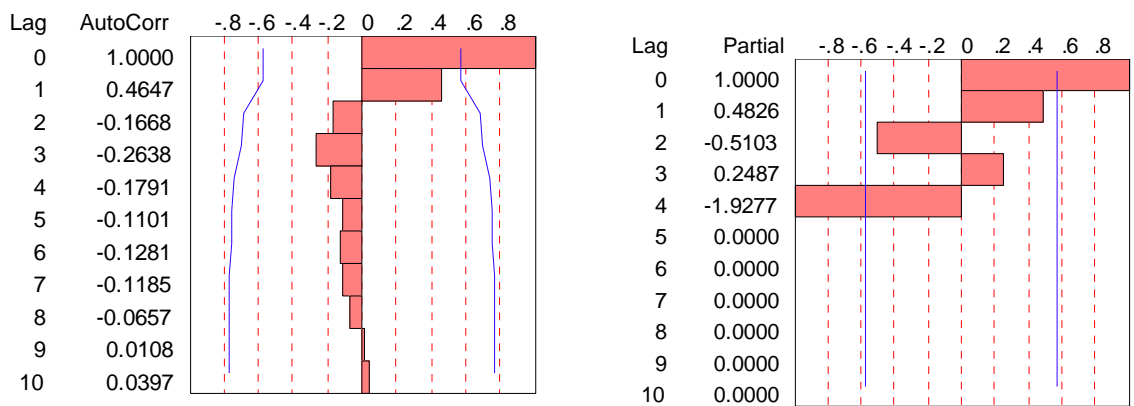


Figure 3c: Auto correlation and partial Auto correlation correlogram of NO<sub>x</sub>.

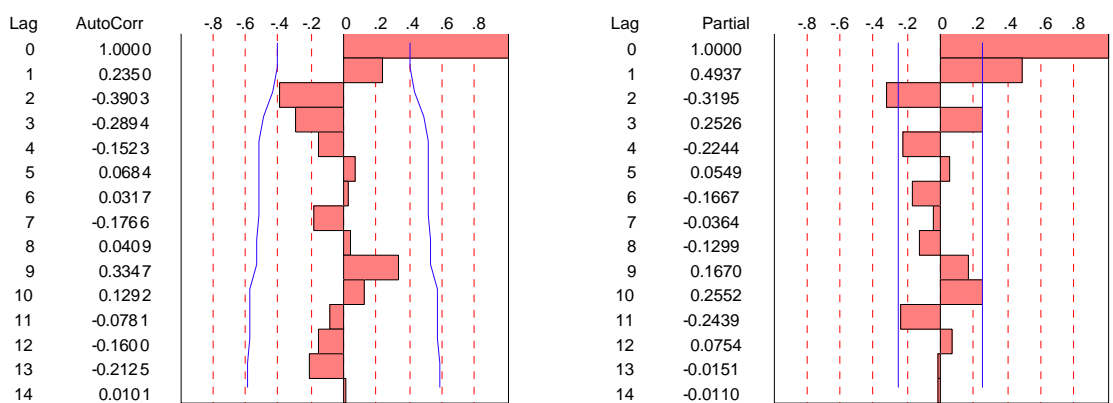


Figure 3d : Autocorrelation and partial Auto correlation correlogram of PM<sub>10</sub>.

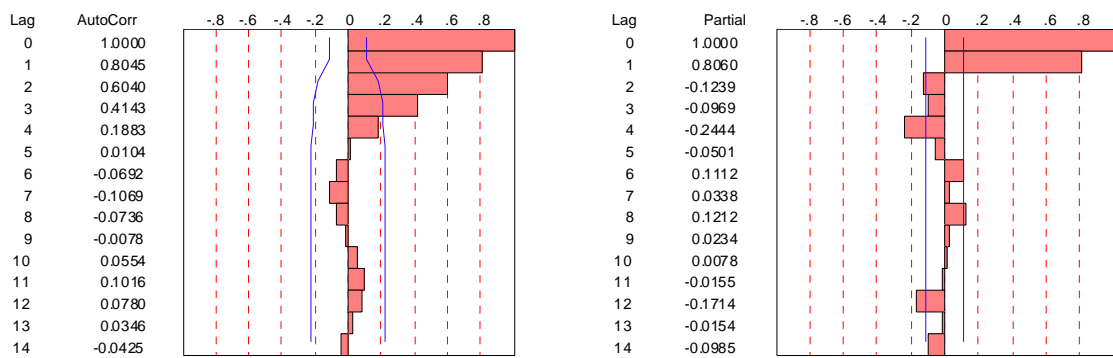


Figure 3e : Auto correlation and partial Auto correlation correlogram of SO<sub>2</sub>.

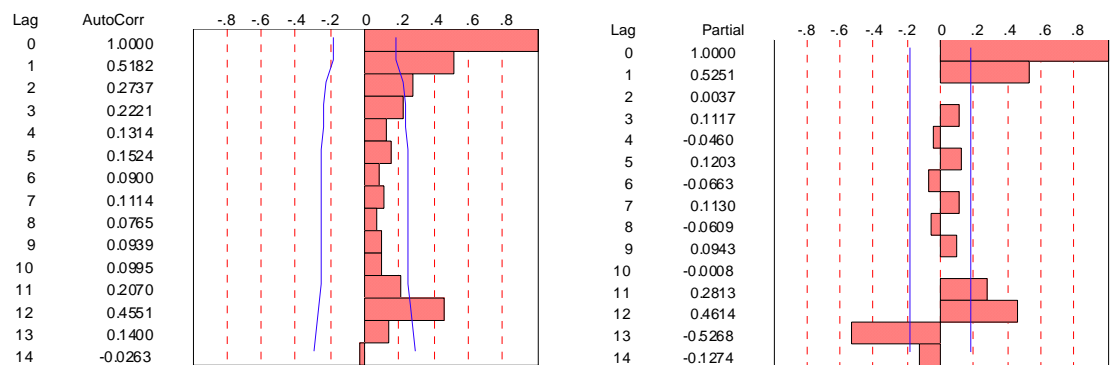


Figure 3f : Auto correlation and partial Auto correlation correlogram of TSP.

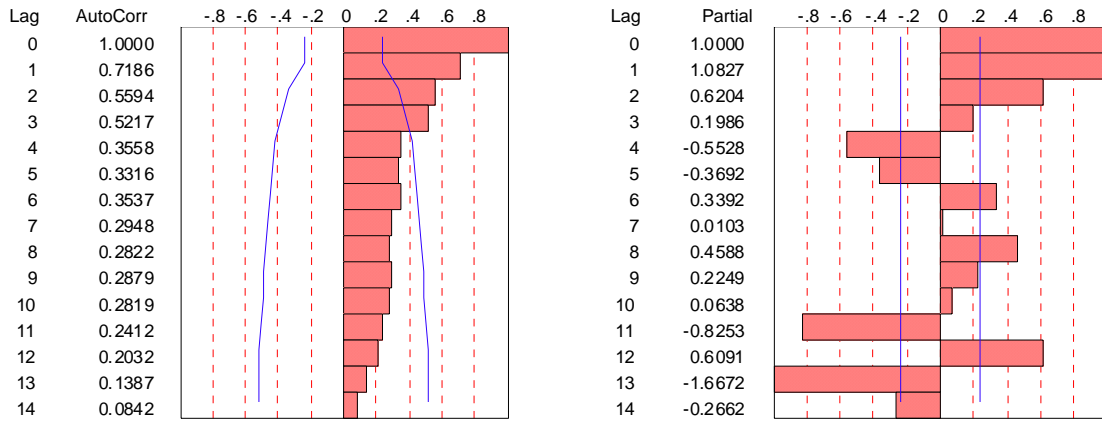


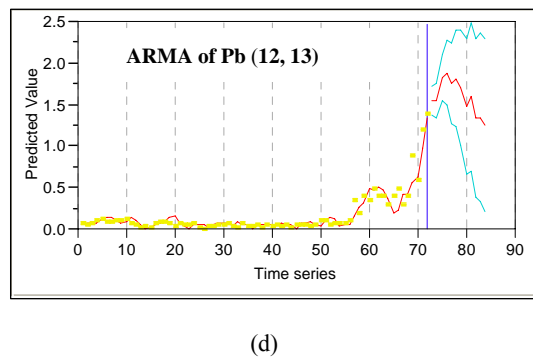
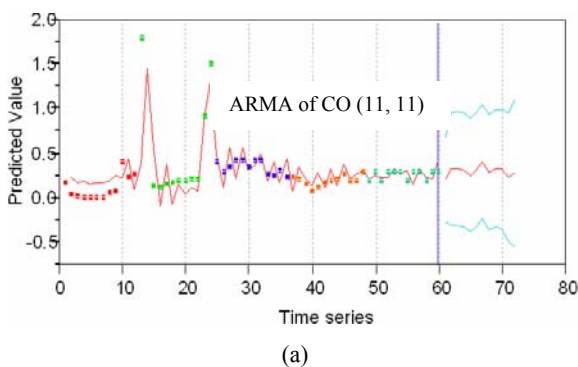
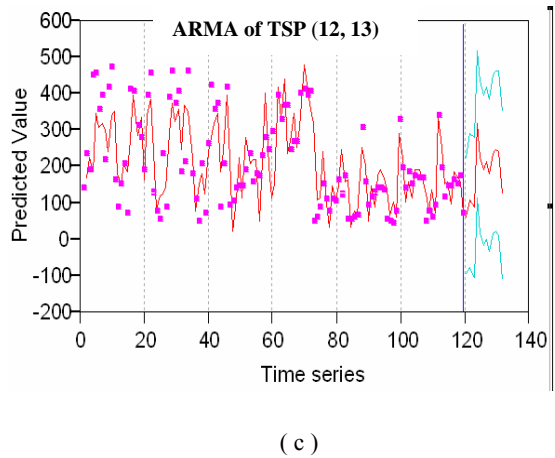
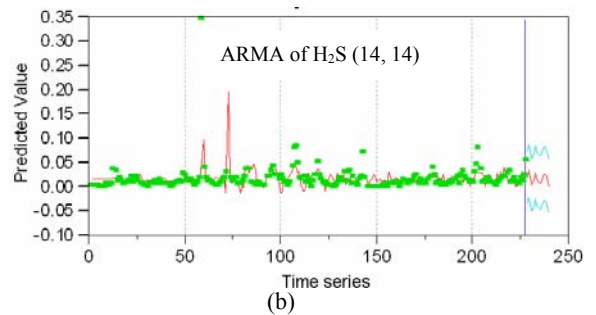
Figure 3g : Auto correlation and partial Auto correlation correlogram of Pb.

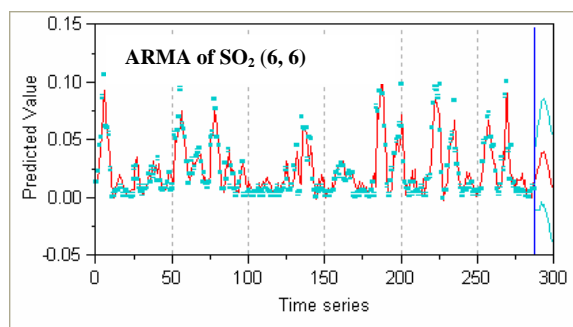
**4. Scenarios:**

Using an ARMA model calibrated on annual time scales, interannual monthly of pollutants were estimated for one year unit, 5 years, and 10 years, respectively, (Table 4). Time series models estimation for predicted yearly air pollutants data showed an overall decreasing trend in ambient air pollutants CO, H<sub>2</sub>S, and TSP, likely due to regulatory measures implemented by the government in the preceding 13 years. There was an increasing trend in PM<sub>10</sub>, NO<sub>x</sub> and Pb, whereas SO<sub>2</sub> did not change much.

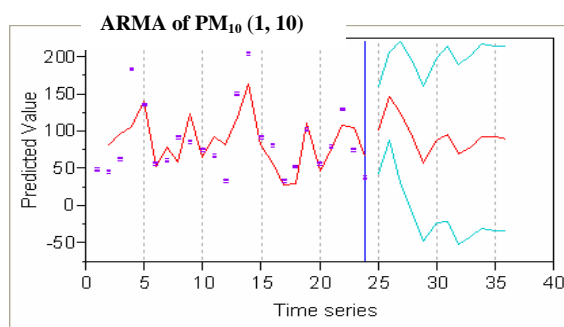
Table 4: The mean of actual and predicted concentration of pollutants for predicted one year, 5 years, and 10 years.

Pollutants	Actual Concentration	Predicted con. For 1 year	Predicted con. For 5 years	Predicted con. For 10 years
CO	0.308	0.306	0.303	0.302
H <sub>2</sub> S	0.0187	0.0186	0.0185	0.0184
NO <sub>x</sub>	0.0086	0.0087	0.0088	0.0088
SO <sub>2</sub>	0.024	0.0250	0.0248	0.0249
PM <sub>10</sub>	85.9	89.3	89.6	89.7
TSP	214.5	211.4	209.5	209.6
Pb	0.173	0.376	0.529	0.524





(e)



(f)

Figure 4: Forecast for Model of ARMA (q,p) of pollutants concentrations.

## 5. Discussion

Annual air pollution time series analysis of Al-Hashimeya area has been performed in this study; and has shown different temporal behavior of different air pollutants. This different time behavior is not only the reason of correlation of different pollutants with each other, but the seasonal variation on increasing or decreasing air pollutants as well. It was also shown that most annual air pollution time series have high persistence of air pollution conditions through time. This persistence is not only harmful for public health but also makes air pollution management and control very demanding.

The best fitted model of  $\text{SO}_2$  concentration at 95% CIs were given for the current ARMA (6,6). This ARMA model shows the smallest AIC, SBC, Variance and DF values, and largest value of  $R^2$  with a significant parameters. Time-series analysis showed that  $\text{SO}_2$  does not change through the predicted years at all. The best fitted model of  $\text{H}_2\text{S}$ , TSP and CO concentrations were given for the current ARMA (14,14) ARMA (12,13) and ARMA (11, 11), respectively. Time-series analysis has shown decreasing trend in the predicted years for these pollutants.

## 6. Conclusion

Results have shown that pollution becomes more elastic to the inter-annual perturbations over time at Al-Hashimeya area. Furthermore, it has also shown that forecasted pollution could be identified with the help of ARIMA analysis. Time series analysis of Al-Hashimeya annual air pollution data for the period 1992–2004 showed an overall decreasing trend in ambient air pollutant for TSP. This is likely attributable to regulatory measures implemented by the government in the preceding 13 years. There was an increasing trend in  $\text{PM}_{10}$ ,  $\text{NO}_x$  and Pb,

## 7. Acknowledgments

We thank the Royal Scientific Society and the Ministry of Environment for providing us with the data used in this study.

## References

- [1] Bencala, K.E., and Seinfeld, J.H., 1979. On frequency distribution of air pollutant concentrations. *Atmos. Environ.*, 10:941-950.

- [2] Brockwell, P.J., and Davis, R.A., 2001. *Introduction to Time Series and Forecasting*. Springer-Verlag, New York.
- [3] Gouveia, N., and Fletcher T., 2000. Time series analysis of air pollution and mortality: Effects by cause, age and socioeconomic status. *J. Epidemiol. Commun. H.*, 54:750-755.
- [4] Hertzberg, A.M., and Frew, L., 2003. Can public policy be influenced. *Environmetrics*, 14: 1-10.
- [5] Hies, T., Treffeisen R., Sebald L., and Reimer E., 2003. Spectral analysis of air pollutants. Part I: elemental carbon time series. *Atmospheric Environment*, 34:3495-3502.
- [6] Kocak K., Saylan L., and Sen O., 2000. Nonlinear time series prediction of  $\text{O}_3$  concentration in Istanbul. *Atmospheric Environment*, 34:1267-1271.
- [7] Kyriakidis, P.C., and Journal, A.G., 2001. Stochastic modeling of atmospheric pollution: a special time series framework. Part II: application to monitoring monthly sulfate deposition over Europe. *Atmos. Environ.*, 35:2339-2348.
- [8] Lee, C. K., 2002. Multiracial characteristics in air pollutant concentration time series. *Water Air Soil Poll.*, 135: 389-409.
- [9] Roberts, S., 2003. Combining data from multiple monitors in air pollution mortality time series studies. *Atmos. Environ.*, 37:3317-3322.
- [10] Sall J., Lehman A., and Lee Creighton. (2001). *JMP Start Statistics, Using JMP and JMP IN Software*. Copyright: 2001 by SAS Institute Inc. Duxbury Thomson LEARNING.
- [11] Salcedo R.L.R., Alvim Ferraz M., Alves C., and Martins F., 1999. Time series analysis of air pollution data. *Atmos Environ.*, 33:2361-2372.
- [12] Schwartz J., and Marcus A., 1990. Mortality and air pollution in London: a time series analysis. *Am. J. Epidemiol.*, 131:85-194.
- [13] Smith, R.L., 1998. Extreme value analysis of environmental time series: an application to trend detection in ground-level ozone. *Statistical Science* 4:367-383.
- [14] Touloumi, G., Atkinson R., and Terte A.L., 2004. Analysis of health outcome time series data in epidemiological studies. *Environmetrics*, 15:101-117.
- [15] Voigt, K., Welzl G., and Bruggemann, R., 2004. Data analysis of environmental air pollutant monitoring.
- [16] [http://en.wikipedia.org/wiki/Autoregressive\\_integrated\\_moving\\_average](http://en.wikipedia.org/wiki/Autoregressive_integrated_moving_average) (cited 24 March 2008).

- [17] Yee E., and Chen, R., 1997. A simple model for the probability density functions of concentration fluctuations in atmospheric plumes. *Atmos. Environ.*, 31:991-1002



# Analyzing Correlation Coefficients of the Concentrations of Trace Elements in Urinary Stones

Iyad Ahmed Abboud\*

*Mineralogy and Geochemistry, Institute of Earth and Environmental Sciences, Al al-Bayt University, Al-Mafraq, Jordan.*

## Abstract

The present study aims at deducing correlation coefficients between concentrations of trace elements and their metals, and determining the most important geochemical and environmental factors contributing to the formation of urinary stones. The researcher distributed 460 questionnaires to patients in different hospitals in Jordan, 282 of which were retrieved yielding a percentage of 61.3%. Seven groups were identified by using XRD namely calcium oxalate, oxalate/apatite, struvite/apatite, oxalate/uric acid, cholesterol, uric acid, and cystine. Urinary stones have been distributed as follows; gallbladder 65.3%, kidney 25.2%, ureter 8.1%, and bladder 1.4%. Males are found more likely to be infected with lithiasis about 51.1% with an average age of 50 years at (44.3%). Married people of both sexes make up to 87.2% of people infected. People with lower income (<100 JDs) are more likely to be infected with the disease by 46.9%; stones formation correlates inversely with socio-economic status. The daily amount of water a patient drinks ranges from 1 to 1.5 liters (40.4% of daily need) leading to high concentration of the nucleus of salts and formation of stones. The weekly average consumption of meat by patients was low (0-2 meals by 64.5%). It is obvious that eating more meat, green leaves, in addition to taking large quantities of milk, eggs, and dairy participate to the increase of calcium and phosphorous in the body leading to the formation of urinary stones that are made up of oxalate or phosphate.

© 2008 Jordan Journal of Earth and Environmental Sciences. All rights reserved

*Keywords:* Medical Geochemistry, Urinary Stones, Kidney Stones, Gallbladder Stones.

## 1. Introduction

Urinary stones are one of the most widespread diseases in the world (Marshall and Ryall, 1981). In Jordan, however, over 40% of urinary disease cases are urinary stones (Malki, 2000; Al-Fawaz, 2006). It increases in people older than 30 years old (Scott, 1985; Mhailan, 1992; Malki, 2000). Its proportion in males is higher than in females (Malki, 2000; Al-Fawaz, 2006). Recent studies have attempted to explain its spread by exploring the reasons behind forming stones in the human body and explaining the environmental factors that play a major role in its creation.

More than 40 chemical elements in the human body affect the biological processes related to the health of body. These elements have different concentrations and functions. For example, a small presence of some trace elements negatively affects the biological processes in the body. Recently, attention has been paid to studying the concentration of trace elements in the body and their effects on such processes (Wandt and Underhill, 1988). These elements are often present in the body as contaminations (Feinendegen and Kasperek, 1980) and not as major constituents.

Hammarsten (1929) determined the effect of some trace elements on patients in forming urinary stones. Concentration of Co, Mg, and Ni affects Ca in the human body through the increase of dissolution of crystallized calcium oxalate stones. Meyer and Angino (1977) determined many of trace elements ions affecting the crystallization of urinary stones especially oxalate and phosphate stones. Furthermore, Levinson *et al.*, (1978) explained the effect of some trace elements on the dissolution and the crystallization of urinary stones.

Many studies try to put an account for the problem of urinary stones and its relation to the environmental and pathological factors. These studies also attempted to determine the mineralogical and chemical composition of stones (Abboud, 2008b). Joost and Tessadri (1987) indicated that the presence of stones in the human body is an old phenomenon, and apatite has been the first mineral to be discovered. Meyer and Angino (1977) have studied the role of trace elements in the growth of calcium oxalate and calcium phosphate. Donev *et al.*, (1977) explained that amount of some of heavy metals found in stones are higher than the amount found in the ordinary blood. However, Levinson *et al.*, (1978) studied concentration of some trace elements in the kidney, and found many of the concentrated elements in the oxalate stones. Furthermore, Wandt and Pougnet (1986); Joost and Tessadri (1987); Durak *et al.*, (1988); Wandt and Underhill (1988); Al-Maliki (1998); Al-Fawaz (2006); Abboud (2008a), among others conducted studies attempting to determine concentrations of heavy and trace elements. They tried to

\* Corresponding author.; iyad.abboud@yahoo.com

relate them to geochemical, environmental, and health factors. However, statistical studies have not dealt with the percentage of the spread of urinary stones and linking them to environmental factors.

Reviewing the medical records of those who went to the department of abdominal disease and surgery in Jordanian hospitals in the last 10 years, It was noticed that a great number of people suffer from urinary stones (ureter, bladder, kidney, and gallbladder). Also the number of people who check in the above-mentioned departments increases in summer.

Recently, statistical studies of geological and environmental information have become very important, and have developed applications. This study has been conducted by designing a questionnaire requesting some information and many specific questions. Some factors and the main reasons that play an important part in creating urinary stones have been predicted. Many medical and chemical analyses have been performed to 100 urinary stones collected using X-Ray fluorescence to determine their chemical constituents. X-ray diffraction has also been used to determine their minerals and organic constituents. Then results have been discussed by finding out relationships between such elements and their minerals.

## 2. Methodology of the Study

This study focuses on patients suffering from urinary stones who checked into Al-Basheer, Al-Zarqa, Al-Mafraq, King Abdullah, and Princess Basma hospitals from 1/5/2001 until 31/12/2005. The present study is based on the computerized records of patients who checked in the above mentioned hospitals during the study. The computerized data has been ordered and categorized based on the type of the questionnaire. One hundred urinary stones have been collected from both males and females of all ages. The stones have been stored in polyethylene bottles. The organic materials have been removed by  $H_2O_2$ , then dried, after that grinded, and finally made into a homogeneous mix. XRD was used for mineralogical and organic constituents, and XRF was used to determine the major and trace elements of the metals of such stones. The correlation coefficients between the elements and the minerals have been calculated using SPSS software. Finally, the study explained the environmental and health factors that play an important role in creating the urinary stones in humans and their affect on human health.

A statistical questionnaire was designed and distributed to patients. The questionnaire contained a mechanism of distributing stones in the body according to age, sex, weight, nutrition culture, and other variables related to the concentration and distribution of such stones. Next, distribution, concentration, and percentages of each point mentioned in the questionnaire have been calculated. Then, the SPSS was used to examine data in order to determine the effect of each factor.

## 3. Results and Discussion of the Mineralogical and Chemical Analysis

Two hundred eighty two urinary stones have been collected of which the mineralogy of 100 samples have been determined. The samples have been distributed to 7

mineral and organic families (Table 1). As shown in Table 2, the researcher depends on both positive and negative variables to explain relations.

Table 1: Composition percentage of investigated urinary stones analysis by X-ray diffraction collected from adult patients.

Components: Sample type, XRD	No. and % of Stones & No. of Patients
1- Oxalate Stones:	22
a. Calcium Carbonate Oxalate hydrate + Whewellite	5
b. Calcium Oxalate: Weddellite + Whewellite	10
c. Calcium Oxalate: Whewellite	7
2- Oxalate/Phosphate Stones:	17
a. Oxalate/Apatite	
3- Phosphate Stones:	20
a. Struvite /Apatite	
4- Oxalate/Uric Acid Stones:	25
a. Calcium Oxalate (Whewellite)/Uric Acid	14
b. Oxalate/Uric Acid	11
5- Cholesten Stones:	6
a. Cholesten/ Oxalate /Uric Acid	4
b. Cholesten/ Oxalate /Uric Acid/Phosphate	2
6- Urate (Uric Acid) Stones:	7
a. Uric Acid/Uricite	
7- Cystine Stones:	3
a. Cystine	1
b. Cystine /Cholesten /Phosphate	2
	100 %

Table 2 shows that Ca has a strong positive correlation with whewellite and weddellite minerals in the urinary stones. This is because Ca is the fundamental element of whewellite and weddellite which form calcium oxalate. The high percentage of Ca in urinary stones is due to eating foods rich with Ca such as red meat and green leaves, in addition to eggs and milk. Another reason is drinking so much hard water that contains ions of  $Ca^{2+}$ . This is due to extraction of proud water from carbonate aquifers.

Table 2 shows the relationship between Sr and Zn ( $r=0.88$ ). Sr competes with Ca to enter the crystals of whewellite, weddellite, vaterite minerals ( $CaCO_3$ ), and in apatite (Wandt and Underhill, 1988 in Sobel *et al.*, 1949). Sr resembles Ca and processes of metabolism, and accompanies it with the precipitated salt in the urine. Sr's mechanism of exchange with Ca increases intake in crystal structure when its percent increases (Neuman and Neuman, 1953). The positive correlation between apatite content and Sr ( $r=0.89$ ), and between P and Sr ( $r=0.84$ ) in oxalate/apatite stones supports that Sr doesn't play an important role in forming urinary stones in the body (Wandt and Underhill, 1988).

Zn accumulations with apatite supports the relationship between Zn and apatite ( $r=0.77$ ) and between Zn and P ( $r=0.72$ ) in the urinary stones. Schneider *et al.*, (1970); and Wandt and Underhill (1988) supported the result that Zn exchanges with Ca ( $r=0.67$ ) in calcium phosphate, or that it makes a main percent from phosphate as its presence in hopeite mineral.

Table 2: Correlation Coefficients between the components and their trace elements.

	Na	Mg	Al	P	S	K	Ca	Ni	Mo	Co	Mn	Fe	Zn	Sr	Ba	Cr	As	Whe	Wed	UA	Lau	Vat	APA	STR	
Na	1																								
Mg	.63	1																							
Al	.79	.33	1																						
P	.79	.62	.78	1																					
S	-.18	-.29	.28	.23	1																				
K	.93	.82	.68	.48	.11	1																			
Ca	.69	.18	-.23	.21	.29	.38	1																		
Ni	.29	-.42	-.24	.72	-.20	-.28	.12	1																	
Mo	.21	.72	.29	.54	-.55	-.14	.09	-.21	1																
Co	.09	-.07	-.04	.38	-.16	.22	-.11	.12	.39	1															
Mn	.19	-.21	-.48	.27	-.44	.27	.14	.48	-.47	-.01	1														
Fe	.15	-.18	.19	-.08	.38	.55	.34	.25	.77	-.13	.38	1													
Zn	.92	.24	.93	.72	.95	.93	.67	-.20	-.54	-.35	-.05	-.38	1												
Sr	.84	.62	.38	.84	.44	.84	.74	-.18	.16	.38	-.51	.75	.88	1											
Ba	-.21	-.23	-.60	.35	-.54	-.38	.33	.65	-.19	.08	.67	.24	.82	-.16	1										
Cr	-.08	.26	-.53	-.28	-.56	-.17	.60	-.32	.21	-.40	-.08	.06	-.27	.28	-.20	1									
As	-.16	-.11	-.80	.46	-.41	-.22	.35	.85	-.23	-.16	.46	.06	.81	.78	.84	-.21	1								
Whe	-.30	.14	-.32	-.54	-.35	-.23	.87	-.18	.25	-.25	-.14	.53	.86	.89	-.24	.57	-.08	1							
Wed	-.33	.03	-.15	-.80	-.20	-.29	.53	-.15	.15	-.33	-.23	-.13	.67	.67	-.13	.31	-.32	.27	1						
UA	-.17	-.25	-.23	-.55	-.51	-.45	.06	.03	-.47	-.25	-.26	-.10	-.02	-.40	.85	-.40	.92	-.25	-.35	1					
Lau	.95	.91	.21	-.19	.46	.82	-.21	.33	.14	.43	-.54	.78	-.33	-.33	-.33	.90	-.37	-.78	-.1	.72	1				
Vat	.29	.28	-.35	-.82	-.34	-.28	.45	-.28	-.19	-.25	.41	-.14	-.35	-.44	-.02	.66	-.19	-.29	.32	-.27	.74	1			
APA	.82	.78	.84	.62	.56	.68	.13	.22	.09	.40	-.01	.43	.77	.89	.08	-.40	-.16	-.25	-.25	-.25	-.27	-.25	1		
STR	.86	.76	.77	.74	.58	.82	-.58	.21	-.27	.26	-.24	-.27	.43	.45	-.62	-.62	-.61	-.38	-.35	-.38	-.38	-.32	.26	1	

Whe: Whewellite; Wed: Weddellite; UA: Uric Acid; Vat: Vaterite; APA: Apatite; STR: Struvite; Lau: Lautite

The reason behind the presence of P in some kinds of urinary stones is high concentration of P in water and food besides the excessiveness of drinking milk and eating cheese, eggs, and some kinds of vegetables which increase phosphorous.

Sr (r=0.84) and Zn (r=0.92) have relationships with concentrations of Na especially in oxalate stones with whewellite mineral (Sr: r=0.89, Zn: r=0.86) and oxalate whewellite/apatite stones (Sr: r=0.89). In a group of oxalate stones, Sr and Zn have strong correlation with K (Sr: r=0.84, Zn: r=0.93). This happens because of the relation between Ca and K in this group (r=0.93). This result is consistent with the correlated results of Wandt and Underhill (1988).

Potassium (K) correlation is negative with all minerals except with lautite (r=0.52), apatite (r=0.68), and struvite (r=0.82). This element appears because of drinking water and eating foods rich with K (Al-Maliki, 1998).

Elements like arsenic (As) with Sr (r=0.78) and Zn (r=0.81), and K with Na (r=0.93) can be substituted with Ca in apatite minerals especially in its crystal surface (Simpson, 1968; Wandt and Underhill, 1988). There are some processes of small amount of substitutions through the combination of crystal especially in oxalate stones.

Fe which is concentrated in urine usually comes from cells in the human urine channel (Lentner, 1981), which increases its percentage in the urinary system and allows it to enter oxalate (r=0.53) and calcium phosphate stones (r=0.43) (Wandt and Underhill, 1988). Fe ions increase in the kidney stones if there is an enrichment of citric acid (Meyer and Thomas, 1982). However, Al percent increases in apatite stones if citric acid increases, which does not affect the presence of Al in calcium oxalate (Meyer and Thomas, 1982). In this study, Al has a correlation with P (r=0.78) and with apatite (r=0.84). This result is consistent with those of Wandt and Underhill (1988), which was (r=0.82).

Some concentrations of S in some urinary stones, which were analyzed, indicate its concentration in cystine stones. It is also found in low concentrations in oxalate stones (Lautite) (r=0.46), oxalate with apatite stones, and apatite stones (r=0.62). Another reason for S concentration in oxalate stones is the alteration between inorganic

sulfur (S with Ca) in the crystal structure during the growth of stones crystal (Schwille *et al.*, 1985; Wandt and Underhill, 1988). There are no obvious correlation coefficients between S in the urinary stones and the reason behind diseases (Wandt and Underhill, 1988).

Molybdenum (Mo) plays a secondary role in the statistical results of this study. It has low concentrations decreasing its effect. Mo has a correlation with Fe (r=0.77) as a result of the harmony of the geochemical relation in the ionic exchange.

Other trace elements such as; Ni, Mn, Ba, Cr, Co, As have negative or positive correlations with all elements and minerals. Generally, correlation coefficients become between elements that make mineral stones when the element enters the chemical formation of that element, or when it has geochemical relations with the radius and/or are charges of major elements.

Many theories have been proposed to link and explain the relation between concentration of some trace elements and their role in forming the urinary stones in humans. However, no direct relation has been found linking the concentration of trace elements in urinary stones and the reasons behind it. It can be said, based on the results of this study, that the concentration of many trace elements in different stones is due to environmental and nutrition reasons. These contributed to increased calcium concentrations inside the human body reaching the urinary system, preparing the biological and physical conditions for gathering many nuclei forming the stones.

#### 4. Analysis and Discussion of the Results

Four hundred and sixty questionnaires have been distributed between 1 /5/2001 and 13/12/2005 on urinary stones patients in selected hospitals in Jordan. Two hundred and eighty two questionnaires have been retrieved representing 61.3 % of the total. This is a high percent and validates the study. These 282 stones have been relieved for those who filled the questionnaires.

Table 3 clarifies the diagnosis of the disease. The urinary stones are 4 kinds: gallbladder, kidney, ureter, and bladder. The distribution is similar to the study of Dajani *et al.*, (1988) with all kinds except for the stones in the gallbladder. The percentages also matched those of

Mhailan (1992) in the types of stones in the bladder and kidney. They were fewer than those in the ureter.

Table 3: Type and percentage of urinary stones in patients and numbers (282 patients).

Gallbladder Stones		Kidney Stones		Ureter Stones		Bladder stones	
No.	%	No.	%	No.	%	No.	%
184	65.25	71	25.2	23	8.15	4	1.4
Total							282

Al-Maliki (1998) had the same percentages in the kidney and ureter. The percentages of the study were consistent with Malki (2000) and Zargooshi (2001). There have been no gallbladder stones in the previous studies, whereas they represent the highest percentage in this study. The kidney stones include the stones that are formed because of increased amount of salt in blood because of filtration through its passage inside the urinary units in the kidney, or that some disorder affected the urinary system. Stones in ureter move from the kidney and settle in the ureter as a result of some stoppage in the urinary passage. The stones in the bladder are formed by a gland of tumor (Al-Attar, 1970). An important factor creating urinary stones is the amount of salts in urine. The formation of nuclei in the urinary system and the process of the salt crystallization help in creating urinary stones in the body (Hashem, 1990).

Table 4: Sex of patients (282 patients)

Sex	No.	%
Male	144	51.06
Female	138	48.94
Total	282	100

In this study, there have been 144 male patients and 138 female patients. Table 4 shows that males are more exposed to urinary calculus. The results of this study are consistent with the results in Dajani *et al.*, (1988), Slimon (1994), Al-Maliki (1998), Stein *et al.*, (1998), Yagisawa *et al.*, (1999), Malki (2000), Goel and Hemal (2001), Naya *et al.*, (2002), and Al-Fawaz (2006), with minor differences in percentages. We noticed that females are more exposed to urinary calculi after adolescence. The reasons behind the presence of stones in females more than in males include hormones of pregnancy. This decreases chenodeoxy cholic-A which decreases the cholesterol forming the stones leading to crystallization of stones in gallbladder (Belal, 1994).

Table 5 shows the distribution of patients of urinary stones in terms of age. The patients range between 5-90 years. The average age of people suffering from urinary diseases is between 45-50 years. The total number of people with this disease is 125 (44.3%). This percentage is consistent with Mhailan (1992), Al-Maliki (1998), Yagisawa *et al.*, (1999), Goel and Hemal (2001), McConnell *et al.*, (2002), Naya *et al.*, (2002), Angwafo *et al.*, (2004), and Al-Fawaz (2006). Second, comes the age group of 31-45 years with 39.4%, then 16-30 (8.5%) followed by 71-90 with 4.6%. Finally the age group of 15> with 93.2%. Urinary calculi are also present in children,

which supports Al-Maliki (1998) about the Iraqi patients and Al-Fawaz (2006) regarding Jordanian patients. The reasons for its presence in children is the excessive eating of eggs, drinking milk, bad health conditions, malnutrition, and the nature of social life of children.

Table 5: Distribution of urinary stones in patients depends on age and sex (282 patients)

Age (year)	Male	%	Female	%	Total	%
5-15	6	4.17	3	2.17	9	3.2
16-30	12	8.33	12	8.7	24	8.5
31-45	55	38.2	56	40.58	111	39.4
46-60	63	43.75	62	44.93	125	44.3
61-75	8	5.55	5	3.62	13	4.6
Total	144	100	138	100	282	100

Married couples (246 patients with an average 87.2%) are more exposed to this disease, which is dominated by people who are more than 45 years old. The number of the unmarried couples is 36 (12.8%) (Table 6).

Table 6: Distribution of urinary stones in patients depending on social status (282 patients)

Marital status	Male	%	Female	%	Total	%
Single	20	13.9	16	11.6	36	12.8
Married	124	86.1	122	88.4	246	87.2
Total	144	100	138	100	282	100

Table 7 shows the distribution of the percentage of the diseases in weight as follows the most exposed to the disease are between 61-80 kg (43.3%) then weights between 81-100 kg, 41-66 kg, and 51-40 kg (28.4, 24.1, 4.3)% respectively. Fat as a result of diets leads to the fact that the gallbladder can not drain its extract and thus creating stones (Al-Attar, 1970). Obesity helps in creating stones. Other studies showed that the possibility of this disease increases with people who quickly lose weight (Al-Attar, 1970; Bakkar, 1995).

Table 7: Weight of patients and frequency (282 patients)

Weight (Kg)	Frequency	%
40-20	12	4.3
60-41	68	24.1
80-61	122	43.25
100-81	80	28.35
Total	282	100

Table 8 shows the time span of suffering form the urinary calculi distributed in three periods as follows 2001-2005 (56.8%), 1996-2000, 1990-1995 (34.8%), and (8.5%) respectively. In 2001-2005 the proportion was high because the polluted water in Jordan led to shortage of clean water. This led to the increase in the concentration of solid hard nucleus crating stones.

The repetition of this disease has been determined if the patient has made previous removing operations. Many patients have not recorded removing operations (77%)

(Table 9). Bakkar (1995) indicated the possibility of iterative disease over the years (67%).

Table 8: Urinary stones distribution depending on year periods

Periods	No.	%
1990-1995	24	8.5
1996-2000	98	34.75
2001-2005	160	56.75
Total	282	100

To determine if patients have other diseases linked with the occurrence of calculi 80.2% of patients hadn't had any others disease, but (19.9%) have been linked with diseases like diabetes or hypertension (Table 10). Many drugs which are taken by patients result in forming stones. Women who take Estrogens, for example, are exposed to the calculi by 2 to 3.7 times as much the women who do not. Furthermore, women who take contraceptives show more risk (Mendo, 2000).

Table 9: Surgery frequency (282 patients)

Surgery	No.	%
No	217	77
Yes	65	23
Total	282	100

We have also determined the relationship between the urinary calculi and heredity through determining if patients have a relative or family member suffering from the disease. 65.6% of patients do not have relatives suffering from this problem (Table 11). This is what Slimon (1994), Bakkar (1995), Abu Ali (1998), Malki (2000) have assumed with 18% of the patients. Table 12 shows that 66.3% of the sick relatives do not have kinship with the patients. The disordered genes can cause calculi disease (Bakkar, 1995) because it results in diseases like kidneys' acidity which causes urinary stones with 73% (Slimon, 1994). The disease of belya cystine is an inherited disease that increases cystine for more than 600g in the urine each day (Takla, 1985). Also, the inherited readiness of the urinary stones has a probable influence which differs from generation to generations (Bakkar, 1995).

Table 10: Urinary stones with other diseases (282 patients)

Another disease	No.	%
No	226	80.15
Yes	56	19.85
Total	282	100

The study has determined the proportion of people suffering from the disease by relating the disease to the educational level of the patient: 12.8% with elementary school, more 9.9% with high school, 26.6% with Al-Tawjihi (secondary certificate), 14.9% with diploma, 21.3% with bachelors' degree, 8.2% with masters, and finally 6.4% with Ph.D. degree (Table 13). Therefore, we notice that the educational level has no obvious association with the urinary calculus in people.

There is a connection between people's salary and the presence of the disease. People with the salary between 0-

100 JD are more exposed to the disease (46.8%), followed by people who get 101-200 JD (33%), followed by those of 201-300 JD (12.4%), and people who get more than 300 JD (7.8%) (Table 14). The urinary calculi are in reverse with the social status. People with low social status have malnutrition leading to the disease (Takla, 1985).

Table 11: Urinary stone disease in another people from family (282 patients)

Disease in another family people	No.	%
No	97	34.4
Yes	185	65.4
Total	282	100

Table 12: Family member suffering from the disease (282 patients)

Family degree	No.	%
Husband	20	7.1
Mother	25	8.87
Sons	28	9.93
Brothers	22	7.8
Nothing	187	66.3
Total	282	100

Table 13: Relation between educational level and urinary stones (282 patients)

Educational Level	No.	%
Elementary	36	12.77
High school	28	9.93
Al-Tawjihi	75	26.59
Diploma	42	14.88
Bachelor	60	21.27
Master	23	8.18
Ph.D.	18	6.38
Total	282	100

Table 14: Relation between deposit incoming and urinary stones (282 patients)

Deposit (JD)	No.	%
0-100	132	46.8
101-200	93	33
2001-300	35	12.4
>300	22	7.8
Total	282	100

Table 15: Water resources

Water resources	Frequency	%
Authority	242	85.8
Commercial treatment	10	3.55
Minerals water	20	7.1
Another	10	3.55
Total	282	100

The results of the statistical analysis of water data taken from patients are as follows: The main water sources come from the competent Authorities (85.8%), followed by commercially treated water (7.1%). The third kind is the least in use which is treated water and other resources like water from rain (3.6%) (Table 15). Most houses don't have filters (87.6%) (Table 16).

Table 16: Equipment of water filtration

Filter	No.	%
No	247	87.6
Yes	35	12.4
Total	282	100

Table 17: Daily amount of drinking water

Amount (litter)	Frequency	%
0.5	21	7.45
1	64	22.7
1.5	114	40.42
2	53	18.8
>2	30	10.63
Total	282	100

The amount of water the patients take daily is a liter and a half (40.4%). 22.6% of the patients consume one litter daily. However, 18.8% consume 2 liters daily, 10.63% consume more than 2 litters daily, and 7.5% consume half liter daily (Table 17). Two hundred and one houses consume less than 50m<sup>3</sup> in one quarter (71.3%) followed by 61 households that consume 51-100 m<sup>3</sup> (21.6%). The least number is 20 households consuming 101-150 m<sup>3</sup> (7.1%) (Table 18).

Table 18: Water amount consumed during period/m<sup>3</sup>

Water consumed (m <sup>3</sup> )	frequency	%
0-50	201	71.28
51-100	61	21.62
101-150	20	7.1
Total	282	100

Table 19: Weakly consumption of meat

Type	No.	%	No. f meals	No.	%
Cow meat	35	12.4	0-2	182	64.54
Cheep meat	63	22.3	3-4	78	27.66
Chicken	184	65.3	5-6	22	7.8
Total	282	100		282	100

There are two factors related to drinking water and making urinary calculi: one is the amount of water, and another is the salt and metal found in water. More water intake decreases the proportion of creating urinary calculi. The amount of solid and dissolved materials in water has a relation with creating stones. The proportion of dissolved Ca in water increases the possibility of the disease. Furthermore, the presence or the absence of certain elements in water affects creating the stones. Zn for example, prevents the crystallization of Ca and low Zn in urine increases the possibility of this disease (Malki, 2000). By analyzing water, we found a high proportion of dissolved Ca in water because the water reserve is made of carbonate.

Regarding food, the researcher has noticed that most of the people suffering from this disease eat chicken by 65.3%, sheep meat by 22.3%, and beef with 12.4% (Table 19).

Table 20: Weakly consumption of yogurt, cheese, and milk

Type	No.	%	No. f meals	No.	%
Milk	32	11.35	0-2	46	16.3
Cheese	44	15.6	3-4	61	21.63
Labaneh	108	38.3	5-6	77	27.3
Yoghurt	98	34.75	7	98	34.77
Total	282	100		282	100

The weekly consumption of meat is low. 64.5% of the patients consume 0-2 meals a week, 27.7% consume 3-4 meals a week and 7.8% consume 5-7 meals a week (Table19). Yoghurt consumption was 38.3% and 34.8% cheese 15.6%, and milk 11.4% (Table 20). The above-mentioned averages indicate that 34.8% eat 7 meals a week, 27.3% eat 5-6 meat a week, 21.6% eat 3-4 meals a week and 16.3% eat 0-2 meals a week (Table 20). Regarding the consumption of eggs, it is found that most people suffering from the disease consume 21-30 eggs a week (35.1%), 11-20 eggs a week (33.3%), less than 10 eggs a week 23.1% and 31-40 eggs a week (8.5%) (Table 21).

Table 21: Weakly consumption of eggs

Amount	No.	%
0-10	65	23.07
11-20	94	33.33
21-30	99	35.1
31-40	24	8.5
Total	282	100

Regarding vegetables with green leaves, Jew mallow was the most consumed one (55.3%), cabbage (19.5%), lettuce (13.5%) and spinach (11.7%) (Table 22). It was previously mentioned that eating eggs, red meat, green leaves, and drinking hard water containing Ca help increase Ca in the urinary stones in the body. The researcher also mentioned that some kinds of vegetables, eggs, cheese and milk increase phosphorous and its concentration in the stones. Phosphorous concentration in water may also increase the risk.

Table 22: Weakly consumption of green vegetables

Type	No.	%
Spinach	33	11.7
Jew mellow	156	55.3
Lettuce	38	13.5
Cabbage	55	19.5
Total	282	100

## Acknowledgements

This research was sponsored by a grant from Al al-Bayt University. The author highly appreciates the help of Dr. Ali Ahmed Bani Nasser, Dr. Arwa Shathel Taqa, and Mr. Musa Al-Zghoul for their invaluable comments during all stages of this research.

## References

- [1] Abboud, I.A. (2008a). Concentration effect of trace metals in Jordanian patients of urinary calculi, *Environmental Geochemistry and Health*, Springer, Nether land, Vol. 30, No. 1, P. 11-20.
- [2] Abboud, I.A. (2008b). Mineralogy and chemistry of urinary stones, patients from north Jordan, *Environmental Geochemistry and Health*, Springer, Nether land, Vol. 30, No. 5, P. 445-463.
- [3] Abu Ali, Kh. (1998). Study of coral kidney stones. *M. Sc. Thesis, Halab University*, Halab, Syria, P87. (in Arabic).
- [4] Al-Attar, M.A. (1970). Urolithiasis of urinary system, *M. Sc. Thesis, Damascus University*, Damascus, Syria, P70. (in Arabic).
- [5] Al-Fawaz, M.M. (2006). Diagnostic of environmental effects in stone formation and traces on human health–northeastern of Jordan, Study in Medical Geochemistry. *M. Sc. Thesis, Al al-Bayt University, Jordan*, P124.
- [6] Al-Maliki, M.A. (1998). Renal stones a study in medical geochemistry. *M. Sc. Thesis, Baghdad University*. Baghdad, Iraq, P101. (in Arabic).
- [7] Angwafo III, F.F., Takongmo, S., and Griffith, D. (2004). Determination of chemical composition of gall bladder stones: Basis for treatment strategies in patients from Yaounde, Cameroon. *World J Gastroenterol*, Vol. 10, No. 2, P. 303-305.
- [8] Bakkar, M. (1995). Study of unity of kidney stones in hospitals of Higher Educational Governorate. *M. Sc. Thesis, Halab University*, Halab, Syria. P88. (in Arabic).
- [9] Belal, M. (1994). General surgery. *Damascus University Publishing*, Damascus, Syria, P. 37-47. (in Arabic).
- [10] Dajani, A., Abu Khadra, A., and Baghdadi, F. (1988). Urolithiasis in Jordanian children. A report of 52 cases. *Brit. J. Urol.*, Vol. 61, P. 482-486.
- [11] Donev, I., Mashkarov, S., Maritchkova, L., and Gotsev, G. (1977). Quantitative investigation of some trace element in renal stones by neutron activation analysis, *J. of Radio Analytical chemist*, Vol. 37, P. 441-449.
- [12] Durak, I., Yasar, A., Yurtarslani, Z., Akpoyraz, M., and Tasman, S. (1988). Analysis of magnesium and trace elements in urinary calculi by atomic absorption spectrophotometry, *British Journal of Urology*, Vol. 62, P. 203-205.
- [13] Feinendegen, L.E. and Kasperek, K. (1980). Medical aspects of trace element research. In Trace Element Analytical Chemistry in Medicine and Biology. *Proceedings of First International workshop*, ed. Bratter, and Schramel, P. 1-37. Berlin: de Gruyter.
- [14] Goel, A., and Hemal, A.K. (2001). Upper and mid-ureteric stones: a prospective unrandomized comparison of retroperitoneoscopic and open ureterolithotomy. *BJU International*, Vol. 88, P. 679-682.
- [15] Hashem, M.A., Basha, W.A., and Al-Sabbag, A. (1990). Kidney urolithiasis, *Damascus University Publishing*, Damascus, Syria.
- [16] Hammarsten, G. (1929). On calcium oxalate and its solubility in the presence of inorganic salts with special references to the occurrence of oxaluria. C R. Traw. Lab. *Carlsberg*, Vol. 17, P. 1-85. In Wandt, M. A. E. and Underhill, L. G. (1988): Covariance biplot analysis of trace element concentrations in urinary stones. *Brit. J. Urol.*, Vol. 61, P. 474-481.
- [17] Joost, J., and Tessadri, R. (1987). Trace elements investigation in kidney stones patients, *Europe Urology*, Vol. 13, P. 264-270.
- [18] Lentner, C. (1981). Geigy Scientific Tables. English edition. Vol. 1, P. 53-107. Basle: Ciba-Geigy.
- [19] Levinson, A.A., Nosal, M., Davidman, M., and Prien, E.L. (1978). Trace elements in kidney stones from three areas in United States, *Investigation Urology*, Vol. 15, No. 4, P. 270-274.
- [20] Malki, A. (2000). Study of kidney and ureter stones in Halab University Hospitals during period between “1988-1999”. *M. Sc. Thesis, Halab University*, Halab, Syria, P121. (in Arabic).
- [21] Marshall, V.R., and Ryall, R.L. (1981). Investigation of urinary calculi. *Journal of Hospital Medicine*, Vol. 26, P. 389-392.
- [22] McConnell, N., Campbell, S., Gillanders, I., Rolton, H., and Danesh, B. (2002). Risk factors for developing renal stones in inflammatory bowel disease. *BJU International*, Vol. 89, P. 835-841.
- [23] Mendo, W. (2000). Percentage determination of abnormal and normal gallbladder stones and determination f type diseases caused it. *M. Sc. Thesis, Damascus University*, Damascus, Syria, P58. (in Arabic).
- [24] Meyer, J.L., and Angino, E.E. (1977). The role of trace metals in calcium urolithiasis, *Investigation Urology*, Vol. 14, No. 5, P. 347-350.
- [25] Meyer, J.L., and Thomas, W.C., Jr. (1982). Trace metal-citric acid complexes as inhibitors of calcification and crystal growth. II. Effects of Fe(III), Cr(III) and Al(III) complexes on calcium oxalate crystal growth. *J. Urol.*, Vol. 128, P. 1376-1378.
- [26] Mhailan, M.M. (1992). The management and treatment of 400 patients with urolithiasis. *Dirasat J.*, Vol. 19(B), No. 4, P. 57-71.
- [27] Naya, Y., Ito, H., Masai, M., and Yamaguchi, K. (2002). Association of dietary fatty acids with urinary oxalate excretion in calcium oxalate stone-formers in their fourth decade. *BJU International*, Vol. 89, P. 842-846.
- [28] Neuman, W.F., and Neuman, M.W. (1953). The nature of the mineral phase of bone. *Chem. Rev.*, Vol. 53, P. 1-45.
- [29] Schneider, H.-J., Straube, G., and Anke, M. (1970). Zink in harnsteinen. *Z. Urol.*, Vol. 63, P. 895-900.
- [30] Schwille, P.O., Hamper, A., and Sigel, A. (1985). Urinary and serum sulfate in idiopathic recurrent calcium urolithiasis. In *Urolithiasis and Related Clinical Research. Proceedings of the Fifth International symposium*. P. 339-342. New York: Plenum.
- [31] Scott, R. (1985). Epidemiology of stone disease. *British Journal of Urology*, Vol. 57, P. 491-497.
- [32] Slimon, W. (1994). Kidney Stones, *M. Sc. Thesis, Damascus University*, Damascus, Syria, P79. (in Arabic).
- [33] Stein, R., Fisch, M., Andraea, J., Bockisch, A., Hohenfellner, R., and Thuroff, J.W. (1998). Whole-body potassium and mineral density up to 30 years after urinary diversion, *British Journal of Urology*, Vol. 82, P. 798-803.
- [34] Simpson, D.R. (1968). Substitution in apatite: I. Potassium-bearing apatite. *Am. Mineral.*, Vol. 53, P. 432-444.
- [35] Sobel, A.E., Nobel, S., and Hanok, A. (1949). The reversible inactivation of calcification in vitro. *Proc. Soc. Exp. Biol. Med.*, Vol. 72, P. 68-72. In Wandt, M.A.E. and Underhill, L.G. (1988): Covariance biplot analysis of trace element concentrations in urinary stones. *Brit. J. Urol.*, Vol. 61, P. 474-481.
- [36] Wandt, M.A.E., and Pougnet, M.A.B. (1986). Simultaneous determination of major and trace elements in urinary calculi by microwave-assisted digestion and inductively coupled plasma atomic emission spectrometric analysis. *Analyst (London)*, Vol. 111, P. 1249-1253.
- [37] Wandt, M.A.E., and Underhill, L.G. (1988). Covariance biplot of trace element concentrations in urinary stones, *British Journal of Urology*, Vol. 61, P. 474-481.
- [38] Yagisawa, T., Hayashi, T., Yoshida, A., Okuda, H., Kobayashi, H., Ishikawa, N., Goya, N., and Toma, H. (1999). Metabolic characteristics of the elderly with recurrent calcium oxalate stones. *BJU International.*; Vol. 83, P. 924-928.

[39] Takla, M. (1985). Kidney stones in Halab University Hospital, *M. Sc. Thesis, Halab University*, Halab, Syria, P114. (in Arabic).

[40] Zargooshi, J. (2001). Open stone surgery in children: is it justified in the era of minimally invasive therapies?. *BJU International*, Vol. 88, P. 928-931.

# Structural Control on Groundwater Distribution and Flow in Irbid Area, North Jordan

Al-Taj, M.

The Hashemite University, Department of Earth and Environmental Sciences., P.O. Box 330159 Zarqa 13133, Jordan

## Abstract

This study aims to evaluate geologic and structural influences on groundwater in Irbid area as an essential resource in that area. This importance increases in the light of the rapid increase in human population, industrial expansion, and agricultural activities. The geology of the area is comprised of Upper Cretaceous limestone, silicified limestone and marly limestone, and all overlain by thick layers of soil. Amman Silicified Limestone and Wadi As Sir Limestone Formations form good aquifers in the study area. The influence of faults and joints on groundwater in the study area is two fold. N-S and NE-SW joints and faults act as drainage channels of groundwater flow and also as aquifers in the area. On the other hand, ESE-WNW normal faults, forming a horst and graben system, form a barrier or semi-barrier to the ground water flow. They are responsible for the dryness of wells in Dayr Yusof, Al Husn Camp, and Huwwarah. All these wells are on the down thrown side of these faults.

© 2008 Jordan Journal of Earth and Environmental Sciences. All rights reserved

**Keywords:** structure, horst and graben, Irbid area, groundwater flow.

## 1. Introduction

Water is the most important component of the development of any area. Human settlement depends to a large extent on the availability of water resources in close proximity to the settled localities. There has been a tremendous increase in human population in Irbid area. Moreover, there has been a lot of industrial expansion and farming activities within the area. These factors have overstretched water demands in the area.

The present research is important for understanding the factors influencing the distribution, flow, and yield of groundwater. The study area is located in the northern part of Jordan. The area ranges in elevation between 770 m above sea level in the southern part and 480 m in the northeastern part. The area is bounded by latitudes  $32^{\circ} 25' 38''$  N and  $32^{\circ} 33' 21''$  N and longitudes  $35^{\circ} 45' 02''$  E and  $35^{\circ} 57' 20''$  E, which is equivalent to 221-240 E and 202-220 N of Palestine Grid. It is about  $340 \text{ km}^2$  (Figure 1).

Irbid area is located on the northern end of Ajloun dome, which is very close to the Dead Sea rift. Thus, it was affected by subsequent movements during the formation of the Dead Sea rift. The formation of the Dead Sea rift was accompanied by faulting, tectonic movement, and volcanic activity. The rift margins were affected by these events (Abed, 2000). Faults have influenced the occurrence of groundwater in terms of its distribution, flow, and yield. Faults can make rocks excellent aquifers.

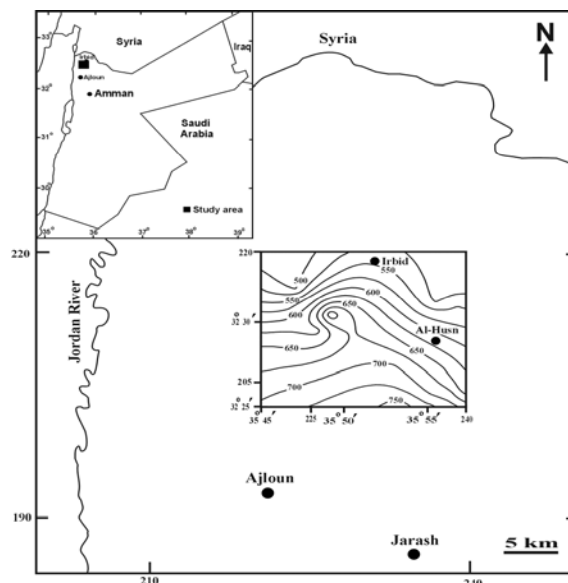


Figure 1: Location and topography of the study area. Contour lines are indicated on the map.

The yield from boreholes drilled into such rocks is thus high. Alternatively, faults act as drains, lowering water table and thus affecting the distribution of groundwater (Mulwa *et al.*, 2005). Further, faults act as barriers to the flow of groundwater if filled with impermeable material such as marl and clays (Kulkarni and Deolankar, 1993). These factors have a strong influence on the aquifer yields through boreholes, static water levels, flow, and hence distribution of groundwater. Therefore the amount of water available in a faulted region would be influenced. A comprehensive understanding of the influence of structures on groundwater is necessary for the selection of drill sites of

\* Corresponding author. maltaj@hu.edu.jo;

productive boreholes in this area and in other areas of similar geological setting.

## 2. Hydrogeological Setting

The study area forms part of the Yarmouk basin, which is the major source of groundwater in north Jordan (Al-Ta'ani, 1989). The rocks outcropping in the study area are mostly of Late Cretaceous age. Wadi As Sir Limestone Formation (WSL) (A7), of Turonian age, is the oldest exposed rock unit and covers most of the area (Figure 2). It consists of limestone and dolomitic limestone. It is exposed as a result of the folding in the area (Atallah and Mikbel, 1992). The total thickness of this formation is about 100 m. It is overlain by Wadi Umm Ghudran Formation (WG) (B1) (Santonian). The Formation is 40 m thick and consists of laminated and bedded chalk. The overlying Amman Silicified Limestone (ASL) (B2) (Campanian-Maestrichtian) consists of chert beds, limestone, and laminated and fossiliferous chalk (Moh'd, 1997). It is about 80m thick. Soil covers the eastern part of the study area (Figure 2). Aquifers in the area are replenished by the precipitation that infiltrates into the underground. WSL and ASL are the main aquifers in the area. They are highly permeable and have secondary porosity due to jointing, faulting, karstification of limestone beds, and brecciation of chert.

Due to large portion of chalk WG acts as an aquiclude separating the WSL and ASL aquifers. WSL and ASL in north and central Jordan are considered as one aquifer system that has high potentiality. Table (1) summarizes the characteristics of the Late Cretaceous Formations.

Forty six boreholes were used in this study. The boreholes data were available at Ministry of Water and Irrigation. Generally, the hydraulic gradient decreases toward the north. According to Momani *et al.* (1989), groundwater in the southern part moves toward the northeast, changing its direction in the northern part to move toward the north. In the western part, it moves to the northwest. Numerous wells drilled in the area and penetrated this aquifer system. In the southern part, they are high yield (24-91 m<sup>3</sup>/hr); examples are AB1375, AD1219, AB1441 and AD1234 wells. While in the north, they aren't high yield (producing 1-5 m<sup>3</sup>/hr). Examples of such wells are AD1220, AD1206, AE1032 and AE1006 wells.

## 3. Structures in The Area

Fracturing and folding result in a high degree of inhomogeneity in the hydrogeological characteristics of different aquifers. This inhomogeneous character causes aquifer yields and ground water flow direction to vary over a whole area (Mulwa *et al.*, 2005).

Bender (1968) considered the study area (i.e., the Irbid area) a part of the fault block mountain east of the rift. Later, Atallah and Mikbel (1992) and Atallah (1996) studied north Jordan in detail, and explained that the study area is a part of Halawa-Al Husn fold belt. It extends from Wadi El Yabis in the west to the basalt plateau in the east. Faulting, folding, and jointing are clear in the area (Figure 2).

Black and white aerial photographs at the scale of 1:10,000 were used in the identification and relocation of

faults and fractures in the study area. A mirror stereoscope was used in the interpretation of structural data. The data was plotted on transparent sheets at the same scale as that of the aerial photographs, and the structural data were then transferred onto a topographic map (scale 1:50,000). Consequently, the main structural features such as faults, folds, and joints in the study area were identified (Figure 2).

### 3.1. Faults and Joints Analysis

Lattman and Parizek (1964) established a relationship between the occurrence of groundwater and fracture traces for carbonate aquifers, particularly in lineaments underlain by zones of localized weathering, increased permeability, and porosity. Researchers' interest in this relationship has grown most rapidly since the introduction of aerial photographs into geological studies (Caran *et al.*, 1982).

The faults in the study area are grouped into two sets. The first set consists of normal faults strikes NW-SE to WNW-ESE, while the second strikes E-W, and they are strike-slip faults. Faults are of Late Tertiary in age (Abdelhamid, 1995). The major fault of the study area is Dayr Yusof fault. It strikes WNW-ESE and can be traced for 6 km before being covered with soil (Figure 2). A fault breccia zone up to 1 m wide was found. The breccia consists of limestone fragments cemented by coarse crystalline calcite (Mansoor, 1998). Geophysical studies showed that it extends east to Al Husn Camp (Azmy Al Mufty Camp) (Al-Bis, 1994). The down thrown block is the northern one. Based on boreholes data, its throw is estimated to be 50 m (Figure 3). Also, there are two remarkable faults; the first lies near Juhfiyeh, 1 km south of Dayr Yusof fault. While the second lies just north of Al Mazar (Figs. 2 and 3). Juhfiyeh fault strikes WNW-ESE and can be traced for about 4 km (Figure 2). In several localities, it is detected due to the truncation of the Wadi As Sir Limestone strata (upthrown) in the south against the Wadi Umm Ghudran (downthrown) in the north. In addition, topographic change between the step-like steep cliffs of the upthrown block and the gentle slopes of the downthrown block is clear evidence of the fault (Mansoor, 1998). Al Mazar fault strikes WNW with a remarkable throw (Figure 3). Dayr Yusof, Juhfiyeh and Al Mazar faults represent the horst and graben system extending from Dayr Yusof to the north of Kitim (Figs. 2 and 3). This system is associated with several high angle minor faults, which are of N-S direction, almost perpendicular to the major faults (Figure 2).

The joint system in the study area consists of four sets (Figure 4). The first set, which constitutes the major set, trends WNW-ESE (120°). The other sets trend: N-S (10°), NNW-SSE (150°) and ENE-WSW (70°) (Figure 4).

### 3.2. Folds Analysis

Folds are obvious in the central and northwestern parts of the area. The fold axes are of two trends; the first is NNE-SSW, and the other is ENE-WSW. Generally, they are plunging to the north. The first trend is formed due to WNW-ESE compression related to Syrian Arc system, while the second trend is younger than the first; and is caused by NNW-SSE compression; and is related to Dead Sea system (Eyal, 1996, Diabat *et al.*, 2004 and Al-Khatib, 2007).

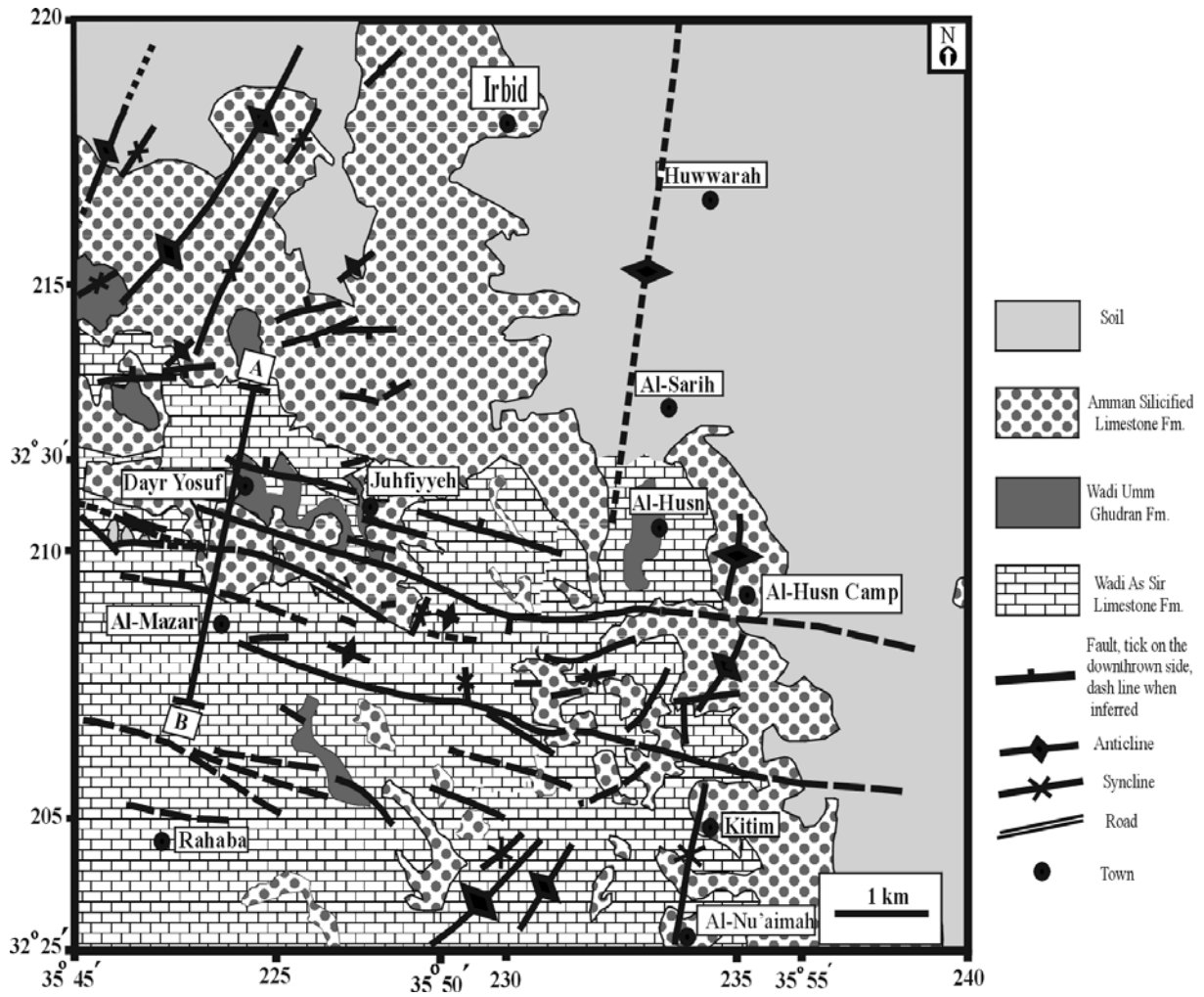


Figure 2: Geology of the study area.

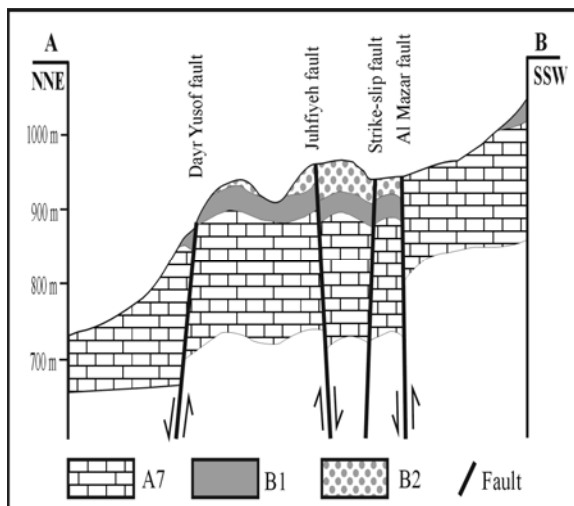


Figure 3: N-S cross section in the area (based on boreholes data). The location is shown on the map of Figure 2.

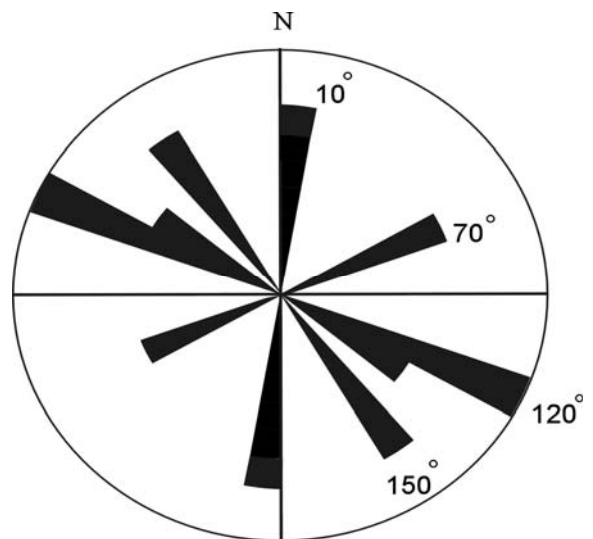


Figure 4: Rose diagram representing main trends of joints in the area.

Table 1. Geological and hydrogeological classification of the Upper Cretaceous rocks (Abed, 2000).

Period	Epoch	Group	Formation	Symbol	Lithology	Thickness (m)	Aquifer Potentiality	Permeability (m/s)
Late Cretaceous	Maestrichtain	Balqa	Muwaqqar Chalk Marl	B3	Chalk, marl and chalky limestone	80	Poor	Permeable
	Campanian		Al Hisa Phosphorite and Amman Silicified Limestone	B2	Chert, limestone with phosphate	80	Excellent	Permeable
	Santonian		Wadi Umm Ghudran	B1	Chalk, marl and marly limestone	40	Poor	Impermeable
	Turonian	Ajlun	Wadi As Sir Limestone	A7	limestone; dolomitic and some Chert	100	Excellent	Permeable
	Cenomanian		Shu'ayb	A5-6	limestone interbedded with marls and marly limestone	60	Poor	Impermeable

#### 4. Results and Discussion

In order to understand geological and structural influence on groundwater, two maps were prepared as described below:

##### 4.1. The groundwater flow map

The groundwater flow map (Figure 5) was prepared based on the boreholes in the area and contouring at 25 m interval. The map shows recharge and discharge zones in the area. It also shows how groundwater flow is influenced by faults, or hidden structures, or divides (Figure 5). This water divide coincides with the trend of some fold axes. So, it may be explained as resulting from a hidden fold. Moreover, the map shows that groundwater flows from elevated regions (Ajloun area in the south) to low lying discharge areas in the northern part of the area (Figure 1). Joints trending N-S may facilitate this movement.

Faulting is an outstanding phenomenon in the area, and the flow model is modified by the presence of major faults and folds. As a result, flow in the northern side occurs laterally (NE and NW). A characteristic feature of aquifers tapped through boreholes located along or close to faults, which divert the lateral flow of groundwater, is that all of them have water yield in excess of 20 m<sup>3</sup>/hr, and can be considered a reasonably good yield. Such boreholes include AB1375, AD1219, AB1441, AD1234, AD1305, AD1221, AD1235 and AD1220 (Figure 6). Therefore, faults and joints act as conduits through which groundwater flows.

##### 4.2. Aquifer yields map

A second map showing aquifer yields of boreholes was prepared by contouring the water yield at intervals of 2 m<sup>3</sup>/hr (Figure 7).

This map is important because it relates water yield from aquifers to geology and structures. The aquifers yielding more than 20 m<sup>3</sup>/hr are located in the southern region of the area, on the upthrown block of the fault system (Figure 3). The high yield from these aquifers can be explained by a correlation of the location of wells (Figure 6), and aquifer yield (Figure 7) maps. The regions with aquifers yielding over 20 m<sup>3</sup>/hr are those immediately close to joints and faults. The discharge regions to the north have low yields, less than or equal to 5 m<sup>3</sup>/hr, except in very few areas with anomalous high yield ranging between 5 m<sup>3</sup>/hr and 10 m<sup>3</sup>/hr. All wells with low yield are located on the downthrown block of the main faults.

Aquifers close to fault zones have a mean yield of 46 m<sup>3</sup>/hr, and boreholes sited on such fault zones are quite deep with an average total depth of 300 m. However, the respective aquifers were struck at relatively shallow depths. The average aquifer depth is 130 m below ground surface.

Aquifers yielding more than 50 m<sup>3</sup>/hr of water are only located on or near fault zones in the study area. Such aquifers, for example, are those tapped by boreholes AB 1375, AD1219 and AB1441 and their mean yield is 63 m<sup>3</sup>/hr (Figure 6). These aquifers occur in the central part of the study area where jointing and faulting are dominant.

The water yield in Irbid area therefore depends on the location of an aquifer, whether on the upthrown or downthrown block of the faults. However, the occurrence of multiple aquifers in boreholes does not always guarantee high water yield. Some boreholes associated with multiple aquifers have low water yield (i.e. AD1266), whereas other yields that are associated with only a single aquifer have high water yield (i.e. AD1234).

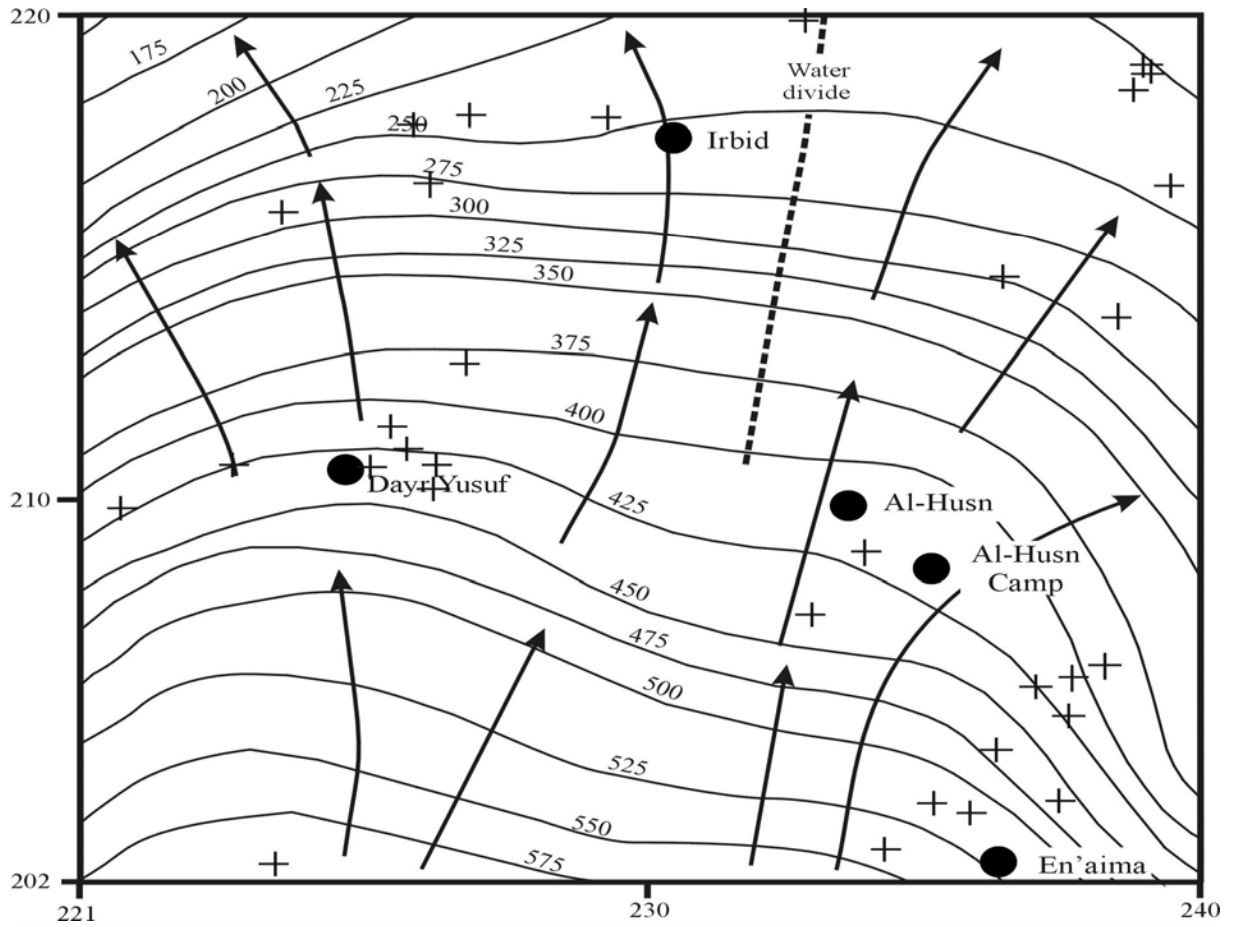


Figure 5: Groundwater flow in Irbid area. Contour lines represent the groundwater level. Crosses represent boreholes locations.

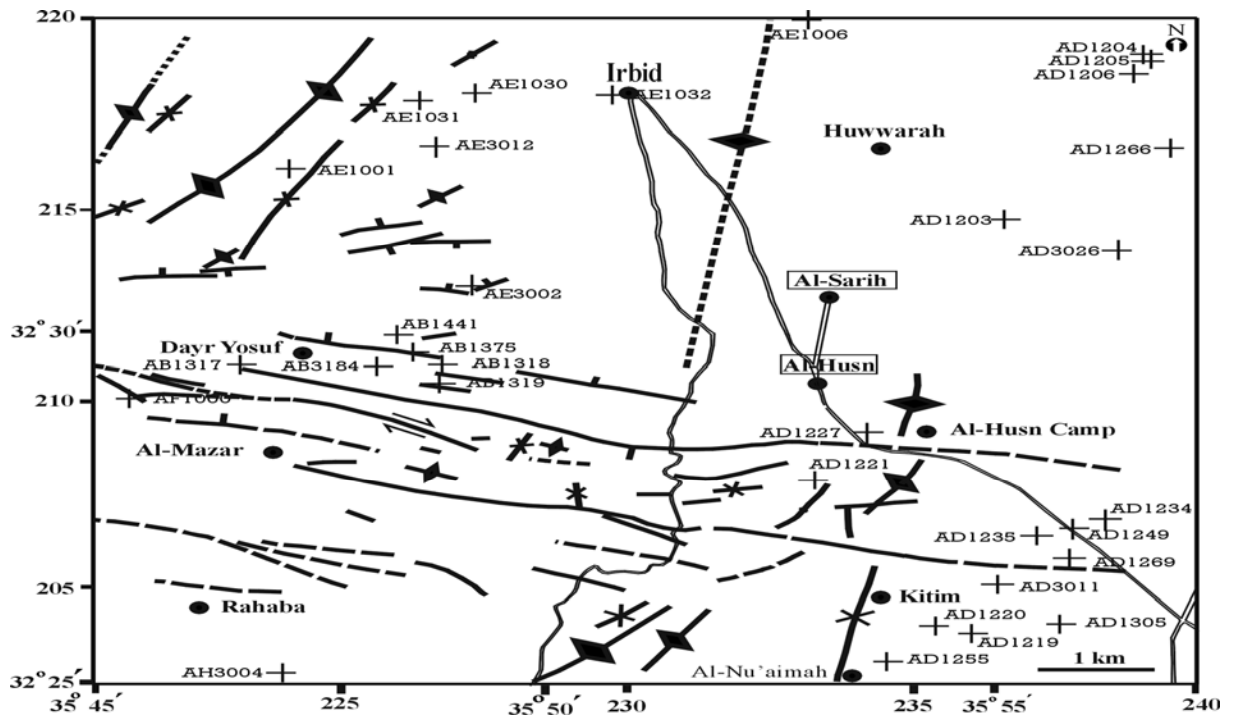


Figure 6: Location of boreholes and their relation with structures in Irbid area. For symbols see Figure 2.

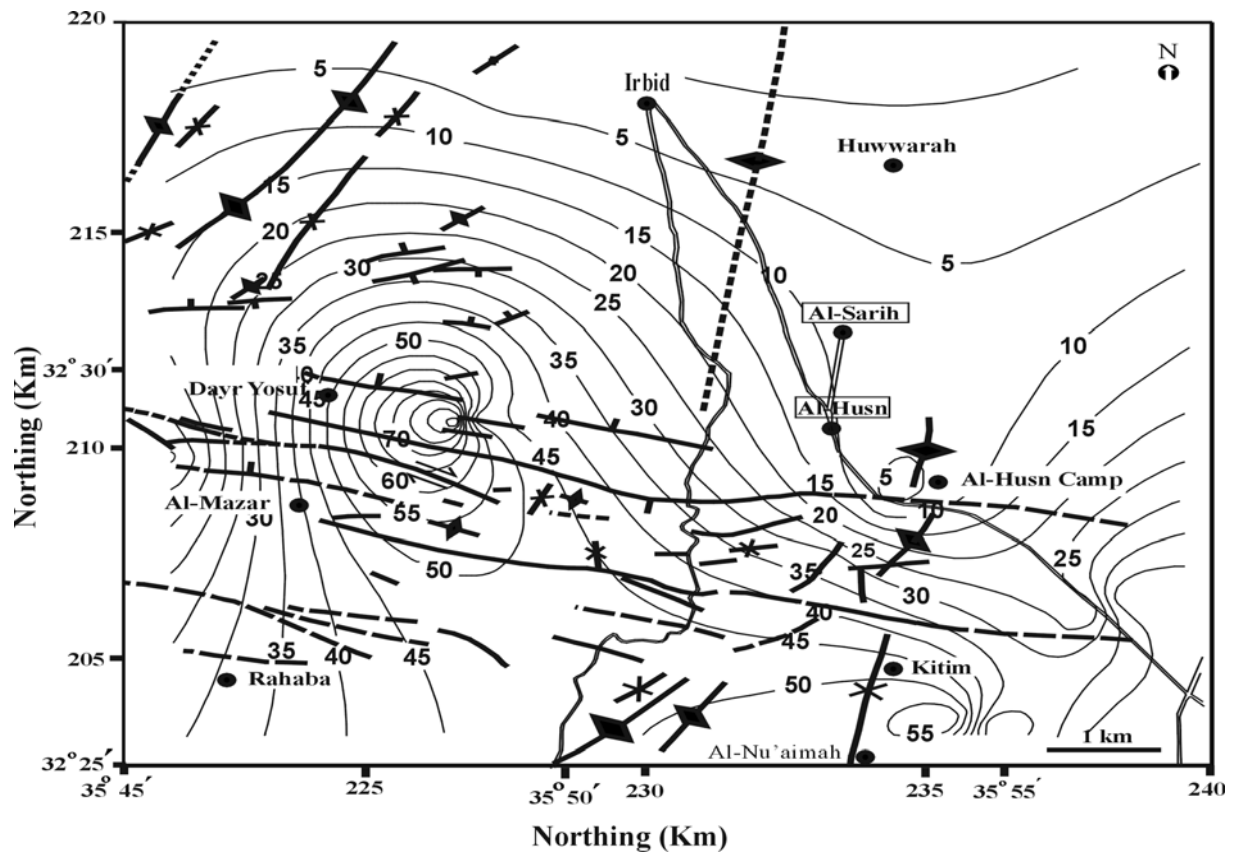


Figure 7: Contour map of boreholes yield and their relation with structures. For symbols see Figure 2.

In the southern region on the flanks of Ajloun dome, recharge is excellent due to high rainfall, which favors infiltration of a good quantity of rainwater (Al-Ta'ani, 1989). Aquifers in the area tend to be modified by structures, both on a small scale by creating local fracture systems which comprise many aquifers and, to a large scale, forming regional hydraulic barrier (Garza *et al.*, 1986, Kulkarni and Deolankar, 1993).

## 5. Conclusions

Groundwater in Irbid area occurs within Amman Silicified limestone and Wadi As Sir Limestone Formations. The groundwater potential in the area is generally acceptable since the mean yield of all aquifers is about 21 m<sup>3</sup>/hr. Aquifers on fault zones have the highest water yield; and are very deep as depicted by the depths of boreholes tapping water from such aquifers. The depths of these boreholes signify that faults have drained groundwater to deeper levels. Generally, clay layers and dense compact rock units underlying aquifers often act as controls to the downward migration of groundwater. Their absence in the study area (Abdelhamid, 1995) has contributed to migration of groundwater to deeper levels, especially along the joints and faults. The faults in the area are excellent aquifers and excellent conduits to the flow of groundwater.

The groundwater flow direction which is determined by the groundwater flow map (Figure 5) shows that the recharge zone is the southern region, and the discharge zone is the northern region. High water yield from aquifers

(>20 m<sup>3</sup>/hr) in the recharge zone is due to an immediate recharge by joints and faults or rainwater infiltrating into the subsurface. Aquifers with high water yield are located on the upthrown side on the WNW-ESE normal faults system. The discharge region is characterized by aquifer yields either less than or equal to 5 m<sup>3</sup>/hr, and all these wells are located on the downthrown block of the main faults. The water yield from these aquifers is less than 5 m<sup>3</sup>/hr and has an average of 3 m<sup>3</sup>/hr. The excessively high yield from aquifers tapped through boreholes in the central region of the study area, mean 46 m<sup>3</sup>/hr, is due to the influence of the numerous faults in this region. The WNW-ESE faults and joints act as barriers or semi-barriers to the groundwater flow, while joints trending N-S facilitate the groundwater flow. The permeable rocks in the upthrown block (B2/A7) in the south face impermeable rocks of the down thrown block in the north (B1). The lateral flow of groundwater along the fault zones has led to deeper flow paths.

## Acknowledgement

Special thanks are due to the Ministry of Water and Irrigation in Jordan for providing most of the borehole data used in this study. Thanks are also due to the Department of Earth and Environmental Sciences, Yarmouk University, for granting permission to use aerial photographs. Thanks are also extended to Prof. Dr. Nasser Athamneh for proof reading.

## References

- [1] Abdelhamid, G., 1995. The geology of Jarash area. Map sheet 3154 I, Bull. 30. Natural Resources Authority, Amman, Jordan.
- [2] Abed, A., 2000. Geology of Jordan (In Arabic), 1st. edition. Geological Association of Jordan, Amman, Jordan.
- [3] Al-Bis, A., 1994. Geophysical evaluation of the underground water situation in Ramtha basin. M.Sc. Thesis (Unpubl.), Yarmouk University, Irbid, Jordan.
- [4] Al-Khatib, N., 2007. Paleostress analysis of the Cretaceous rocks in northern Jordan. M.Sc. Thesis (Unpubl.), Yarmouk University, Irbid, Jordan.
- [5] Al-Ta'ani, A., 1989. Hydrogeology of Amman-Wadi El-Sir aquifer system in Yarmouk Basin in Jordan. M.Sc. Thesis (Unpubl.), Yarmouk University, Irbid, Jordan.
- [6] Atallah, M. and Mikbel, Sh., 1992. Structural analysis of the folds between Wadi El-Yabis and basalt plateau, Northern Jordan. *Dirasat*, 19B: 43-58.
- [7] Atallah, M., 1996. Joints and faults analysis in Al-Husn fold belt, northern Jordan. *Abhath Al-Yarmouk*, 5:187-201.
- [8] Bender, F., 1974. Geology of Jordan. Gebruder Bontraeger, Berlin, Germany, 196p.
- [9] Caran, C., Woodruff, C., and Thompson, E., 1982. Lineament analysis and inference of geologic structure--examples from the Balcones/ Ouachita Trend of Texas: University of Texas at Austin, Bureau of Economic Geology. *Geological Circular*, 82(1): 59-69.
- [10] Diabat, A, Atallah, M. and Salih, M., 2004. Paleostress analysis of the Cretaceous rocks in the eastern margin of the Dead Sea transform, Jordan. *Journal of African Earth Sciences*, 38: 449-460.
- [11] Eyal, Y., 1996. Stress fluctuations along the Dead Sea rift since the Middle Miocene. *Tectonics*, 15:157-170.
- [12] Garza, L., Raymond, M. and Slade, R., 1986. Relations between areas of high transmissivity and lineaments-the Edwards aquifer, Barton springs segment, Travis and Hays counties. In Abbott, Patrick, L. and Woodruff, C. (eds.), the Balcones Escarpment, Central Texas: Geological Society of America, p.131-144.
- [13] Kulkarni, H. and Deolankar, S., 1993. Groundwater abstraction from shallow unconfined Deccan basaltic aquifers of Maharashtra, India; In: Selected papers on Environmental Hydrogeology, 4:107-119.
- [14] Lattman, L., and Parizek, R., 1964. Relationship between fracture traces and the occurrence of groundwater in carbonate rocks: *Journal of Hydrology*, 2: 73-91.
- [15] Mansoor, N., 1998. An assessment of geological and engineering properties of limestone in Dayr Yusof area, North Jordan. M.Sc. Thesis (Unpubl.), Yarmouk University, Irbid, Jordan.
- [16] Moh'd, B., 1997. The geology of Irbid area. Map sheet 3155 II, Bull.46. Natural Resources Authority, Amman, Jordan.
- [17] Mulwa, J., Gaciri, S., Barongo, J., Opiyo-Akech, N. and Kianji, K., 2005. Geological and structural influence on groundwater distribution and flow in Ngong area, Kenya. *African Journal of Science and Technology, Science and Engineering Series*, V. 6, No. 1: 105-115.



# Characterization of A Hard Opaline Clayey Bed Overlying Phosphates from Esh-Shidiya Area, SE of Jordan.

Zayed Al-Hawari \*

*Department of Environmental and Applied Geology, University of Jordan, Amman 11942, Jordan.*

## Abstract

The top two meters of a yellowish clayey bed in Esh-Shidiya area are characterized by using X-ray diffraction (XRD), X-ray fluorescence (XRF), and Scanning electron microscope techniques. The clay rich bed is composed of dioctahedral smectite (100% expandability), quartz, and goethite. The SEM photos have indicated that there is a close relationship between the dioctahedral smectite and silica phases (quartz and amorphous silica). The porous nature of the silica rich bed that overlies a porcelanite (tripoli) layer and the nature of the continuous growth of smectite plates suggest a diatomite rich precursor.

© 2008 Jordan Journal of Earth and Environmental Sciences. All rights reserved

*Keywords:* Opaline Clay, Phosphates, Jordan, Esh-Shidiya.

## 1. Introduction

Clays of different origin are widely distributed in Jordan. Economical clays are found in different stratigraphic units from Paleozoic to Cenozoic time. Kaolinite, bentonite, and palygorskite deposits are among the most important commodities. Some clay beds are associated with Jordanian phosphorites.

Phosphorites are currently mined from Esh-Shidiya area. The future phosphorite industry in the Esh-Shidiya area is estimated around more than 1000 million tons of reserve. The area is located to the south-east of Jordan, approximately 50km south-east of Ma'an (Figure1). The geology and mineralogy of the clays in this area were reported by Khaled (1980). He mentioned that montmorillonite, kaolinite, and mixed-layer illite/smectite are the essential clay minerals that are associated with Esh-Shidiya phosphates. Other studies have concentrated on the phosphorite petrology, geochemistry, and phosphogenesis (Abed et al. 2005), Abed and Abu Murry (1997) studied the rare earth elements distribution, and concluded that upwelling currents played an important role in the deposition of Esh-Shidiya phosphorites. Zghoul(1997) studied the genesis of the palygorskite in the upper part of the sequence overlying phosphorite deposits, and concluded that it was formed from a hypersaline restricted platform or lagoons. Abed et al.(2007) studied evolution of Esh- Shidiya phosphorites, and concluded that palygorskite is of authigenic origin. Systematic study on some clays was carried out by Khoury et. al.( 1988). They reported, for the first time, the presence of palygorskite associated with mixed-layer illite/smectite and kaolinite in the phosphatic beds and marls. The top yellow flat opaline like clayey bed was never investigated. The aim of this

paper is to characterize the opaline clayey bed towards the top of the phosphorite sequence in Esh- Shidiya area.

## 2. Geological Setting

Esh-Shidiya phosphorites are situated in the extreme SE Jordan. It is Upper Cretaceous in age, lower Maastrichtian (Khaled & Abed 1982).High grade phosphorites reserves in this area are around 1000 million tons. Esh-Shidiya phosphorites consist of four phosphorite beds designated from bottom to top: A3, A2, A1, and A0. They are separated by non phosphate materials like chert, marl, dolomitic clay, and porcelanite. These deposits are overlain by yellow marl with varying thickness. The marl is overlain by thick red soil and reddish fluvial conglomerate.

The horizon under investigation is a hard opaline silica horizon. It is tow meters thick, yellow in colour; and is present towards the top of Esh- Shidiya section. It is overlain by the reddish soil and conglomerates and underlain by 0.3m chert, which makes the topmost part of Esh-Shidiya phosphorites (Fig 2).

## 3. Methodology:

A representative sample was collected from the yellow clayey opaline bed. X-ray diffraction (XRD), X-ray fluorescence (XRF), and Scanning electron microscope studies were carried out to characterize the clay sample. The samples were characterized using mineralogical and chemical methods. Size fractionation and the separation of the clay, silt and sand size fractions were accomplished using Atterberg techniques (Jackson, 1975). The cation exchange capacity of the clay was measured using calcium saturation method (Jackson, 1975).

All the analytical work (XRD, XRF, IR and SEM) was carried out in the laboratories of the Federal Institute for Geosciences and Natural Resources, Hanover, Germany.

\* Corresponding author.hawariza@yahoo.com;

A Philips diffractometer PW 3710 (40 kV, 30 mA) with  $\text{CuK}_\alpha$  radiation, equipped with a fixed divergence slit and a secondary graphite monochromator were used. Whole rock 'random powder' samples were scanned with a step size of  $0.02^\circ 2\theta$  and counting time of 0.5 s per step over a measuring range of  $2$  to  $65^\circ 2\theta$ .

Powdered samples were analyzed using a PAN analytical Axios and a PW2400 spectrometer. Samples were prepared by mixing them with a flux material and melting into glass beads. The beads were analyzed by wavelength dispersive x-ray fluorescence spectrometry (WD-XRF). To determine loss on ignition (LOI), 1000 mg of sample material were heated to  $1030^\circ\text{C}$  for 10 min. After mixing the residue with 5.0 g lithium metaborate and 25 mg lithium bromide, it was fused at  $1200^\circ\text{C}$  for 20 min. The calibrations were validated by analysis of Reference Materials. "Monitor" samples and 130 certified reference materials (CRM) were used for the correction procedures.

An ESEM- FEI Quanta 600 FEG scanning electron microscope, operated in low-vacuum mode (0.6 mbar), was used for optical characterization on the  $\mu\text{m}$  scale. Therefore, sputtering of the samples with gold or carbon was not necessary. An EDX-system Genesis 4000 of EDAX was used for chemical characterization.

The infrared samples were prepared using KBr discs; and were studied by using Nexus FT- IR Thermo Nicolet  $150^\circ\text{C}$  dry.

#### 4. Results:

The opaline-like soft clay bed is yellowish to brownish in color due to iron oxides-hydroxides. The hand specimens look dense, but are light in weight. The sampled bed is overlain by porous iron-rich alluvial deposits and underlain by porcelanite (tripoli) layer (Fig. 2).

Fig. 3 shows a typical X-ray diffractogram of the random whole rock preparation of the clayey bed. The diffractogram indicates that the sample is composed of smectite, quartz, and goethite. The same composition is also indicated in the silt size fraction (Fig. 4). The oriented X-ray runs of the clay size fraction have indicated the presence of smectite with 100% expandability and quartz as the essential constituents (Fig. 5). Traces of opal-CT are also indicated by the presence of  $4.18\text{ \AA}$  reflection. The basal reflections of the oriented aggregates are indicated in (Fig. 5). The basal (001) reflection of the dry oriented preparation appears at  $12.6\text{ \AA}$ . The  $12.6\text{ \AA}$  basal reflection expands to  $16.9\text{ \AA}$  upon glycolation.

The chemical composition of the clay and silt size fractions of sample KH16 is given in Table 1.  $\text{SiO}_2$  content is related to quartz, opal-CT and smectites.  $\text{Al}_2\text{O}_3$ ,  $\text{MgO}$ ,  $\text{CaO}$ ,  $\text{K}_2\text{O}$ , and  $\text{Na}_2\text{O}$  content are related to the crystal chemistry of smectite.  $\text{Fe}_2\text{O}_3$  and  $\text{TiO}_2$  are possibly related to both smectite and goethite.  $\text{P}_2\text{O}_5$  is related to some traces of apatite. Loss on ignition (LOI) is related to adsorbed and structural water in the smectite and goethite. The trace elements As, Cr, Cu, Ga, Rb, and V are enriched in the clay size fraction; and possibly enriched in the smectite. Ba, Co, Mo, Ni, Pb, Sr, Zn and Zr are higher in the silt size fraction

The most unique property of smectite minerals is the presence of exchangeable cations that are primarily

adsorbed on the sheet surfaces. The cation exchange capacity of the clay fraction is 30 meq/100g. The most possible exchangeable ions are Ca, Na, and K as indicated from the EDX and chemical results.

The scanning electron micrographs indicate that some phosphate materials (bones) are embedded in the fine matrix (Fig. 6). The texture is homogeneous porous with a dominating crystal size less than 2 microns (Fig. 6). The SEM photos indicate that smectite crystals range in size between 2 microns and 0.2 microns with an average size of about 0.5microns. The matrix is made up of smectite and silica phases, mostly quartz and opal-CT. Fig. 7 shows the continuous growth nature of smectite plates in addition to radial oriented growth. Smectites are found in aggregates, and the neofomed crystals are bridging between the silica phases and grow freely at the expense of the silica phases. The continuous growth of the smectite sheets is well illustrated in (Fig. 8). The lath shaped morphology of the crystallites is dominant, but hexagonal and fibrous varieties are also present.

The EDX results as indicated in (Fig. 9) illustrate that Al and Si are the essential constituents of smectite. Mg and Fe are also present in the smectite structure possibly substituting for Al in the octahedral layer. Fig. 9 indicates also that Ca, K and Na are present in minor amounts possibly as interlayer cations.

The smectite type is a dioctahedral low magnesium type as indicated in (Fig.10). The infrared spectrum confirms the X-ray and SEM results by showing a dioctahedral layer silicate (smectite) and silica phases. The OH water absorbs at  $3400\text{ cm}^{-1}$ . The absorption pattern for the stretching vibrations of the structural OH groups (the principal band at  $3560\text{ cm}^{-1}$ ).

#### 5. Discussion:

The studied clay rich bed is composed of dioctahedral smectite (100% expandability) with quartz and goethite. The field work has indicated that there is a close relation between the dioctahedral smectite and silica phases (quartz and amorphous silica). The porous nature of the silica rich bed that overlies a porcelanite (tripoli) layer suggests a diatomite rich precursor. The released silica from the dissolved frustules is mostly consumed during the growth and neoformation of smectites, opal-CT, and microcrystalline quartz. The transformation of opal-A to opal-CT and finally to quartz is illustrated by Khoury, (1989) and Hesse, (1988). Smectites with a continuous non-interrupted continuous crystal growth indicates a neoformation process possibly as direct crystallization from solution. The radial continuous oriented growth indicates a transformation process from silica phases possibly quartz. The SEM study suggests that the dissolution of diatomite frustules has led to the formation of opal-CT and quartz (Khoury, and Qadan, 2003). The presence of a silica source has helped in the neoformation of smectite. The circulating water moving from the overlying red conglomerate has carried dissolved cations that are incorporated in the structure of smectite. So, the age of smectite is most probably of Pleistocene to Recent.

The most unique property of smectite minerals is the presence of exchangeable cations that are primarily adsorbed on the sheet surfaces.

Table 1: Major oxides and trace elements composition of the clay sample (KH16).

Sample No	SiO <sub>2</sub>	TiO <sub>2</sub>	Al <sub>2</sub> O <sub>3</sub>	Fe <sub>2</sub> O <sub>3</sub>	MnO	MgO	CaO	Na <sub>2</sub> O	K <sub>2</sub> O	P <sub>2</sub> O <sub>5</sub>	LOI	Sum
	%	%	%	%	%	%	%	%	%	%	%	%
KH16/12 Clay Size	68.12	0.406	9.45	7.14	0.054	1.41	0.634	2.36	0.437	0.483	9.16	99.76
KH16/13 Silt Size	75.58	0.46	6.36	6.37	0.225	1.01	1.184	0.03	0.305	0.29	7.87	99.67

Sample No.	(As)	Ba	Ce	Co	Cr	Cu	Ga	Mo	Nb	Nd	Ni	Pb	Rb	Sb	Sc	Sm	Sn	Sr	U	V	Y	Zn	Zr
KH16/12 Clay Size	24	135	<20	9	226	45	11	7	6	<50	65	39	19	6	8	<50	<2	22	3	299	3	276	50
KH16/13 Silt Size	19	601	21	18	127	32	8	13	6	<50	68	42	15	<5	6	<50	10	77	4	275	6	325	67

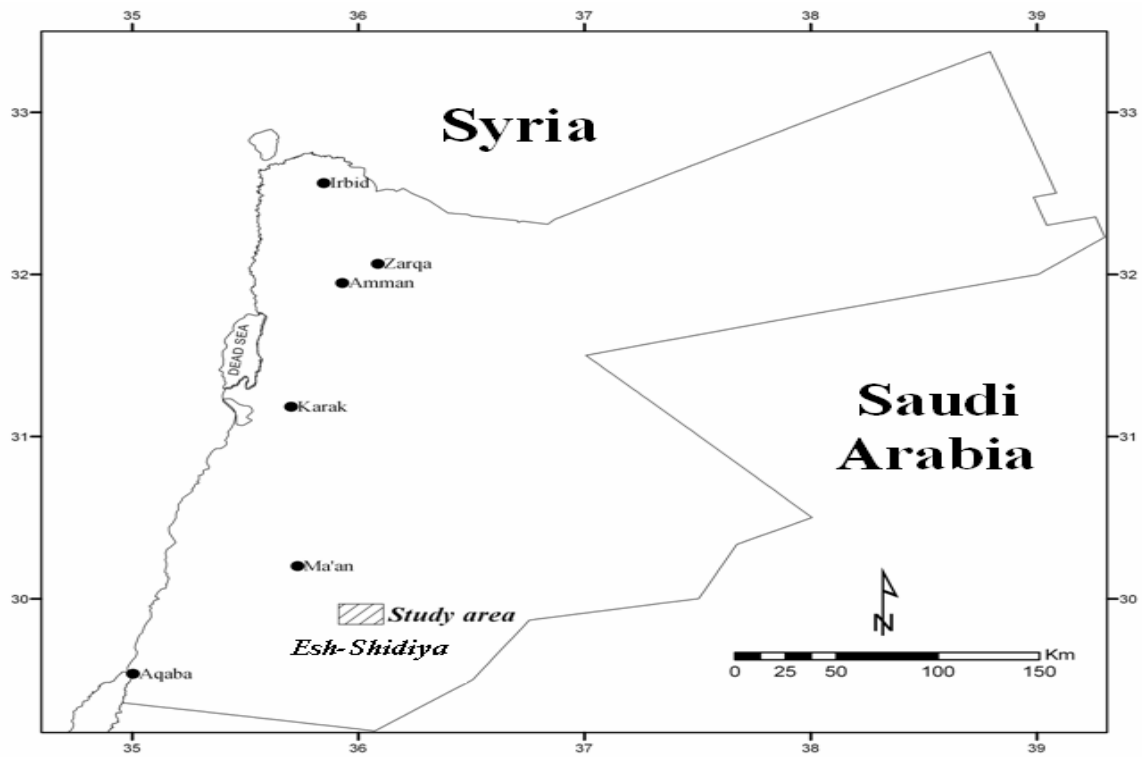


Figure 1. Location map of Esh-Shidiya area

Sample No.	Thickness (m)	Lithology	description
KH16	3 m	[Symbol]	Reddish alluvial sediments
	2 m	[Symbol]	Yellowish hard clay (opaline clay) (Location of the composite sample)
	0.3 m	[Symbol]	Chert and tripoli
	0.2 m	[Symbol]	Clay
	2.5 m	[Symbol]	Thin layers of cherty phosphate and clayey phosphate
	1.5 m	[Symbol]	Soft phosphate (A0)

Figure 2: Columnar section of the upper part of Esh-Shidiya area.

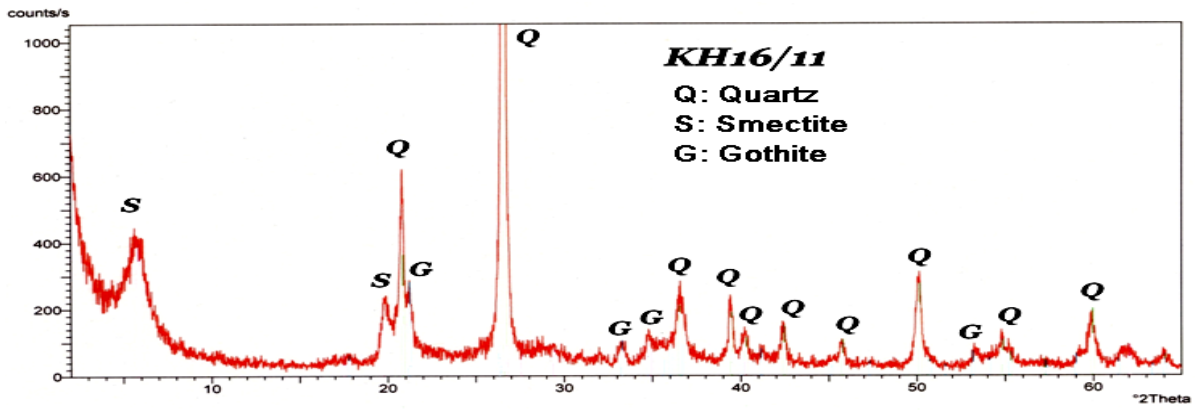


Figure 3 : A trace of X-Ray Diffractogram of the wholeRock Sample (KH16). Figure 4: A trace of X-Ray Diffractogram of the silt size fraction(sample KH16).

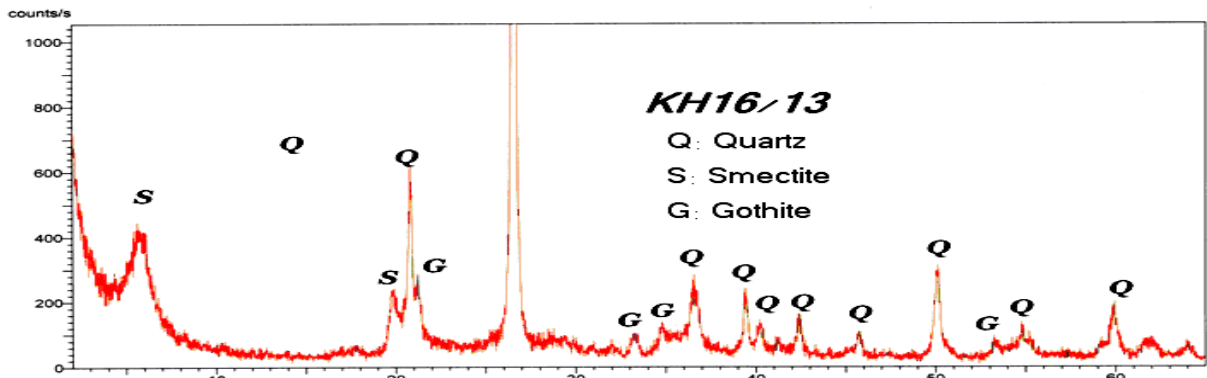


Figure 4: A trace of X-Ray Diffractogram of the silt size fraction (sample KH16).

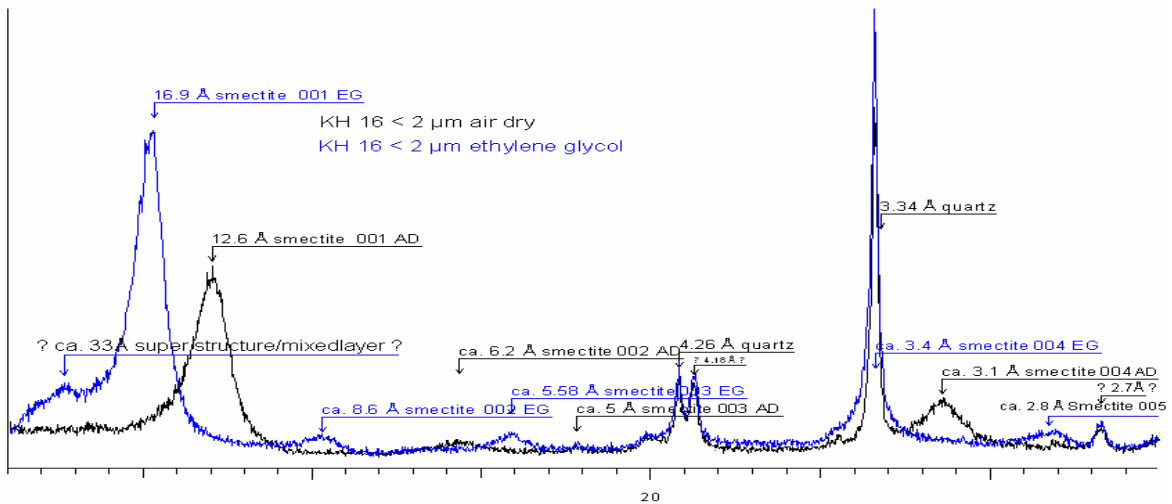


Figure 5: A trace of X-Ray Diffractogram of the clay size fraction sample (KH16).

The aggregation character can have an important influence on physical and rheological properties. This property is very important for using the smectites of the clayey bed for drilling mud.

**6. Conclusions:**

The SEM investigations have indicated that the silica rich bed is formed as a result of diagenetic transformation

process. A diatomite rich precursor (opal-A) is, most probably, the source for silica that has formed dioctahedral smectitic clay and quartz. The clay bed could be utilized for industrial applications.

**Acknowledgments:**

The Federal German Geological Survey Laboratories are highly acknowledged for their help in the analytical

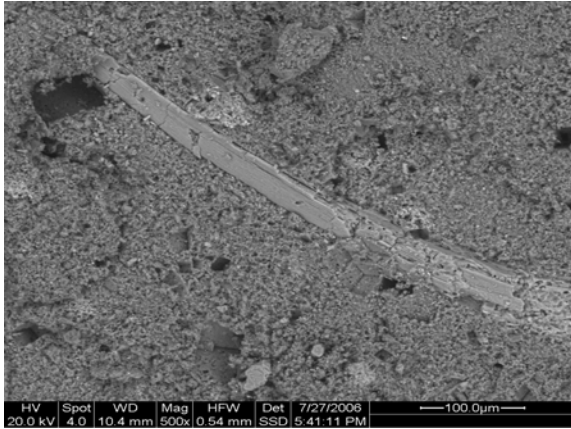


Figure 6: SEM photomicrograph of apatite bone embedded in a clayey matrix.

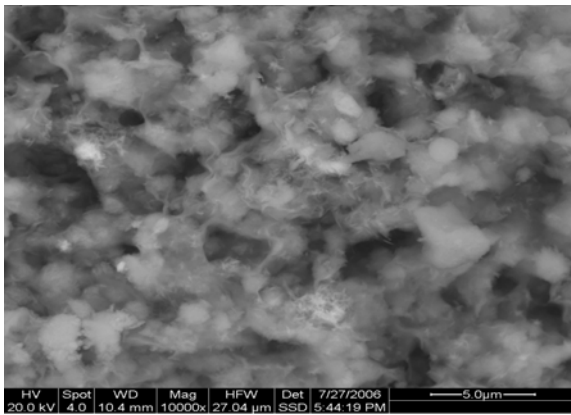


Figure 7: SEM photomicrograph of intergrown smectites with quartz and opaline phases, High porosity.

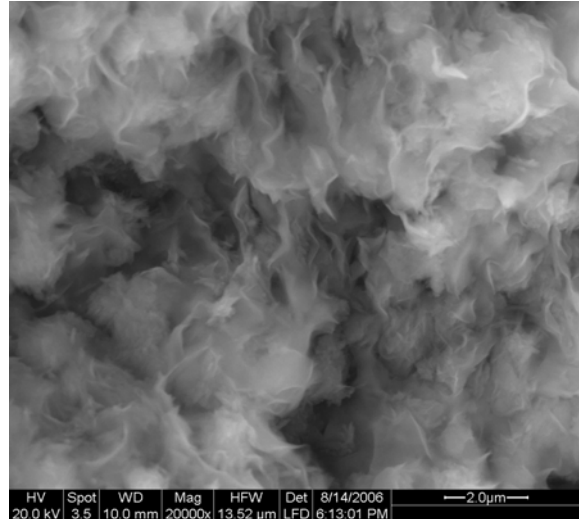


Figure 8: SEM photomicrograph of smectite (Sample KH16) showing a continuous intergrowth.

work. The author is highly indebted to Prof. Hani Khoury and Prof. Abdulkader M. Abed from the Department of Environmental and Applied Geology, University of Jordan, for their critical reading of the manuscript.

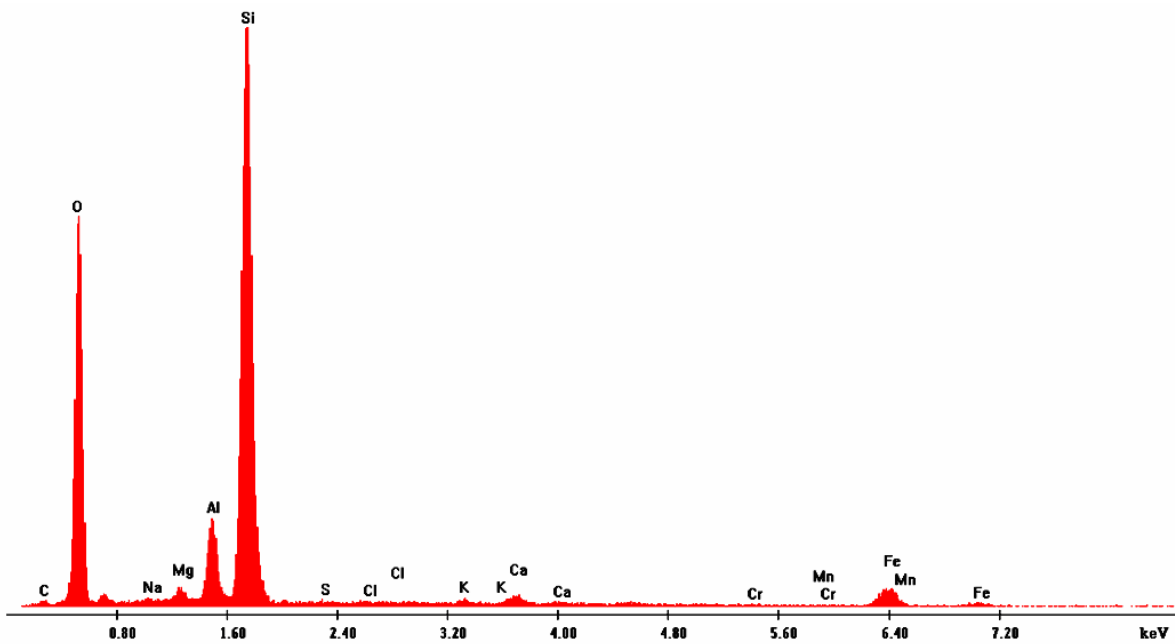


Figure 9:EDX Results of the Smectite of Sample (KH16).

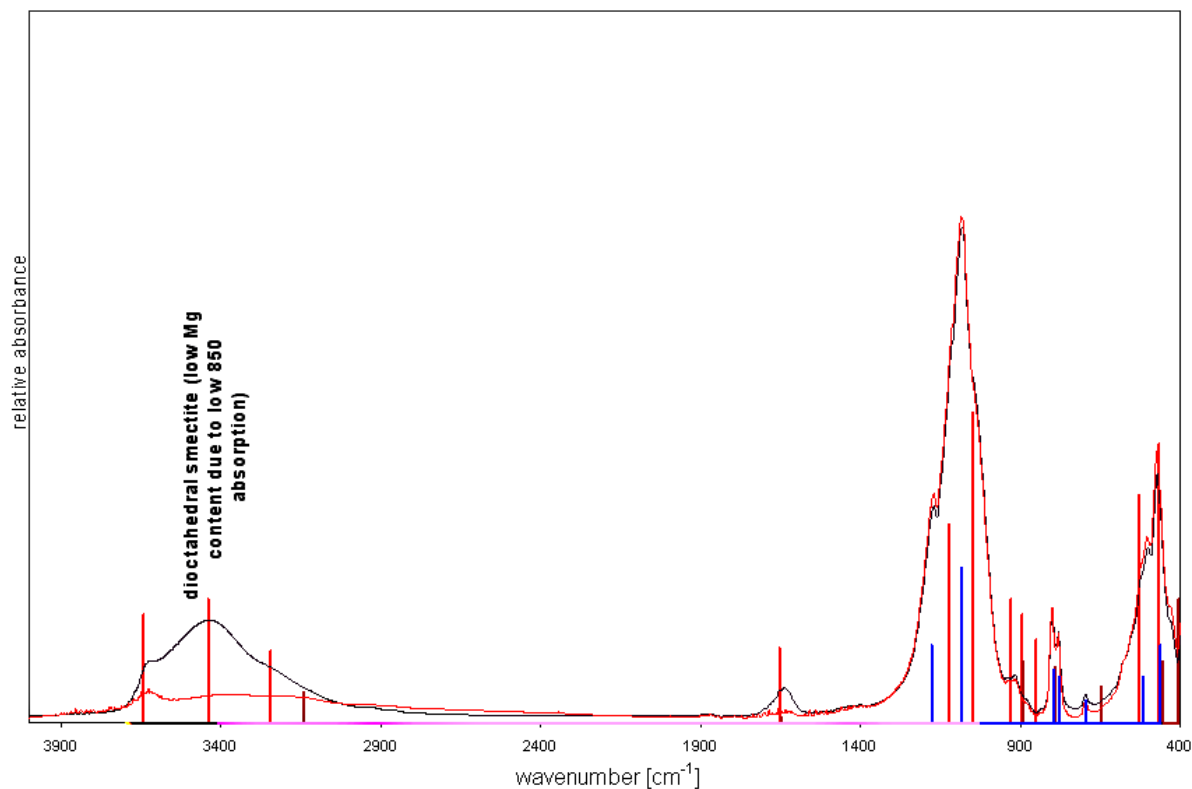


Figure 10: Infrared absorption spectra of the clay size fraction of sample (KH16)

#### References:

- [1] Abed, A.M., Abu Murry, O.S., 1997. Rare earth elements geochemistry of the Jordanian Upper Cretaceous phosphorites. Arab gulf J.Sci.Res.15,41-61.
- [2] Abed, A.M., Arouri, K.H., Boreham, C.J., 2005. Source rock potential of the phosphorite-bituminous chalk-marl sequence in Jordan. Marine and Petroleum Geology, 22,413-425.
- [3] Abed, A.M., Sadaqah, R., Al-Jazi, M., 2007. Sequence stratigraphy and evolution of Eshidiya phosphorite platform, Southern Jordan. Sed.Geol., 198, 209-219.
- [4] Hesse, R., 1988. Origin of chert: diagenesis of biogenic siliceous sediments. Geoscience Canada, 5,(3), 171-192.
- [5] Jackson, M.K., 1975. Soil chemical analysis- advanced course. Madison Wis., 895pp.
- [6] Khaled, H., 1980. Petrology, mineralogy and geochemistry of Esh-Shidiya phosphates. M.Sc thesis, University of Jordan.
- [7] Khaled, H., Abed, A.M., 1982. Petrography and geochemistry of Esh-Shidiya phosphates. Dirasat. 9, 81-102.
- [8] Khoury, H., 1989. Mineralogy and petrology of some opaline phases from Jordan. N.Jb. Miner. Mh., 433-440.
- [9] Khoury, H., Al-Hawari, Z., and El-Surradi, S. 1988. Clay minerals associated with Jordanian phosphates and their possible industrial utilization. Appl. Clay Sci. 3, 111-121
- [10] Khoury, H., and Qadan, M., 2003. Diatomites and diatomaceous earth. published by the university of Jordan, 111pp.
- [11] Zghoul, K.A., 1997. Genesis of the palygorskite and the evolution of Eshidiya platform, southern Jordan. M.Sc thesis, University of Jordan, Amman.





الجامعة الهاشمية



المملكة الأردنية الهاشمية

المجلة الأردنية  
لعلوم الأرض والبيئة

JJIEES

مجلة علمية عالمية محكمة

<http://jjees.hu.edu.jo/>

ISSN 1995-6681

# المجلة الأردنية لعلوم الأرض والبيئة

## مجلة علمية عالمية محكمة

المجلة الأردنية لعلوم الأرض والبيئة : مجلة علمية عالمية محكمة أسستها اللجنة العليا للبحث العلمي، وزارة التعليم العالي والبحث العلمي، الأردن، وتصدر عن عمادة البحث العلمي والدراسات العليا، الجامعة الهاشمية، الزرقاء، الأردن.

### هيئة التحرير

رئيس التحرير

الأستاذ الدكتور عبد الرحيم أحمد حمدان

الجامعة الهاشمية، الزرقاء، الأردن.

### الأعضاء

الأستاذ الدكتور إبراهيم الدويري

الأستاذ الدكتور عبد القادر عبد

الأستاذ الدكتور أحمد أبو هلال

الأستاذ الدكتور هاني خوري

الأستاذ الدكتور عيسى مخلوف

الأستاذ الدكتور زهير العيسى

### فريق الدعم

#### تنفيذ وإخراج

م.أسامة الشريط

#### المحرر اللغوي

الدكتور وائل زريق

### ترسل البحوث إلى العنوان التالي:

رئيس تحرير المجلة الأردنية لعلوم الأرض والبيئة

عمادة البحث العلمي والدراسات العليا

الجامعة الهاشمية

الزرقاء ١٣١٣٣ - الأردن

هاتف : ٣٩٠٣٣٣٣ ٥ ٠٠٩٦٢٠ فرعي ٤١٤٧

Email: [jjees@hu.edu.jo](mailto:jjees@hu.edu.jo)

Website: [www.jjees.hu.edu.jo](http://www.jjees.hu.edu.jo)